RHEOLOGICAL AND PHYSICO-CHEMICAL PROPERTIES OF PALYGORSKITE CLAY AND ANIONIC POLYACRYLAMIDE POLYMER SLURRIES USED IN DRILLED SHAFT CONSTRUCTION

By

HWEE YAN KHENG

A DISSERTATION PRESENTED TO THE GRADUATE SCHOOL
OF THE UNIVERSITY OF FLORIDA IN PARTIAL FULFILLMENT
OF THE REQUIREMENTS FOR THE DEGREE OF
DOCTOR OF PHILOSOPHY

UNIVERSITY OF FLORIDA

1989

Dedicated with love and gratitude to

my parents
Kheng Chin Hock and Kwok Hung Fun
and
my life-long friend
Leong Ah Kow

who treasure education, but unfortunately,
missed the opportunity to receive
the traditional education they deserved.

ACKNOWLEDGEMENTS

Above all, I am grateful to the graduate program of the United States, for allowing me to have an opportunity to hold graduate assistantships which enable me to financially support myself for my graduate education.

I wish to sincerely thank Dr. Paul Y. Thompson, my supervisory committee chairman, for his thorough review of the manuscript and the support he constantly offered me.

My utmost gratitude goes to Dr. David Bloomquist, the cochairman of my supervisory committee. He has taught me how to put simple ideas to work and has given me hands-on demonstration on how things work. His concern and unselfish help have provided me great encouragement, especially during those days where things did not go right.

I wish to express my appreciation and gratitude to Dr. Frank C. Townsend for his help in obtaining the financial support for this research, his guidance, and encouragement during this research.

Special thanks and respect go to Dr. James L. Eades, who offers me his suggestions regarding clay mineralogy, provides me access to the X-ray diffractometer and scanning electron microscope at the department of Geology, and his support and friendship.

I also wish to thank Dr. Douglas L. Smith for service beyond the call of duty as an external member of my committee.

Sincere thanks is extended to Dr. R. Dean Rhue for using his laboratory to conduct part of the research and for enriching my knowledge in clay chemistry.

The financial support of the Florida Department of Transportation and the Lee Foundation, Singapore, which made this research possible, is greatly appreciated.

The industrial support from Dr. Joseph Caliendo of the Florida Department of Transportation, Mr. Earl Stebbins of the Coastal Caisson Drill Co., and Mr. Ronald Williams of Williams & Associates, is appreciated.

I wish to express my sincere thanks to Messrs. Bill Reve, Ed Dobson, Bill Studstill, Daniel Richardson, and Kirk Waite for their technical skills, help and support.

I also wish to thank the student assistants, Chon Lam Wong, Paula Hirshman, John Philips, and Angela Ramirez, for their conscientious help.

I am grateful to the teachers who inspire me in the various fields of knowledge, and/or offer help that directly or indirectly related to my research: Dr. John L. Davidson, Dr. Michael C. McVay, Dr. Frank N. Blanchard, Dr. Guerry H. McClellan, and Dr. Willie H. Harris.

I wish to thank many of my former and present graduate fellows for sharing of knowledge and creating a congenial working environment; special on the list are Dr. Ramon

Martinez, Dr. Kwasi Badu-Tweneboah, Dr. Prasit Soongswang, Fernando Parra, Curt Basnett, and Bob Casper.

Finally, my heartfelt thanks goes to my parents, Chin Hock Kheng and Hung Fun Kwok, and my best friend, Ah Kow Leong, for their unfailing long-distance love and support towards this special endeavor.

TABLE OF CONTENTS

Abstract of Dissertation Presented to the Graduate School of the University of Florida in Partial Fulfillment of the Requirements for the Degree of Doctor of Philosophy

RHEOLOGICAL AND PHYSICO-CHEMICAL PROPERTIES OF PALYGORSKITE CLAY AND ANIONIC POLYACRYLAMIDE POLYMER SLURRIES USED IN DRILLED SHAFT CONSTRUCTION

By

Hwee Yan Kheng

December, 1989

Chairman: Paul Y. Thompson
Cochairman: David Bloomquist
Major Department: Civil Engineering

Deep foundation construction known as drilled shaft construction (D.S.C.) is gaining popularity throughout the United States. The construction usually requires the use of a drilling mud or slurry during excavation. Slurry of high density, gel strength, and viscosity is good for maintaining an open hole and suspending cuttings after drilling operations cease but is undesirable for clean displacement by concrete during tremie operations. Consequently, proper control of the conflicting properties is essential.

To gain insight into the rheological and physico-chemical properties of two types of slurry commonly used in D.S.C., extensive laboratory tests were performed. A Palygorskite clay (trade name Florigel H-Y) and an anionic

polyacrylamide polymer (Super Mud) slurries were studied. A 20-foot (6.096 m) settling column was designed to study the settling characteristics of sands (cuttings) in slurries.

The mixing method was found to be much more important than hydration for the clay slurry. Organic tannic acid was more effective than inorganic hydrochloric acid in reducing the viscosity, yield point, and gel strength of the slurry. Sodium hydroxide turned the slurry into a "fluid" at pH 11. Addition of calcium hydroxide (lime) caused flocculation and subsequent settlement.

The polymer slurry showed a density of 1000 kg/m^3 at a viscosity as high as 50 s Marsh funnel viscosity. The tests indicated a stable viscosity for pH above 6. However, viscosity decreased when the pH fell below 6. Rejuvenation of the viscosity in this pH range by soda ash was almost futile.

Full scale settling tests showed that gel strength was the principal factor in a slurry's ability to suspend sand particles. The polymer slurry, lacking gel strength, was unable to suspend any sand, whereas the clay slurry, which developed gel strength, was capable of suspending sand. The length of time the sands remained in suspension was dependent on the slurry viscosity.

Preliminary centrifuge model tests were conducted to investigate the viability of using high accelerations to

model hole integrity, filter cake formation, and slurry settlement. It appeared that this technique might model full scale D.S.C.

CHAPTER 1
INTRODUCTION

Background

The use of slurry in well drilling was certainly more of an art than a science in the early days of its usage. For example, the properties of slurry did not merit recording and 13 years were required, after the first successful application of slurry in oil-well drilling in 1901, to have the first publication on the subject appear in the literature (Rogers 1953).

Marsh (1931, 234), the inventor of the funnel viscometer currently used in the field for measuring the slurry viscosity, stated in 1931:

> The subject of mud (slurry) sounds so simple, uninteresting and unimportant that it has failed to receive the attention it deserves, at least as applied to the drilling of oil wells. As a matter of fact, it is one of the most complicated, technical, important and interesting subjects in connection with rotary drilling.

Since then, numerous papers on rotary mud have appeared in the oil-well drilling related literature. However, literature pertinent to slurry performance in drilled shaft construction is still meager today even though slurry has been used in constructing drilled shafts for more than half a century.

Drilled shafts are foundation elements used for supporting structures. Drilled shafts are also called drilled piers, drilled caissons, or bored piles (British usage). A drilled shaft is constructed by placing fresh concrete in a cylindrical drilled hole. Reinforcing steel can be installed in the drilled hole before placing the concrete, if desired.

When drilling soils which tend to cave in, such as sandy soil, a slurry can be used to keep the hole open. Figure 1-1 shows the slurry method of constructing a drilled shaft. The types of slurry method of drilled shaft construction range from shallow, a few meters, utility drilling to foundation drilling, as deep as 94.50 m (Veder 1953). Reese and O'Neill (1987) have cited a few examples where deep foundations could not have been built without the use of slurry.

Drilled shaft construction is gaining popularity throughout the United States and many parts of the world (Greer and Gardner 1986). According to Reese and O'Neill (1987), bentonite slurry has been used in the construction of many drilled shafts in the United States but documentation of the specific number is not available.

The slurry method of drilled shaft construction is not flawless. Heavily contaminated slurry, i.e., slurry that is heavily laden with cuttings, is detrimental to the integrity and load carrying capacity of the shaft later constructed.

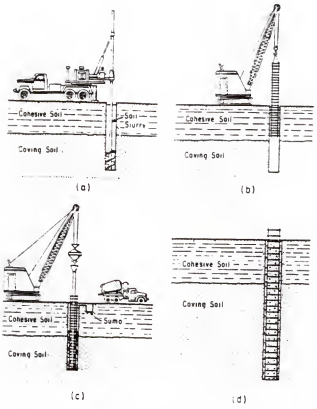

Figure 1-1. Slurry method of drilled shaft construction (a) drilling to full depth with slurry; (b) placing rebar cage; (c) placing concrete; (d) completed shaft. [From Reese 1978]

Settlement of cuttings can occur while waiting for concreting. The gritty, thick, and heavy slurry-cuttings concentrated at the bottom of the hole may not be displaced by the concrete. If not displaced, the end bearing capacity of the shaft will be greatly reduced. Even if the mass of slurry-cuttings is displaced by the concrete from the bottom, the displacement may not be thorough. Muddily thick slurry-cuttings around the steel reinforcement may still be trapped by the concrete, resulting in poor bonding and a defective shaft.

The success of drilled shaft construction using slurry depends heavily on the proper construction techniques and a good quality control on the properties of slurry and concrete. Unfortunately, the slurry must possess conflicting properties, because of the different functions it has to serve in the construction of drilled shafts. For example, a slurry of high density, high gel strength (shear strength), and high viscosity is good for suspending the cuttings when drilling operations stop but is not good if clean displacement by concrete is required. Therefore, a good control of the slurry properties in the field is not a straightforward task.

Fortunately, slurry specifications (see Chapter 2) have been written by organizations and individuals to control the properties of slurry in drilled shaft construction. However, specifications that are suitable for certain

construction conditions may not be suitable for others. Strict compliance of a particular set of slurry specifications, without proper modifications to suit the field conditions, may not be practical.

The majority of slurry specifications are meant for bentonite clay (which is composed mainly of the smectite clay minerals with sodium as the major exchangeable cation) slurries, the most popular clay slurries. Also, there is a wealth of information on the rheological and physico-chemical properties of the bentonite clay slurries. However, limited information is available on drilling clay slurry composed mainly of the palygorskite/attapulgite clay mineral. The Florigel H-Y clay (a specially-processed palygorskite clay) slurry is the most popular mineral slurry used in the State of Florida for the construction of drilled shafts, especially for drilled shaft construction in the salt water environment.

Smectite and palygorskite clays are different both physically and chemically. Smectite clays are flakes composed of tiny platelets. Because of the weak bonding between the platelets and high repulsive surface charge on the platelets, water can enter between them causing the smectite clays to swell when placed in water. On the other hand, palygorskite clay consists of bundles of laths and has low surface charge. Unlike the smectite clay slurries, the palygorskite clay slurry shows small variations in viscosity

and gel strength with large variations in electrolyte content (Grim 1962).

Since the smectites and palygorskite clays are different in shape and properties, slurry specifications written for bentonite clay slurries may not be suitable for palygorskite clay slurry. Therefore, it is important to investigate the Florigel H-Y clay slurry properties used in drilled shaft construction.

Super Mud (an anionic polyacrylamide polymer) is a relatively new product for use as a polymer slurry in drilled shaft construction in the United States. Its obvious superiority to the mineral slurry is its biodegradable nature that alleviates the problems of disposing spent slurry. But, whether Super Mud can perform better, as a drilling slurry, than the mineral slurry in constructing the drilled shafts is yet to be determined.

The slurry properties to be controlled during drilled shaft construction are density, viscosity, pH, sand content, and gel strength. Since the ultimate goal of drilled shaft construction is to construct a shaft that will carry the design load, it is important to study the rheological properties of the slurry, the settling characteristics of cuttings in the slurry, and the integrity of the hole.

Objectives

The objectives of this research on the Florigel H-Y clay slurry and the Super Mud polymer slurry are as follows:

1. To determine the proper slurry preparation method to achieve the desired slurry density/viscosity.
2. To investigate the flow characteristics of the slurries.
3. To study the effect of pH on the rheological properties of the slurries.
4. To design a full scale settling column and to use it to study the settling characteristics of cuttings in slurries.
5. To examine the current available slurry specifications based on the results obtained from the above studies.
6. To attempt to use centrifuge modeling to study the integrity of a slurry-filled hole.

Scope

The research involved extensive and systematic laboratory studies to achieve the objectives stated in the previous section. These laboratory studies consisted of three parts: the rheological study, the settlement study, and the centrifuge modeling.

The rheological properties of slurries are influenced by several factors: concentration, slurry preparation method, stress history, and pH. These factors were studied. The slurry preparation method involved consideration of soaking, mixing time, and mixing speed. The effect of pH on the rheological properties was studied using organic and

inorganic acids and inorganic bases to lower and raise the slurry pH.

The settlement study was an investigation of the settling characteristics of sands (cuttings) in slurries. Sands were used as cuttings because drilling with slurry in Florida is most commonly done in sandy soil. Variables such as density, sand content, and viscosity of the slurry were related to the depth of slurry and different settling times. The settling tests would help in identifying conditions where cuttings could be suspended, and the duration they could be suspended.

Since no available literature has reported the use of centrifuge modeling to study the slurry performance in drilled shafts, it was attempted to determine whether the centrifuge was a viable tool for the nature of this research. The testing program consisted of designing a sample container with a mechanism such that the integrity of a slurry-filled hole could be studied under a high acceleration environment. This phase of the research served as a preliminary study for investigating the potential use of centrifuge modeling to examine the full scale slurry method of drilled shaft construction.

The following chapters present (a) a review of pertinent literature, (b) laboratory studies on the various factors that affect the rheological properties of both the Florigel H-Y clay slurry and the Super Mud polymer slurry,

(c) a unique design of a 20-ft (6.096 m) settling column, (d) the settling tests of sands in the slurries using sedimentation cylinders and the settling column, (e) the centrifuge modeling tests of slurry-filled holes, and (f) a final chapter on the conclusions and recommendations.

CHAPTER 2
LITERATURE REVIEW

Introduction

This chapter presents a review of literature relevant to the research. A brief introduction of the development and use of drilling slurry is presented first, followed by a discussion of the slurry materials. The functions of slurry in drilled shaft construction are stated and explained. A more thorough review is made on the properties of slurry, with emphasis on the rheological properties. Finally, slurry specifications currently available for controlling the slurry properties are presented and reviewed. Note that literature on centrifuge modeling of slurry method of drilled shaft construction is not found.

Development and Use of Drilling Slurry

The original application of slurry support may go back to the origin of water-well drilling as suggested by Boyes (1975). In 1901, slurry was employed for drilling the first successful oil well in Texas, U.S.A. (Heggem and Pollard 1914). The oil-well drilling practice was later extended to civil engineering construction by a Chicago contractor named Charles Leslie Powell in 1926 (Mayo 1973).

Powell filed an application for a patent "relating to the construction and formation of caissons, abutments, piles and the like and particularly to such as are formed from concrete or other plastic compounds" (Mayo 1973, 163). The chief advantage Powell cited for his innovation was its speed. In 1958, Joseph Elliott, the founder of the slurry process of constructing drilled shafts in Florida, termed the process cast-in-place piling construction (Stebbins and Williams 1986). He combined the tremie concrete methods of bridge pier construction with the slurry drilling techniques used to do soil testing borings without casing.

The use of slurry drilled shaft construction is especially suitable to ground conditions where there are cohesionless soils, particularly below the water table (Terzaghi and Peck 1967). Stebbins and William (1986) point out that stability problems seldom occur when drilling or augering large-diameter holes below the water table using only slurry for hole stability. Also, caving within the shaft even in the sandiest soils simply does not occur with proper techniques. Although historically, slurry drilled shaft construction has been used almost exclusively by the utility industry, it is gaining popularity in deep foundation construction where the ground conditions and cost warrant its application.

Slurry Materials

Bentonite, a highly colloidal and plastic clay, was first used in drilling slurry in 1929 (Xanthakos 1979). This clay was originally found near Fort Benton in the Cretaceous beds of Wyoming, U.S.A., and is largely composed of smectite clay minerals (Grim 1968). It can swell to several times its original volume when placed in water. Its excellent gel forming and thixotropic properties made it the most popular drilling clay worldwide. However, the rheological properties of both sodium and calcium bentonite gels are reported to be susceptible to electrolyte concentration (Van Olphen 1956 & 1959). Bentonite clay is therefore not suitable for drilling conditions where salt contamination is encountered or anticipated.

Clays composed of palygorskite/attapulgite mineral show small variations in viscosity and gel strength with large variations in electrolyte content. Note that the name palygorskite has priority over attapulgite (Bailey et al. 1971) for the mineral with ribbonlike structure in which the ribbons have a width of two pyroxene-like chains. Palygorskite is rare in nature. At present, the most important deposit is in the Meigs-Attapulgite-Quincy district, Georgia and Florida, U.S.A. The minimal sensitivity of rheological properties of palygorskite suspension to the presence of electrolyte has been partly

explained by Grim (1962). He attributes the inert response to the hollow channels through the aggregates of this clay mineral into which sodium ions could penetrate and become non-reactive. The detailed structure of palygorskite that is now generally accepted was proposed by Bradley (1940).

The rapid decline of Wyoming bentonite (Hostermann 1985) and the growing concern of environmental pollution problems have led to the search for a biodegradable surrogate bentonite. In Japan, a polymer known as Telmarch was introduced in the early 1970s to take the place of bentonite clays (Ikuta 1974), but no artificial bentonite was known to be used in Europe at that time (Institute of Civil Engineers 1977). In the U.S.A., the loosely termed "polymer drilling slurries" have had an increased use by the oil industry in recent years (Bouse 1987). Nesbitt and Sanders (1981) report that the synthetic polymers used in drilling slurry--the polyacrylamides and polyacrylates--are biologically nearly inert and biodegradable.

Functions and Properties of Slurry

Due to the popular use of bentonite clays in drilling slurry, literature pertinent to functions and properties of drilling slurry is, in general, referred to the bentonite clay slurries.

Functions

Although originally required only to remove cuttings from the holes, the drilling slurry was later recognized as a vital factor in preventing caving and collapse of holes and maintaining cuttings in suspension when drilling operations were stopped. Hutchinson et al. (1975) state that the slurry has functions that required conflicting properties, i.e., a dense viscous slurry versus a fluid slurry. To support a drilled hole and suspend cuttings, a denser and more viscous slurry is required. For clean displacement of slurry by tremie concrete, the slurry should be more fluid.

To accomplish a successful drilling job, the slurry must be able to form a relatively impermeable filter cake on the interface between the walls of the drilled hole and slurry. Without this impermeable filter cake, the stabilization of the hole by slurry will disappear (Lorenz 1963). For drilled hole stability, the slurry in the hole exerts an outward hydrostatic pressure against the impermeable filter cake, thus prevents the inward collapse of the hole. During excavation, the slurry level should be maintained well above the groundwater level to ensure a positive outward pressure (Reese and O'Neill 1987).

As stated, the outward hydrostatic pressure exerted by the slurry on the walls of a drilled hole is recognized as the main stabilizing factor (Johston et al. 1977, 60).

Hence, the slurry itself should be a colloidally stable suspension of fine clay particles, i.e., no sedimentation of clay particles should occur (Lorenz 1963). In addition, the slurry should be able to suspend cuttings to avoid sludge layers building up at the bottom of the excavation (Hutchinson et al. 1975). If the sludge layers at the bottom of a drilled hole refuse to be displaced by the tremie concrete, the bottom of the concrete shaft will be seriously weakened (Greer and Gardner 1986). Also, the loose sediment that is trapped at the bottom of the drilled shaft will reduce the end bearing of the shaft (Reese and O'Neill 1987).

Hutchinson et al. (1975) describe three different filtration mechanisms--surface filtration, deep filtration, and rheological blocking--that can occur under various conditions during formation of filter cake. Surface filtration occurs when a filter cake is formed by the bridging of hydrated bentonite particles on the soil surface, with negligible penetration of bentonite. Deep filtration occurs when slurry penetrates into the soil, slowly clogging the pores and form a filter cake of several centimeters into the soil. Rheological blocking occurs when slurry flows into the ground, as deep as several feet, until restrained by its gel strength.

The phenomenon of rheological blocking has been shown by McKinney and Gray (1963). They show the gelling of

bentonite slurry in the pores of loose gravel, thereby preventing further entry of slurry from the drilled hole into the gravel.

Properties

To fulfill the above functions of stabilizing a drilled hole, the slurry must be thixotropic. The term "thixotropy" was introduced in 1927 by A. F. Peterfi and used by H. Freundlich to describe the phenomenon of isothermal, reversible gel-sol transformation in colloidal suspensions (Mitchell 1960). Since a thixotropic slurry is one that forms gel while at rest and turns fluid upon agitating, its gel can hold cuttings in suspension when drilling operations stop and its fluidity is restored by breaking the gel structure when agitation resumed.

The flow properties of a slurry are controlled by the rheological parameters, i.e., yield point and viscosity, where rheology is a science of deformation and flow of matter.

Flow models. Most drilling slurries do not conform exactly to any flow models to be mentioned below. However, for practical purposes, these models can be used to predict slurry behavior with sufficient accuracy (Gray and Darley 1980). Flow models are usually visualized by means of flow curves (or consistency curves), which are plots of shear stress versus shear rate.

The plastic flow characteristics of a clay-water suspension were first recognized by Bingham in 1916 (Bingham 1916). Ambrose and Loomis (1931, 1933) were among the first to recognize the plastic flow properties of drilling slurry. Figure 2-1 shows the flow curve for an ideal Bingham plastic flow, the equation for which is

$$\tau - YP = PV.s$$

where τ = shear stress,

YP = yield point,

PV = plastic viscosity, and

s = shear rate.

Yield point (or yield stress) is the stress required to initiate flow. The plastic viscosity is defined as the shear stress in excess of the yield point that will induce unit rate of shear. Thus

$$PV = \frac{\tau - YP}{s}$$

The total resistance to shear of a Bingham plastic flow may be expressed in terms of an effective viscosity, μ_e, at a specified shear rate. Figure 2-1 shows that effective viscosity at shear rate s_1, is given by

$$\mu_{e1} = \frac{\tau_1 - YP}{s_1} + \frac{YP}{s_1}$$

$$= PV + \frac{YP}{s_1}$$

Thus effective viscosity may be considered as comprising two components: plastic viscosity, which corresponds to the viscosity of a Newtonian fluid, and structural viscosity, which represents the resistance to shear caused by the tendency for the particles to build a structure. As shown in Figure 2-1, YP/s forms a decreasing proportion of the total resistance to shear as the shear rate increases, so that the effective viscosity decreases with increase in shear rate. The decrease in viscosity as the shear rate increases is due to the gradual alignment of the particles in the direction of flow (Gray and Darley 1980). Note that the value of effective viscosity is meaningless unless the rate of shear at which it is measured is specified.

The flow curve of the ideal Bingham plastic flow as shown in Figure 2-1 is based on the behavior of a suspension that has a high concentration of approximately equidimensional particles, such as printing inks and paints. The concentration of solids in the suspension is high enough to build a structure by grain-to-grain contact. This structure resists shear through interparticle friction. Once the yield point is exceeded, flow commences, the viscosity is influenced by the volume the particles occupy and not particle interaction (Gray and Darley 1980).

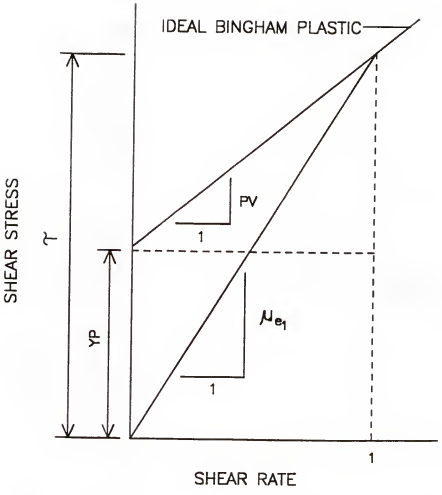

Figure 2-1. Flow curve of an ideal Bingham plastic flow.

The clay particles in the drilling slurries are highly anisodimensional, e.g. bentonite clays (smectites) are platy in shape and palygorskite clay has a needle shape. Also, the clay particles can build a structure at very low solid concentration through the surface attractive and repulsive forces. Because of the influence of the shape and surface forces of the clay particles at low shear rate, the initial part of the flow curves of drilling slurries deviates from that of the ideal Bingham plastic flow. This is illustrated in Figure 2-2.

Although the Bingham plastic model is still in use in the drilling industry, the Ostwald-deWaele power law model for the pseudoplastic slurry gained acceptance in the 70s. Drilling slurries which consist of long-chain polymers are typical pseudoplastics. At rest, the chains are randomly entangled, but they do not set up a structure because the electrostatic forces are predominantly repulsive (Gray and Darley 1980). When in motion, the chains tend to align themselves parallel to the direction of flow; this tendency increases with increase in shear rate, so that the effective viscosity decreases.

Pseudoplastic flow has no yield point; the flow curve passes through the origin as shown in Figure 2-3. The nonlinear curve approaches linearity at high shear rates. Thus, a yield point similar to that of a Bingham plastic flow can be obtained by extrapolation as shown in Figure

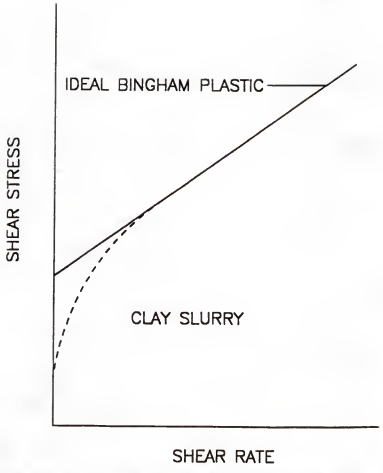

Figure 2-2. Flow curves showing the deviation of clay slurry flow from ideal Bingham plastic flow.

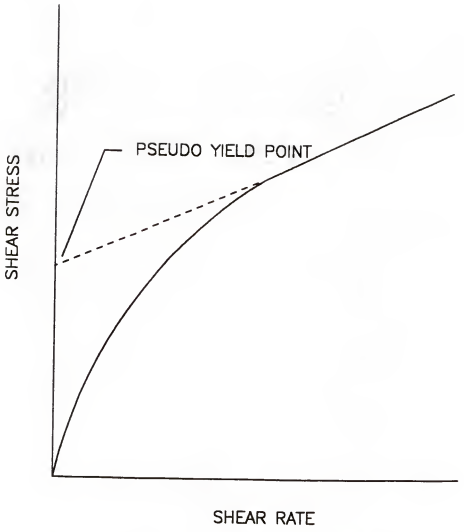

Figure 2-3. Flow curve of a pseudoplastic flow.

2-3; hence the name pseudoplastic. The flow curve of the ideal pseudoplastic flow is described by the power law model, which is

$$\tau = k\, s^n$$

and $n < 1$

where τ = shear stress,

k = consistency index,

s = shear rate, and

n = flow behavior index.

A logarithmic plot of shear stress versus shear rate of the power law model gives a straight line as shown in Figure 2-4.

The flow characteristics of most drilling slurries are intermediate between the ideal Bingham plastic and the ideal pseudoplastic. Zamora and Bleier (1977) propose the Herschel-Bulkley model to describe the yield-pseudoplastic slurry. This model states that

$$\tau - \tau_y = k\, s^n$$

where τ = shear stress,

τ_y = yield point,

k = consistency index,

s = shear rate, and

n = flow behavior index.

The Herschel-Bulkley model is the general case of the Bingham plastic model (when n = 1) and the Ostwald-deWaele power law model (when $\tau_y = 0$). Thus it can be seen that

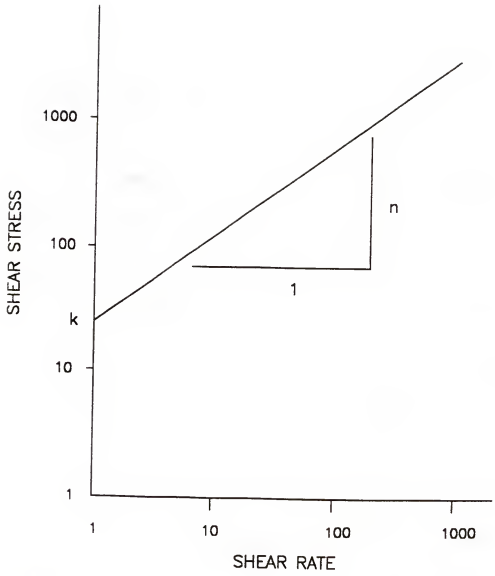

Figure 2-4. Logarithmic plot of flow curve of an ideal power law model.

resistance to flow is composed of two parts; first, dependent on the rate of shear, and second, independent of the rate of shear.

Yield point. Bingham's original concept of yield point was that it resulted from friction between the clay particles in the clay suspension (Bingham 1916, 330). If friction were the only cause of yield point, a straight line flow curve (Figure 2-2) would be formed with a definite intercept on the stress axis. However, a non-linear flow curve is formed which is the result of not only friction, but also flocculation forces between the clay particles that resist flow (Green 1949). Lilienthal (1952) also recognizes the yield point as a measurement of the interparticle forces in the slurry. Consequently, yield point is a function of concentration of slurry solids and factors such as surface charge and potential, which affect the interparticle forces (Melrose and Lilienthal 1951).

As shown by Kelly (1983) and Gray and Darley (1980), the calculated yield point obtained by the American Petroleum Institute (API) (1985) method (see Appendix B) may not correspond to the true yield point. They suggest that the initial gel strength (gel strength is mentioned in the following "Gel and gel strength" section, and the measurement of initial gel strength is described in Chapter 3) is probably the best measure of the true yield

point. Of course, complete flow curves are the best way to obtain the true yield point.

Viscosity. Viscosity is that part of flow resistance in a slurry which represents mechanical friction (1) between solids in the slurry, (2) between the solids and the liquid which surrounds them, and (3) of the shearing of the liquid itself. Higher concentrations of solids will have more resistance to flow because of the greater chance for solid particles rubbing against one another, thus resulting in higher viscosity. Particle shape also has a marked influence on the viscosity, the more asymmetric the particles the more viscous the flow (Lilienthal 1952). Size distribution of slurry solids particles has been shown by Burke (1935) to have an intimate relationship with viscosity. Slurries having greater percentage of small particles have higher viscosities.

Gel and gel strength. When a thixotropic slurry is allowed to come to rest, forces resulting from positive and negative electrical charges located on or near particle surfaces tend to move the solid particles around until they reach a geometrical arrangement where the attractive and repulsive forces are best satisfied. Gelation then occurs and a single "floc," which extends throughout the available volume, is formed. Platelike particles may associate to rigid "card-house" structures

and rods or needles may build a scaffolding arrangement (Van Olphen 1977).

The term "gel strength" can be defined as the measurement of the peak shear stress value upon the sudden application of a 5.11 s^{-1} shear rate. The strength of the gel is dominated mainly by the electrostatic force between individual clay particles. This force depends upon the cations present, the attractive force between the particles, and the size, number, and asymmetry of particles present in the suspension (Jessen and Toktar 1960). Since both gel strength and yield point are functions of the interparticle force, as the yield point decreases, the gel strength will usually decrease (Chisholm and Kohen 1954). Timed gel-strength measurements denote the thixotropic properties of the drilling mud, which are measurements of a condition at rest, while yield point is a measurement under flowing conditions. The rate of gel strength increase is highest at the start and gradually approaches some constant amount as time goes on (Halnouty 1937).

A high gel strength slurry will, in general, be quite viscous, but the reverse is not necessarily true. A high viscosity slurry will have high gel strength if its viscosity is due to highly dispersed clays, but it will have little or no gel strength if the viscosity is caused by a high content of relatively inert solids (Williams 1951).

Cuttings suspending ability. Settling of cuttings is prevented by the gel-forming colloids which do not allow particles to settle in accordance with Stokes' law. The dropping out of cuttings is controlled by the degree of flocculation, and the yield point apparently determines the ease with which they start to drop. The viscosity of the slurry tends to stop the settling of cuttings (Marsh 1913). For settling of sand grains in a slurry, Herrick (1932) states that there is for each slurry a minimum size of sand grain that can settle out. Any grain smaller than this minimum size does not have sufficient stress (due to its weight) to shear the slurry, and so cannot settle any faster than the clay particles. Dilution of the slurry allows such grains to settle by reducing the "yield point." In examining the correctness of the yield-point value, Kelly (1983) cautions that true yield point should be used in assessing the cuttings-carrying capacity of a slurry. Loomis et al. (1934) explain the settling rate of cuttings in terms of effective viscosity of the slurry. The viscosity of a slurry is not a constant but increases as the shearing stress to which it is subjected is decreased. The settling rate of cuttings is dependent upon the shearing stresses that are exerted by the cuttings on the slurry. Lower shearing stress will be opposed by a higher effective viscosity.

Carico (1976) developed an easy test to measure the relative suspending abilities of several polymer slurries. The suspension test uses a standard API sand content tube (described in Chapter 3). Slurry to be tested is filled to the mark labeled "water level" (about 100 mL), and 1 g of sand is placed into the tube. The tube is then vigorously shaken and then placed upright. The time taken for the sand to reach selected graduated marks at the bottom of the tube is recorded. Although the test is very simple and rapid, it cannot give accurate results for opaque slurries.

Carico (1976) found that the American Petroleum Institute's (1985) yield point correlation was marginal and could give erroneous suspension information. However, there is an extremely good correlation of the settling rate with the 3-rpm Fann V-G viscometer dial reading. His explanation is that the shear rate experienced by the sand he used may be close to the 3-rpm shear rate, 5.11 s^{-1} (Carico 1976).

The relationship between the shear strength of slurry and the diameter of a spherical particle that the slurry can suspend has been proposed by both Weiss, as noted in Xanthakos (1979), and Cardwell, as given by Morgenstern and Amir-Tahmasseb (1965). Weiss gives

$$D = \frac{3\ \tau_s}{2\ (d - d_s)}$$

and Cardwell suggests

$$D = \frac{6\,\tau_s}{(d - d_s)}$$

where D = diameter of spherical particle,

τ_s = shear strength of slurry,

d = unit weight of the particle, and

d_s = unit weight of slurry.

Note that the two equations are similar in form but differ by a factor of 4. From the derivation of Weiss's equation, the factor of 4 is likely due to the area of the sphere for calculating the shearing resistance to fall in the slurry. Weiss used the projected area of a sphere, i.e. the area of a circle. Cardwell might have considered the whole spherical area which is four times the area of a circle. Nevertheless, Weiss's equation is a more conservative one in terms of the particle size a slurry with a certain shear strength can hold.

Control of Slurry Properties

Prior to 1930, literature pertinent to field or laboratory testing of drilling slurry was scarce. In 1931, Marsh (1931) introduced the funnel instrument for field measurement of viscosity. After 1931, the studies of the properties of drilling slurries progressed rapidly by the oil-well drilling industry. Means of slurry testings were developed in the 30s. The year 1937 marked the final assembly of drilling slurry testing techniques

and apparatus in use today by both the oil-well and the civil engineering drilling industries.

Among the various slurry properties to be tested and controlled in constructing drilled shaft, density and viscosity are customarily thought to be synonymous. They are, in fact, independent properties and must be considered separately. Marsh (1931) emphasizes the importance of distinguishing the two properties. Other important slurry properties include the pH, sand content, and gel strength (shear strength).

The importance of density and viscosity is obvious, because they control the stability of the drilled hole. Higher viscosity helps suspend the cuttings thus increases the slurry density which in turn increases the slurry hydrostatic pressure against the inward collapse of the hole.

The gel strength is needed to maintain an open hole by suspending cuttings and forming a filter cake. Gel sets in the excavated soil pores and its strength prevents further slurry penetration into the soil. Hence, a relatively impermeable filter cake is formed at the soil/slurry interface for slurry pressure to exert on.

The sand content is important for controlling the amount of cuttings in the slurry. Slurry that is heavily loaded with cuttings cannot be thoroughly displaced by

concrete during tremie operations. The end results will be a defective and low end bearing shaft.

As mentioned above, the rheological properties, such as yield point, gel strength, and effective viscosity, are influenced by the electrochemical environment. The measurement of pH is an indication of the acidity or alkalinity, which gives a chemical index of the slurry. The pH value is especially important when the rheological properties change during drilling operations, and chemical treatments are required to remedy the slurry properties.

Slurry specifications have been written for both slurry walls and drilled shaft construction by several individuals and organizations (American Concrete Institute 1989, Florida Department of Transportation 1988 & 1987, Stebbins and Williams 1986, Federal Piling Specialists 1985, Holden 1983, Millet 1981, Xanthakos 1979, Hodgson 1977, Boyes 1975, Fleming et al. 1975, Hutchinson et al. 1975, Sliwinski and Fleming 1975). Basically, the slurry specifications for the two types of construction are similar. However, due to differences in construction procedures and design methods, desired slurry properties do differ.

Only slurry specifications for drilled shafts are reviewed here; they are those written by the American Concrete Institute, ACI (1989), the Florida Department of Transportation, FDOT (1988 & 1987), Stebbins and Williams

(1986), the Federal Piling Specialists, FPS (1985), and Holden (1983). Tables 2-1 through 2-6 present these slurry specifications.

Among the slurry specifications for drilled shaft construction, those written by the FPS (1985) and Holden (1983) are specifically for the bentonite slurry; others are for mineral slurries in general. The ACI specifications apply to polymer slurries as well. Clean fresh water has been specified by the FDOT (1988 & 1987) and FPS (1985) for preparing slurries. Nonetheless, the FDOT specifications do have a density control limit for salt water slurry. The ACI's specification for water is more flexible; the water can be obtained onsite or offsite from sources approved by the geotechnical engineer in charge. Suggested slurry specifications by Stebbins and Williams (1986) are for fine sandy soils, whereas the bentonite slurry requirements of Holden's (1983) are for the West Gate Freeway project, in Australia, where weathered sedimentary rock is encountered. All specifications, except Holden (1983), are explicitly stated for testing results at 20°C.

Density

The density of slurry is commonly measured by the mud balance (described in Chapter 3). Ranges of slurry densities specified by the ACI (1989) are for slurry sampled 1 ft (0.3048 m) from the pier bottom, and before

Table 2-1. ACI slurry specifications.

Item to be measured	Range of results at 20°C	Test methods
1. Density before concreting, lb/ft^3, for slurry 1 ft from pier bottom		API 13B, Section 1 (Mud Balance)
a. No end bearing	85 maximum	ASTM D 4380
b. With end bearing	70 maximum	
2. Marsh Funnel Viscosity sec/qt, for entry slurry and pier slurry	26 to 50	API 13B, Section 2 (Marsh Funnel and Cup)
3. Sand content by volume, percent, before concreting for slurry 1 ft from pier bottom		API 13B, Section 4 (Sand Screen Set)
a. Piers with design end bearing	4% maximum	ASTM D 4381
b. Piers with no design end bearing	25%	
4. pH, during excavation	8 to 12	API 13B, Section 6 (Paper Test Strips or Glass-Electrode pH Meter)

[From American Concrete Institute 1989]

Table 2-2. FDOT 1988 proposed slurry specifications.

Item to be measured	Range of results at 20°C	Test method
Density	64 - 73 lb/ft^3 (in fresh water) 66 - 75 lb/ft^3 (in salt water)	Mud Density Balance
Prior to concreting	< 74.9 lb/ft^3	
Viscosity	28 - 40 seconds or less than 20 cP	Marsh Cone method Fann Viscometer
Shear Strength (10 min gel strength)	4 to 21 $lb/100\ ft^2$	Fann Viscometer
pH	8 - 12	Electric pH Meter or pH Indicator Paper Strips
Sand content if desanders were used		Sand Content Set
Prior to concreting	< 4%	

[From FDOT 1988]

Table 2-3. FDOT 1987 proposed slurry specifications.

Item to be measured	Range of results at 20°C	Test method
Density	64.3-67.4 lb/ft^3 (in fresh water) 66.1-69.3 lb/ft^3 (in salt water)	Mud Density Balance
Prior to concreting	< 74.9 lb/ft^3	
Viscosity	28 - 40 seconds or less than 20 cP	Marsh Cone method Fann Viscometer
Shear Strength (10 min gel strength)	4 to 21 $lb/100\ ft^2$	Fann Viscometer
pH	8 - 11	Electric pH Meter or pH Indicator Paper Strips
Sand content if desanders were used		Sand Content Set
Prior to concreteing	< 5%	

[From FDOT 1988]

Table 2-4. Slurry specifications of Stebbins and Williams.

Freshly Mixed Mineral Slurry

Item to be Measured	Range of Results at 20°C	Test Method
Viscosity	27 to 40 seconds	Marsh Funnel
pH	8.0 - 12.0	pH indicator paper strips

Shaft Bottom Density

A sample taken from within 1 foot of the bottom of the drilled shaft, immediately prior to beginning concrete operation, shall show a fluid density of not more than 75 pcf.

[From Stebbins and Williams 1986]

Table 2-5. FPS slurry specifications.

Item to be measured	Range of results 20°C	Test Method
Density prior to concreting	< 1.10 g/mL ≤ 1.20 g/mL	Mud density balance
Viscosity	30 - 50 seconds or less than 20 cP	Marsh Cone Fann Viscometer
Shear strength (10 minute gel strength)	1.4 to 10 N/m^2 or 4 to 40 N/m^2	Shearometer Fann Viscometer
pH	9.5 - 12	pH indicator paper strips of electrical pH meter

[From Federation of Piling Specialists 1985]

Table 2-6. Holden's slurry specifications.

Bentonite Property	Mud Supply During Excavation	Socket Slurry During Interruptions	Socket slurry During Concreting
Bentonite type	Sodium bentonite OCMA Spec		
Bentonite Concentration % wt/wt of water	4 min		
Density gm/cc	1.03 min 1.08 max	1.03 min 1.08 max	1.03 min 1.20 max
API Sand content % by volume	0 min 2 max	0 min 2 max	10 max
API Fluid loss mL in 30 min	10 max	10 max	
Cake thickness mm	1 max	1 max	
pH (field check with indicator paper)	8 min 11 max	8 min 11 max	
Plastic viscosity (viscometer) cP	4 min 10 max	4 min 10 max	20 max
Yield Point Pa	14 max	14 max	
10 min gel strength Pa	2 min 10 max	7.5 min	7.5 min 20 max
API Marsh funnel viscosity sec (field check)	30 min 40 max	30 min 40 max	
Head of bentonite	1 m above W.T. (min)	1 m above W.T. (min) 1.5 m above W.T. (max)	1 m above W.T. (min)

[From Holden 1983]

concreting. Maximum densities of 70 lb/ft^3 (≈ 1122 kg/m^3) and 85 lb/ft^3 (≈ 1362 kg/m^3) are specified for piers designed with and without end bearing, respectively.

The slurry specifications currently in used in the state of Florida are the 1987 draft specifications (FDOT 1987). A slurry freshly mixed with fresh water should have a density between 64.3 lb/ft^3 (≈ 1030 kg/m^3) and 67.4 lb/ft^3 (≈ 1080 kg/m^3). For freshly mixed salt water slurry, the density should be between 66.1 lb/ft^3 (≈ 1059 kg/m^3) and 69.3 lb/ft^3 (≈ 1111 kg/m^3). However, a revised FDOT draft specifications (1988) raise the upper limits for both the freshly mixed fresh water and salt water slurries to 73 lb/ft^3 (≈ 1170 kg/m^3) and 75 lb/ft^3 (≈ 1202 kg/m^3), respectively. Both drafts specify a maximum slurry density of 74.9 lb/ft^3 (≈ 1200 kg/m^3) for slurry prior to concreting.

Stebbins and Williams (1986) specify a maximum slurry density of 75 lb/ft^3 (≈ 1202 kg/m^3) for slurry sampled within 1 ft (0.3048 m) from the bottom of the drilled shaft and immediately prior to beginning of concrete operations. Their research in very fine, fine and medium quartz sands has demonstrated that a shaft bottom slurry density of 75 lb/ft^3 can be successfully displaced by concrete.

The FPS (1985) requires the bentonite slurry supplied to the boring to be less than 1100 kg/m^3 (≈ 68.6 lb/ft^3).

For optimum displacement of slurry by concrete, the density near the bottom (about 0.2 m above the base of the pile) should not be greater than 1200 kg/m^3 (≈ 74.9 lb/ft^3).

Holden (1983) considers requirements of supply slurry during excavation, of socket slurry during interruptions, and of socket slurry during concreting. He recommends an upper limit of 1080 kg/m^3 (≈ 67.4 lb/ft^3) and an lower limit of 1030 kg/m^3 (≈ 64.3 lb/ft^3) for both supply slurry during excavation and socket slurry during interruption. For socket slurry during concreting, he recommends an upper limit of 1200 kg/m^3 (≈ 74.9 lb/ft^3) while still maintaining a lower limit of 1030 kg/m^3 (≈ 64.3 lb/ft^3) for hole stability.

Viscosity

Two apparatus are used to determined the slurry viscosity; they are the Marsh funnel and the Fann rotational viscometer as described in Chapter 3. The ACI (1989) specifies a range of 26 to 50 s Marsh for both the entry and pier slurry.

The drafts of the FDOT specifications (1988 & 87) require the viscosity of slurry supplied to drilled shafts to be between 28 to 40 s Marsh, if the Marsh funnel is used. If the Fann viscometer is used, the plastic viscosity shall be less than 20 mPa.s (cP).

Stebbins and Williams (1986) suggest the viscosity of entry slurry to be within the range of 27 to 40 s Marsh. The upper limit of 40 s is meant for coarse permeable zones such as shell bed or gravel lenses.

The FPS specifications (1985) specify the viscosity of bentonite slurry supplied to pile boring to be between 30 and 50 s Marsh, or less than 20 mPa.s Fann plastic viscosity.

The viscosities of bentonite slurry as recommended by Holden (1983) are as follows: plastic viscosity of 4 to 10 mPa.s or 30 to 40 s Marsh for both supply slurry during excavation and socket slurry during interruptions; only upper limit of plastic viscosity of 20 mPa.s is recommended for socket slurry during concreting.

pH

Slurry pH is determined by using either pH indicator paper strips or the glass-electrode pH meter. The ACI (1989) requires the pH of slurry during excavation to fall between 8 and 12. This range is the same as the entry slurry specifications of the FDOT draft (1988) and Stebbins and Williams (1986). The draft of the FDOT (1987) limits the pH range of the supply slurry to 8 to 11.

The range of pH of supply bentonite slurry is specified to be from 9.5 to 12 by the FPS (1985). Holden (1983) recommends a pH range of 8 to 11 for both the

supply slurry during excavation and socket slurry during interruptions.

Sand Content

The sand content of slurry as measured by the American Petroleum Institute (1985) sand content kit (see Chapter 3) is in terms of volume percent and not weight percent. Again, the ACI (1989) considers the sand content limits for piers designed with and without end bearing. For slurry before concreting and sampled 1 ft from the pier bottom, the maximum sand contents are 4% and 25% for design with and without end bearings, respectively.

The FDOT (1988 & 1987) imposes the sand content requirements on slurry prior to concreting only when desanders are used. The sand content at the bottom of the shaft shall not exceed 5% according to the FDOT 1987 slurry specification draft (FDOT 1987). However, the revised draft (FDOT 1988) toughens the sand content control limit to 4%.

Holden (1983) recommends the sand content of both the supply slurry and socket slurry during interruptions be limited to 2%. During concreting, he suggests an upper sand content limit of 10% and states that to prevent sedimentation the slurry should not contain particles larger than 1 to 2 mm (depending on the gel strength).

Gel Strength

The gel strength that is controlled by the slurry specifications is the 10-minute gel strength (refer to Chapter 3 for its determination), which is measured by the Fann viscometer.

The drafts of the FDOT specifications (1988 & 1987) specify a range of 1.9 to 10.1 Pa (4 to 21 lb/100 ft^2) for 10-minute gel strength of entry slurry. However, the FPS (1985) specifies a wider range of 4 to 40 Pa 10-minute gel strength for the supply bentonite slurry.

Holden (1983) recommends a limit of 2 to 10 Pa for the 10-minute gel strength of supply slurry during excavation. Since during interruptions, the slurry has to keep the sand in suspension, he recommends the lower limit of the 10-minute gel strength be increased to 7.5 Pa. However, during concreting, he recommends the gel strength not exceed 20 Pa but requires a minimum of 7.5 Pa to keep medium-coarse (i.e., 1 mm size) sand in suspension.

CHAPTER 3
MATERIALS AND EQUIPMENT

Introduction

The first part of this chapter consists of characterizing the Florigel H-Y clay used in the laboratory studies. Clays of different mineralogical compositions behave differently and possess their own distinct physico-chemical properties. The rheological properties of a clay slurry are governed by the properties of the clay solids, the electrochemical interaction between the clay solids and the makeup water, and the electrochemical interaction of the slurry (composed of clay solids and makeup water) with the groundwater and excavated ground formations. It is thus important to determine the mineralogical composition and the physico-chemical properties of the Florigel H-Y clay.

Mineral identification by x-ray diffraction (XRD), differential thermal analysis (DTA), and scanning electron microscopy (SEM), and physico-chemical properties determination by grain size analysis, Atterberg limits test, Ethylene Glycol Monoethyl Ether (EGME) total surface area test, and cation exchange capacity test, were performed on the Florigel H-Y clay.

No feasible test was performed on the Super Mud polymer. Properties presented in this chapter are based on information provided by the company who produce the polymer. Grain size analysis test was performed on the sands to be used in the settling tests (described in Chapter 5).

The second part of this chapter describes the equipment and the testing methods used in conducting the laboratory tests. The equipment includes the mud density balance, the Marsh funnel, the Fann V-G viscometer, the pH meter and electrode system, and the sand content kit.

Materials

Clay

Florigel H-Y is a light grayish powdered clay specially processed by the Floridin Company at Quincy, Florida, for salt water drilling. During mechanical mixing with the makeup water, which may be fresh, brackish, saturated with salt or may contain either gypsum or cement, Florigel H-Y clay particles are dispersed and interact with each other to form a stable gel-structure throughout the liquid. Slurry made of Florigel H-Y exhibits a much better viscosity stability than does slurry made of Wyoming bentonite under ionic contaminated conditions.

The following sections present the results of the mineralogical and physico-chemical analyses of the Florigel

H-Y clay. Procedures for these analyses are described in Appendix A.

Mineralogical identification

The mineralogical identification was conducted using the GE (General Electric) 11GN1 X-ray diffractometer, the D6000 Deltatherm III differential thermal apparatus, and the ISI (International Scientific Instruments) DS 130, at the Department of Geology of the University of Florida.

X-ray diffraction. Figure 3-1 is a scan of a random mount of the whole clay, while the clay fraction oriented mount X-ray pattern is shown in Figure 3-2. Both indicate that palygorskite, smectite, and quartz are the three detectable minerals in the Florigel H-Y clay. The prism reflections shown in Figure 3-1 agree quite well with the Powder Diffraction File (PDF) cards 21-550, 21-958, and 29-855 Palygorskite diffraction data. The 11.65 Å peak shown in the glycolated pattern remains after 3 days of glycolation suggests that the smectite may consist of magnesium montmorillonite that is not easily expanded by glycolation. The heat treatment pattern shows that the major peak at 10.40 Å of palygorskite is completely eliminated. A fairly high background of the powder mount may have been due to the X-ray amorphous cementitious compounds.

Differential Thermal Analysis. The DTA curve for the whole clay sample is presented in Figure 3-3. It shows the characteristic of the Palygorskite mineral. The peak at

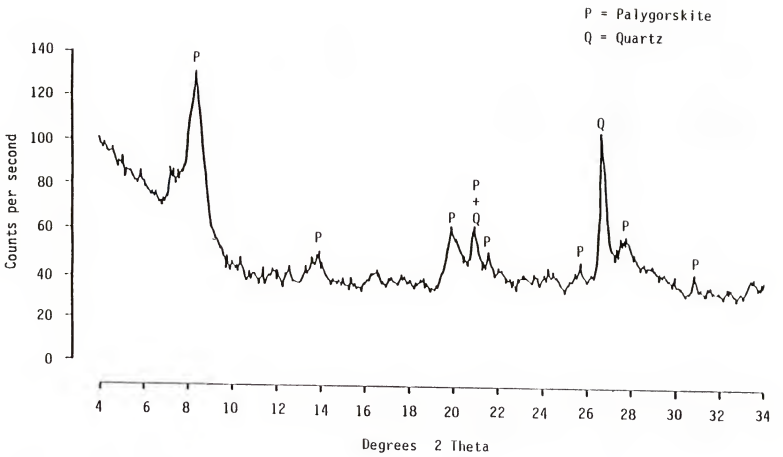

Figure 3-1. X-ray diffraction pattern of Florigel H-Y powder mount (whole sample).

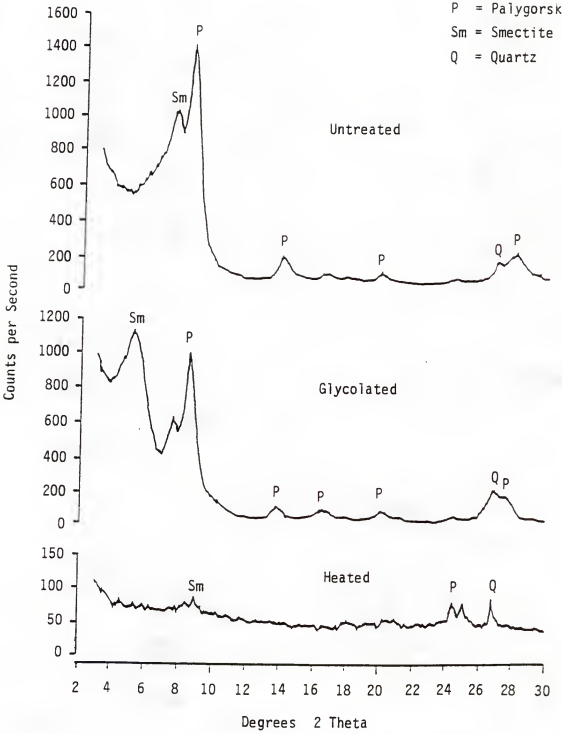

Figure 3-2. X-ray diffraction pattern of untreated, glycolated, and heated Florigel H-Y clay (clay fraction sample).

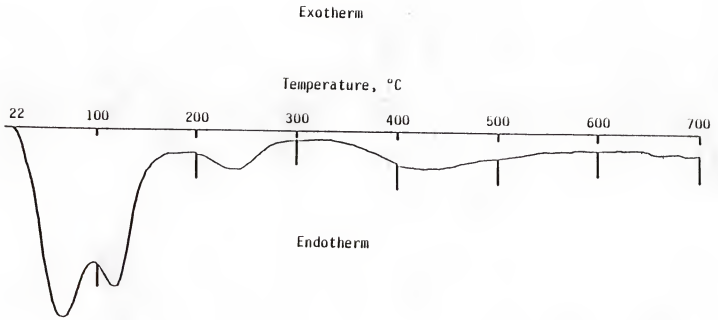

Figure 3-3. Differential thermal analysis (DTA) curve of Florigel H-Y (whole sample).

72°C is probably due to the free water being driven off since the reaction started at slightly higher than the ambient temperature (22°C), and since the sample was air-dried. At slightly higher than 100°C, the interlayer (due to the smectite) and zeolitic water is lost. The peaks at 72°C and at slightly higher than 100°C also indicate the existence of calcium montmorillonite. Between 200°C and 300°C, the OH-H coordination water accounts for the 238°C peak. The endothermic peak at 436°C is caused by the loss of hydroxyl water. A flat endothermic peak at 700°C may be attributed to the smectite. Since the main interest here is the low temperature thermal property, to determine whether drying between 100°C and 110°C has any effect on the zeolitic water, the DTA curve terminates at 700°C. From Figure 3-3, it seems that drying between 100°C and 110°C does not loose much of the zeolite water and the crystal structure can more or less be preserved. This is important since the ASTM standards assume that the free water is driven off between 105°C and 115°C, which may or may not be true for a particular clay.

Scanning electron micrograph. Figure 3-4 is a micrograph of an air-dry sample of a Florigel H-Y clay slurry at 0.5% weight concentration. The micrograph shows the entanglement of the needle-shape particles. The structure resembles a fibrous mesh, and may represent a gel

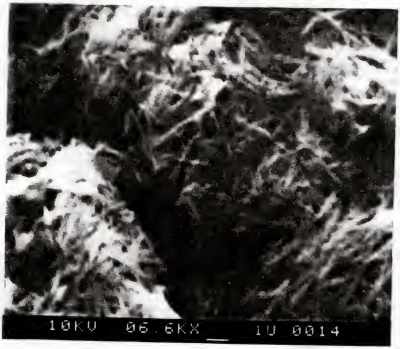

Figure 3-4. Scanning electron micrograph of Florigel H-Y clay slurry (prepared by mixing 30 g clay with 600 mL distilled water and mixed at high speed--18000 rpm for 10 min).

structure, since the slurry forms gel at this concentration.

Physico-chemical properties

The physico-chemical properties of the Florigel H-Y clay are summarized in Table 3-1. The following sections discussed the results.

Table 3-1. Summary of physico-chemical properties of the Florigel H-Y clay.

Properties	Measured values
Grain size	≈ 50% < 2 microns
Liquid limit	324
Plastic limit	124
Plasticity index	200
Activity	4.0
Total surface area	550 - 600 m^2/g
Cation exchange capacity	35 cmol(+)/kg at pH 7

Grain size distribution. The grain size distribution curve in Figure 3-5 shows that about 50% of the clay is of the clay size fraction (< 2 microns). The fine sand fraction consists only a small portion, about 6%. The remaining 45% distributes in a very narrow silt size range.

The accuracy of that portion of the grain size distribution curve obtained by the hydrometer test is uncertain. As pointed out by Bouyoucos (1936), the hydrometer method may not be very successful for materials which will form gel. This is because the gel causes the

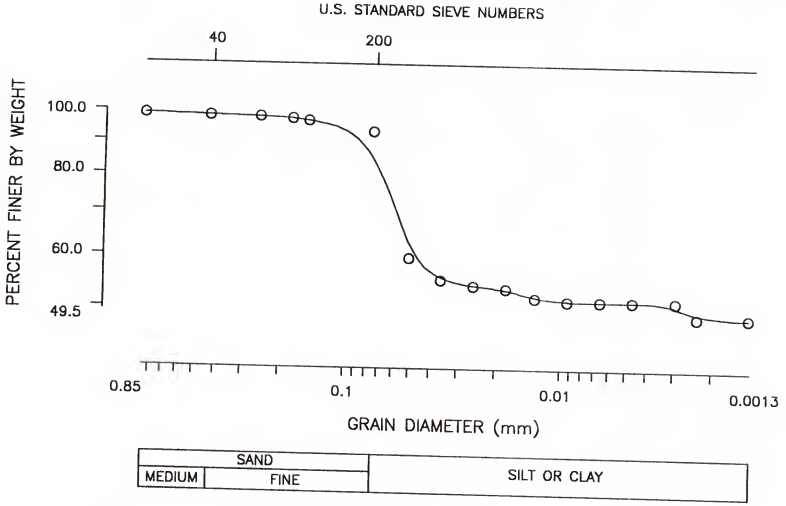

Figure 3-5. Grain size distribution curve of Florigel H-Y clay.

hydrometer to stick and not to float freely as it does in a true suspension. The Florigel H-Y clay suspension for the hydrometer test had a concentration of 20 g/L. It was observed that gelation might have occurred after 8 h of elapsed time, i.e., a constant hydrometer reading after the 8th h. Nevertheless, the primary objective of this test, to obtain an estimated percent clay fraction, was achieved. It can be concluded that about 50% of the Florigel H-Y clay has a clay size fraction.

Atterberg limits. The liquid limit (LL) and plastic limit (PL) of the Florigel H-Y clay are 324 and 124, respectively. Subsequently, the plasticity index (PI), which is the difference between LL and PL, is 200. According to Grim (1962), typical LL values for attapulgite and montmorillonite fall in the range of 160 to 230 and 100 to 700, respectively. Typical PL values for attapulgite range from 100 to 125. It can be seen that the PL of Florigel H-Y is at the high end of the typical attapulgite PL range but the LL falls in the montmorillonite LL range.

From the Atterberg limits (PI = 200) and the hydrometer analysis (50% < 2 microns), the activity of the Florigel H-Y clay is 4.0 which is an active clay based on Skempton's (1953) classification. Mitchell (1976) gives a range of activity values of 0.5 to 1.2 (inactive to normal) for attapulgite and 1 to 7 (normal to active) for smectites. Again, the activity value of the Florigel H-Y

is out of the range for attapulgite but is within the range for smectites.

Total surface area. The total surface area includes the external and internal surface area. The external surface area is the geometric area. The internal surface area is the area between the crystalline layers (of platy clay minerals) or is the area in the intracrystalline channels (of needle-shape clay minerals). The total surface area of the Florigel H-Y was determined to be 524 m^2/g. This value was obtained using an air-dry sample, which included some hygroscopic moisture. Taking into account this moisture, the surface area is between 550 and 600 m^2/g. No reported surface area has been found for palygorskite/attapulgite using the EGME method. This high total surface area might be partly attributed to the smectite content, which has a calculated total surface area of about 800 m^2/g.

By using the Brunauer, Emmett, and Teller (BET) Nitrogen method, the external surface of Florida attapulgite has been found to range from 50 to 136 m^2/g (Van Olphen and Fripiat 1979). Haden and Schwint (1967) reported a 210 m^2/g surface area for commercial colloidal grade attapulgite by the BET method.

Cation exchange capacity. The cation exchange capacity (CEC) at pH 7 of the minus #200 sieve fraction was found to be 35 cmol(+)/kg. Grim (1968) gives the range of

CEC values for palygorskite/attapulgite as 3 to 15 cmol(+)/kg at pH 7. He points out that higher CEC values reported in the past for attapulgite are probably due to montmorillonite contamination. This explanation may well be applied to the Florigel H-Y too.

An attempt has been made to determine the pH dependent CEC of the Florigel H-Y clay. The clay was washed with 1 molar sodium acetate solution buffered at pH 4.00, to remove the carbonates (since the clay effervesced with hydrochloric acid). After a month of washing, there was no more calcium remained in the supernatant of the clay suspension as indicated by the atomic absorption spectrophotometry (AAS). However, magnesium was unexpectedly detected. Readings from the AAS are presented in Appendix B. Since the chemical composition of the ideal palygorskite unit cell, $(OH_2)_4(OH)_2Mg_5Si_8O_{20}\cdot 4H_2O$, shows the existence of magnesium, it is possible that dissolution of clay has occurred. Consequently, the pH dependent CEC test was discontinued.

Polymer

The Super Mud polymer was obtained from the Polymer Drilling Systems Company (PDSCo), Arkansas. The material safety data sheet provided by PDSCo describes Super Mud as an anionic polyacrylamide in water-in-oil emulsion, belonging to the anionic polyacrylamide copolymer chemical family, and having a mixed molecular formula.

According to PDSCo (1989), Super Mud mixes easily in fresh and salt water. The pH of the slurry makeup water should be maintained at 8 or higher. Soda ash is recommended to raise the pH of makeup water if its pH is lower than 8. The use of Super Mud has no environmental concern because it is biodegradable. When dumped on site, it evaporates and provides food for microorganisms and will be gone in 72 h. Quicker disposal can be achieved if mixed with chloride bleach, such as Chlorox, and the resulting fluid discharged within 24 h.

Sands

The sands used in the settling column test (discussed in Chapter 5) were procured form the Feldspar Corporation. A coarse and a fine sand were tested. The coarse sand is the Edgar industrial 8/30 grade sand and the fine sand is the Edgar glass sand. Figure 3-6 shows the grain size distribution curves of the coarse and fine sands. Based on the Unified Soil Classification System (USCS), the 8/30 grade sand falls within the coarse and medium sand size range and the glass sand falls exactly within the fine sand size range. Both are uniform clean quartz sand.

Equipment

The following sections describe the equipment and testing methods used to measure and control the rheological and physico-chemical properties of drilling slurries, details of which can be obtained from API (1985).

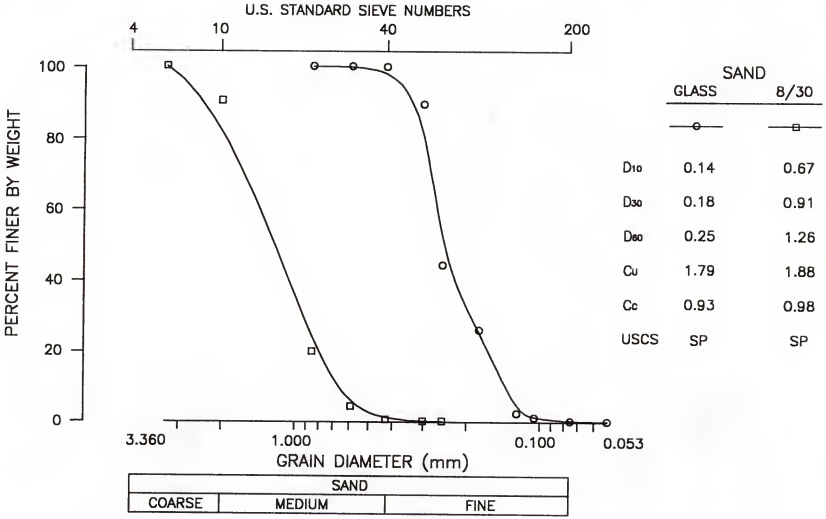

Figure 3-6. Grain size distribution curves of coarse and fine sands.

Mud Density

A mud balance is a beam balance utilizing a constant volume cup fitted with a vented cap as shown in Figure 3-7. After filling with slurry, the cap is put on the filled mud cup and rotated until slurry is expelled through the vent to free any trapped air. Excess slurry must be carefully wiped off. The beam is then placed on a base support and balanced by moving the rider along the graduated scale. A level bubble is mounted on the beam to allow for accurate balancing. Calibration is done with fresh water which gives a reading of 1000 kg/m^3 at 21°C.

Marsh Funnel Viscometer

Routine field tests of slurry viscosity are normally made on the Marsh funnel, illustrated in Figure 3-8. The funnel is of standard dimensions. A wire screen covers half of the top of the funnel. The capacity of the funnel to the bottom of the screen is 1500 cm^3. Testing consists of covering the end of the funnel with a finger, pouring slurry through the mesh to the bottom of the screen, and then removing the finger and measuring the time required to fill a volume of 946 cm^3 (1 U.S. quart) in a cup. The time to the nearest second is the Marsh funnel viscosity. When calibrated with water at 21±3°C, the time of outflow of 946 cm^3 is 26±0.5 s.

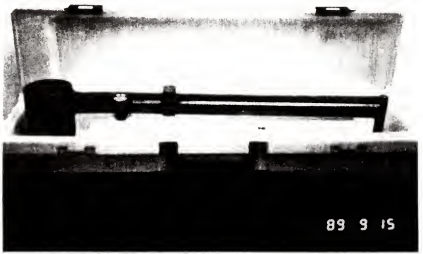

Figure 3-7. Mud balance.

Figure 3-8. Marsh funnel and cup.

Fann V-G Concentric Cylinder Viscometer

The Fann V-G viscometer used is the Model 35A concentric cylinder viscometer. It is a rotational viscometer powered by an electric motor as shown in Figure 3-9. Figure 3-10 is a schematic diagram of the viscometer. Slurry is placed in the viscometer cup and positioned so that the slurry is brought to the scribed line on the outer cylinder, the rotor sleeve. The slurry is then contained within the annular space between two cylinders, the outer cylinder and the inner cylinder, or bob. The rotor sleeve can be rotated at 6 different speeds, 600, 300, 200, 100, 6, and 3 rpm. Rotation of the sleeve produces a torque on the bob which is restrained by a torsion spring. A dial is attached to the bob to indicate its displacement against the spring restraint.

Instrument constants have been adjusted so that plastic viscosity is obtained by using dial readings from rotor sleeve speeds of 300 and 600 rpm. Measurements in the field should be made with minimum delay, within 5 min if possible. With the rotor sleeve rotating at 600 rpm, the steady torque reading corresponding to 600 rpm is recorded. The speed of the rotor sleeve is then reduced to 300 rpm and a corresponding steady dial reading is obtained. The time required to achieve a steady dial reading depends on the slurry characteristics. The difference between the two dial readings is the plastic

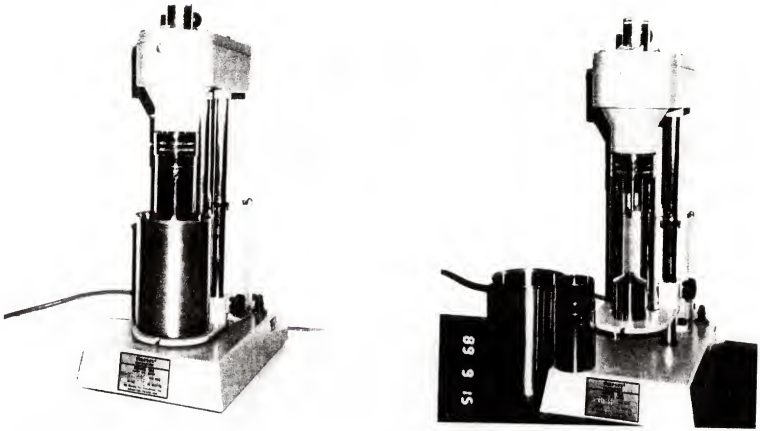

Figure 3-9. Fann V-G viscometer.

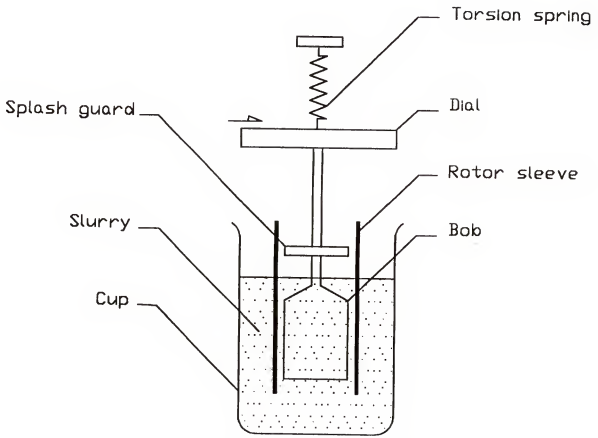

Figure 3-10. Schematic diagram of the Fann V-G viscometer.

viscosity in mPa.s. In addition, with the instrument constants, the effective viscosity and yield point can be calculated from the dial readings. The definitions of effective viscosity, plastic viscosity, and yield point are delineated in Figure 3-11. Appendix C gives the data reduction calculations for the Fann V-G flow measurements.

Gel strength is a measurement of force required to rupture the gel, i.e., it is the maximum dial deflection before the gel breaks. Two gel strength readings, the 10-s and 10-min, can be obtained using the Fann V-G viscometer. Measurement of the 10-s gel strength (also known as initial gel strength) is made by rotating the slurry at 600 rpm for 10 s, allowing it to stand undisturbed for another 10 s, and then recording the maximum dial reading while rotating at 3 rpm. The measurement of 10-m gel strength is similar to that of the 10-s gel strength, except the standing time is 10 min instead of 10 s.

pH Meter and Electrode System

Figure 3-12 shows the pH meter and electrode system used for measuring the pH of slurries. The electrometric method is preferred over using color matching pH paper because the color of the slurry may cause serious errors in pH values. The pH meter has a digital readout with a resolution and accuracy of 0.01 and 0.02 pH unit, respectively. The meter also has an internal temperature compensation feature. The electrode system is a

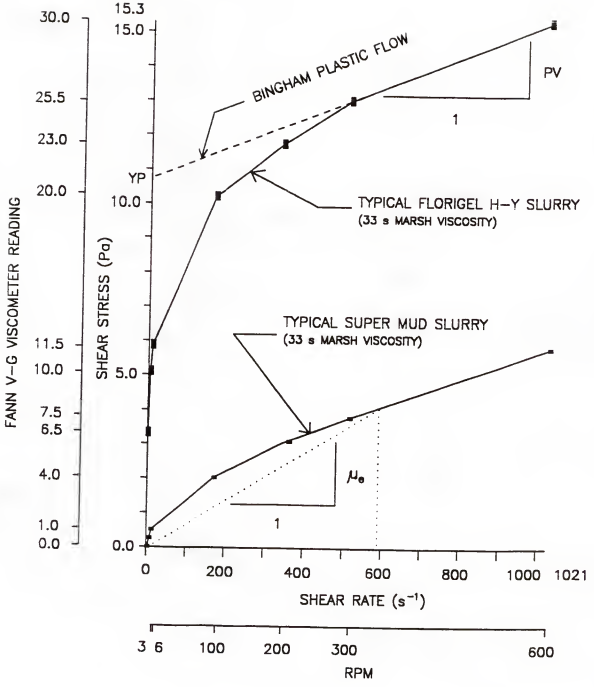

μ_e = EFFECTIVE VISCOSITY

PV = PLASTIC VISCOSITY

YP = YIELD POINT

Figure 3-11. Typical slurry flow curves and definitions of effective viscosity, plastic viscosity, and yield point.

Figure 3-12. pH meter and electrode system.

combination type, i.e., a glass electrode for sensing hydrogen ions and a standard voltage reference electrode are constructed as a single electrode. Buffer solutions of pH 4.0, 7.0, and 10.0 were used to standardize and set the slope of the pH meter prior to sample measurement.

Sand Content Kit

The sand content kit is a sand-screen set as illustrated in Figure 3-13. A funnel is used to connect a #200 sieve to a glass measuring tube. The tube is graduated from 0 to 20% for direct reading of sand content by volume. The measuring tube has marks for both slurry and water, so that fixed quantity of either slurry or water can be added into the tube during testing.

The glass tube is filled with slurry to the "mud" mark and water is added to the "water" mark to dilute the slurry. The mouth of the tube is closed and the slurry is agitated vigorously. The slurry is then poured through the screen, and the diluting and pouring repeated until the tube is clean. The sand retained on the screen is washed free of any remaining mud. The funnel is then fitted upside down over the top of the screen. This assembly is then inverted and the funnel tip inserted into the glass tube. Sand is washed into the tube by a fine water spraying through the screen. The sand is allowed to settle before reading the volume percent of sand.

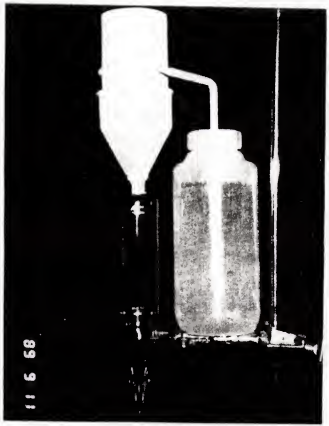

Figure 3-13. Sand content kit.

CHAPTER 4
RHEOLOGICAL PROPERTIES OF SLURRY

Introduction

This chapter presents the rheological study of the Florigel H-Y clay and Super Mud polymer slurries. The clay slurry was investigated more thorough than the polymer slurry due to the complicated nature of the clay slurry. The effect of slurry concentration, slurry preparation, and pH on the rheological properties were investigated. Factors involved in the slurry preparation, i.e., soaking time, mixing speed and time, and stress history, were studied. The effect of pH was studied using hydrochloric acid, tannic acid, sodium hydroxide, and calcium hydroxide. The results of the rheological properties were presented in terms of effective and plastic viscosity, yield point, and gel strength. Finally, comments on the current slurry specifications were made based on the results obtained.

Effect of Slurry Concentration

Methodology

Florigel H-Y clay slurry. At the onset of this experimental study, experimentation was carried out to determine the relationship between the clay concentration

and the density of the slurry. The objective is twofold: to facilitate the control of the slurry properties in this research; and to establish a relationship that can be used as a guide in the field to achieve a specific density.

The weighed clay powder was mixed with tap water using a Hamilton Beach 3-speed mixer. The weight ratio of the dry (as shipped) clay powder to water was predetermined. The range of the ratio was chosen so that it gave a reasonable limit in reference to the slurry specifications of the Florida Department of Transportation (1988 & 1987). The mixing was achieved by both a high and low speed to check whether the speed of mixing would affect the density of slurry. The measurement of the density did not show a difference with different speeds.

Once the relationship between concentration in weight of dry clay to weight of water ratio and density is determined, the concentration can be expressed in terms of weight of dry clay per volume of slurry. In other words, concentration expressed in weight to volume ratio is more practical than that expressed in weight to weight ratio, which is more convenient for laboratory experiments.

Based on some preliminary viscosity tests using the Marsh funnel, the range of clay concentration is limited to the range from 20 to 68 kg/m^3 for investigating the rheological properties, because a high clay concentration gave a high Marsh viscosity which is too thick to be used

in the drilled shaft construction. The weighed clay samples were soaked with tap water for 30 min and then mixed at a high speed (18000 rpm) for 10 min. The rationale for the chosen mixing speed and time will be discussed in the following sections. Both Marsh funnel and Fann viscometer were used to measure the viscosity and gel strength.

Super Mud polymer slurry. The density of the Super Mud polymer slurry was found to be the same as that of water at a viscosity as high as 50 s Marsh viscosity. Note that the density of the liquid Super Mud polymer was measured to be 1020 kg/m^3. Since the polymer came in the form of a liquid, the concentration was expressed in terms of volume of polymer per volume of slurry. To find out the relationship between the concentration and the rheological properties, a range of concentration of 1 to 4 $x10^{-3}$ m^3/m^3 was used. This range of concentration gave an approximate range of Marsh viscosity between 26 to 40 s.

A small quantity of the Super Mud polymer was carefully added to the tap water and later mixed at high speed for 1 min. Experience has shown that mixing time and speed does not affect the rheological properties of the slurry as long as the polymer is fully dissolved in the water.

Results and Discussion

Florigel H-Y clay slurry. The data points of density versus concentration were plotted in Figure 4-1. A linear regression line runs through the points and gives a good fit, with a coefficient of determination, R^2, of 0.9998. The linear experimental result can be used as a guide to prepare a slurry for a specific density. For example, if the minimum density of 1030 kg/m^3 is necessary for supporting the drilled shaft hole, the slurry concentration of about 60 kg dry clay per m^3 slurry (58 kg dry clay per m^3 slurry to be exact) will ensure that the shaft will be supported by slurry of adequate density.

Figure 4-2 is a plot of effective viscosity versus shear rate obtained from the Fann V-G viscometer. Due to the non-Newtonian nature of the slurry, its viscosity varies with shear rate. The highest shear rate occurs at the jets in the bit during drilling and the lowest shear rate in the slurry filled shaft waiting for concreting. The Marsh viscosity for various concentrations is also given in Figure 4-2. Logarithmic scales were used for both the X and Y axes. The effective viscosity increases as the shear rate decreases, which is normal because as the shear rate is low the slurry behaves more viscous. It is obvious that the viscosity increases as the clay concentration of the slurry increases, because higher solid content creates more friction among clay particles and hence more

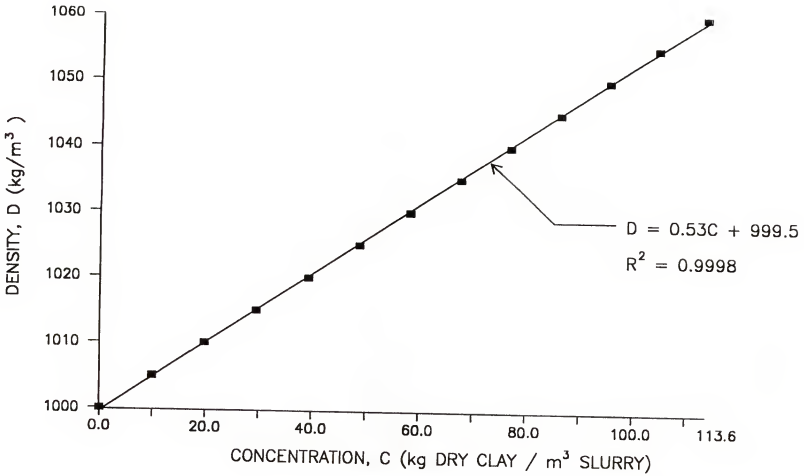

Figure 4-1. Correlation of density and concentration of Florigel H-Y clay slurry.

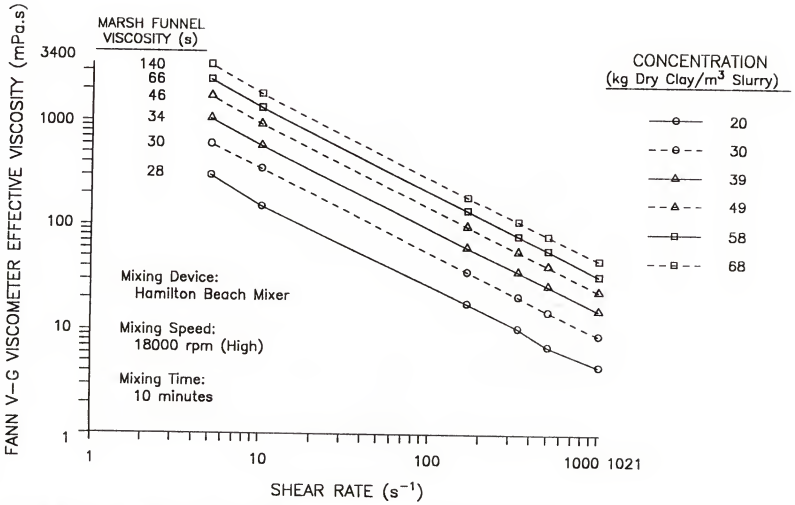

Figure 4-2. Effect of concentration on effective viscosity at various shear rates of Florigel H-Y clay slurry.

resistance to flow. It is shown in Figure 4-3 that the rate of increase in viscosity increases with concentration, especially when the concentration increases above 58 kg/m^3.

The plot of Marsh funnel viscosity versus Fann plastic viscosity shown in Figure 4-3 indicates that the Marsh funnel viscosity increases with increasing Fann plastic viscosity. However, the two viscosities cannot be directly correlated (Chilingarian and Vorabutr 1981); the reasons being measurements obtained from the Marsh funnel are influenced considerably by the rate and degree of gelation and by the density of slurry which varies the hydrostatic head of the column of slurry in the funnel, also, the gel strength of slurry increases with time and the head of slurry decreases with time during the test.

Figure 4-4 shows the plastic viscosity, yield point, and gel strengths obtained from the Fann V-G viscometer versus the clay concentration of the slurry. Consistently, the plastic viscosity, yield point, and the gel strengths all increase as the concentration increases. This is reasonable because as the clay particles in a fixed volume of a continuous phase increases, the slurry becomes more viscous. The yield point increases because it requires more stress to cause the thicker slurry to flow, and the gel strength becomes stronger due to more gel bonds formed and requires stronger force to break the bonds.

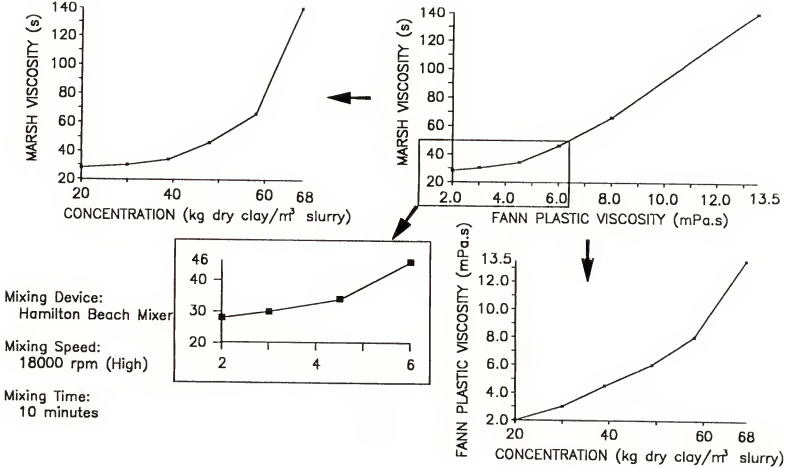

Figure 4-3. Relationships among Marsh funnel viscosity, Fann plastic viscosity, and concentration of Florigel H-Y clay slurry.

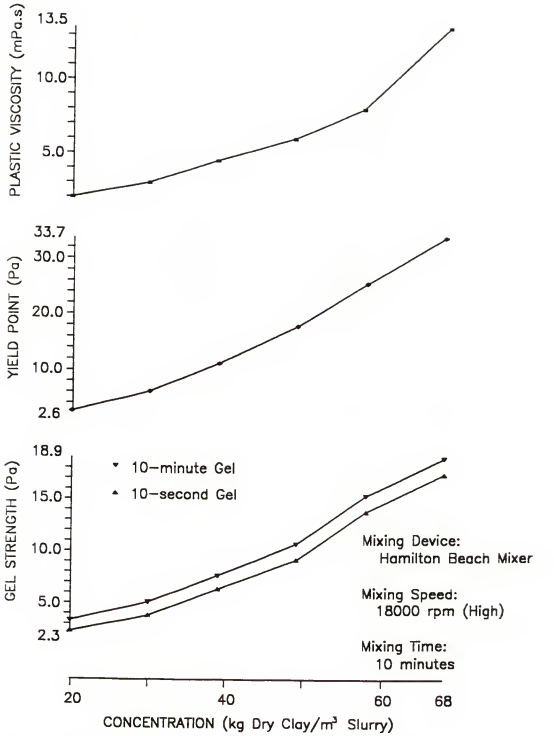

Figure 4-4. Effect of concentration on plastic viscosity, yield point, and gel strengths of Florigel H-Y clay slurry.

Super Mud polymer slurry. The effect of concentration is shown in Figure 4-5. A similar trend as that of the Florigel H-Y is observed, i.e., as the concentration of the polymer slurry increases, the slurry becomes more viscous. At low shear rates, the curves of the slurry of the three lowest concentrations appear to behave differently from those of the clay slurry. This is due to two factors, the low polymer slurry viscosity and the precision of the instrument. On a logarithmic scale plot, the same numerical difference that is not obvious in the high value range (say from 100 to 1000) can be discerned in the low value range (say from 10 to 100). The dial reading of the Fann viscometer can only be estimated to the nearest 0.5 division, which after multiplying by the instrument factor causes the curves to behave in an uncommon manner.

An interesting point that is worth noting is that at the lowest shear rate, 5.11 s^{-1} (refer to Figure 4-2), a clay slurry of 34 s Marsh funnel viscosity corresponds to about a 1000 mPa.s Fann effective viscosity, while a polymer slurry of 40 s Marsh funnel viscosity corresponds to only a 100 mPa.s Fann effective viscosity. However, at the highest shear rate, 1021 s^{-1}, the effective viscosity of the two slurries differs only by about 6 mPa.s. This shows that at low shear rate, the clay slurry behaves much more viscous than the polymer slurry. While as the shear

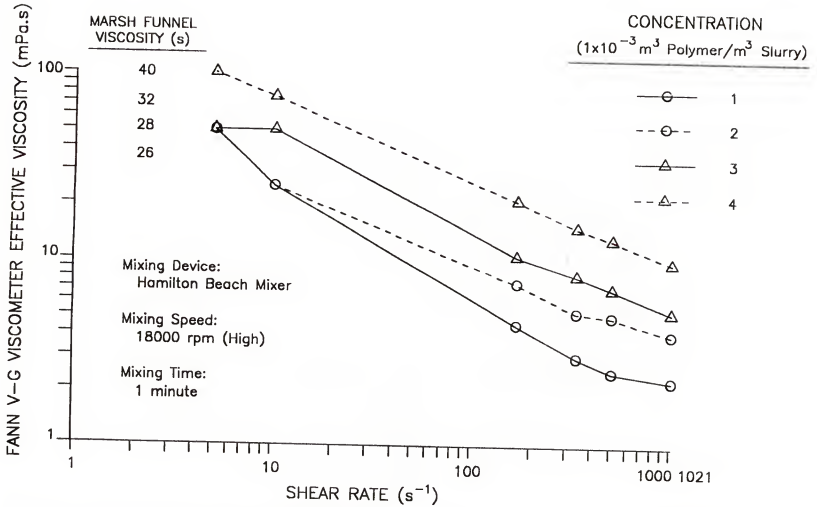

Figure 4-5. Effect of concentration on effective viscosity at various shear rates of Super Mud polymer slurry.

rate increases, the difference in viscosity of the two slurry types decreases.

Figure 4-6 is similar to Figure 4-4; a plot of plastic viscosity, yield point, and gel strength versus polymer slurry concentration. By comparing the yield points, the yield point of a 34 s Marsh funnel viscosity clay slurry is about three times that of a 40 s Marsh funnel viscosity polymer slurry. The 10-m gel strength of the polymer slurry is so low (less than 1 Pa) that the 10-s gel strength is not measurable (i.e., zero gel strength) over the range of Marsh funnel viscosity of 26 to 40 s. On the other hand, the 10-s and 10-m gel strength of the 34 s Marsh funnel viscosity clay slurry are 6.4 and 7.7 Pa, respectively.

The correlation between the Fann plastic viscosity and the Marsh viscosity of the polymer slurry can be seen from Figure 4-7. Again, this curve is plotted only to show the trend, no attempt has been made to obtain a mathematical correlation between the Fann plastic viscosity and the Marsh funnel viscosity.

Effect of Slurry Preparation

Slurry preparation significantly affects the rheological properties of the Florigel H-Y clay slurry. This is not so for the Super Mud polymer slurry, because the polymer is shipped in the liquid form and the slurry is formed by dissolving liquid into liquid. Therefore, as

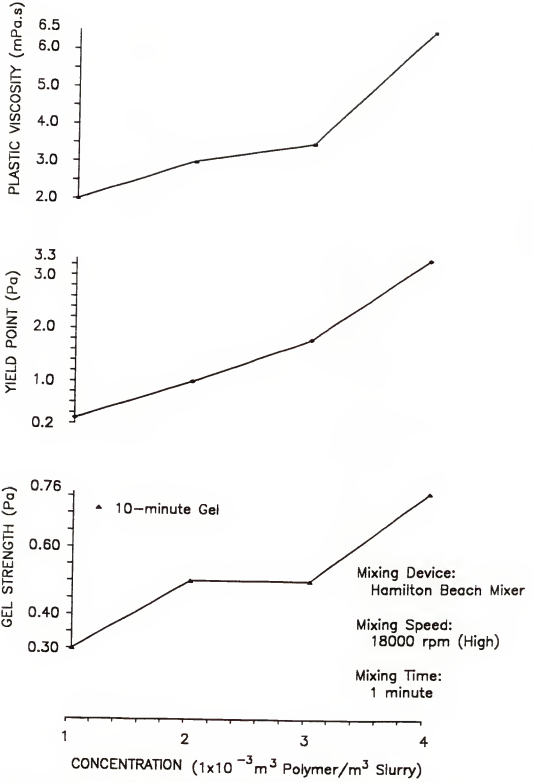

Figure 4-6. Effect of concentration on plastic viscosity, yield point, and gel strength of Super Mud polymer slurry.

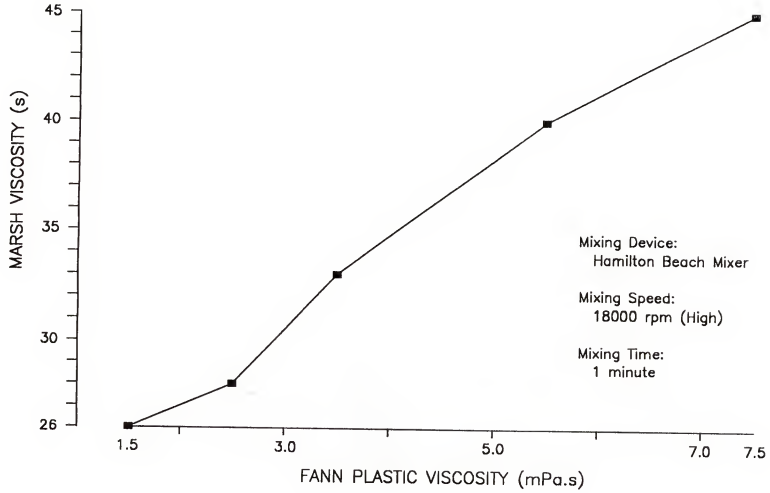

Figure 4-7. Correlation between Marsh funnel viscosity and Fann plastic viscosity of Super Mud polymer slurry.

long as the polymer is fully dissolved and no lump formed, the slurry will perform normally. The Florigel H-Y clay has to be dispersed properly to form a good slurry. The viscosity of the slurry will be low if the clay particles are not dispersed properly by mixing. Because of the complicated clay-water system, efforts were concentrated on the factors that were involved in the preparation of the Florigel H-Y clay slurry.

Methodology

Soaking time. In the field, the mud gun, circulation pit, or other means may be adopted for forming and mixing the slurry before it is used for the drilled shaft construction. The clay powder may or may not be soaked. In the laboratory, it is interesting to find out whether the rheological properties will be improved by soaking the Florigel H-Y clay water mixture in advance, since it is well known that the bentonite clay slurry needs to be presoaked to obtain an optimum performance.

Two samples of clay concentration of 49 kg/m^3 were used for the test. One sample was soaked for 30 min and the other was soaked for 23 h before mixing in the Hamilton Beach mixer for 10 min at high speed. The Fann V-G viscometer was employed to measure the viscosity and gel strength.

Mixing Speed. The Hamilton Beach Mixer used in the laboratory experiment has three speeds, low (13000 rpm),

medium (16000), and high (18000). To find out whether the mixing speed has any effect on the rheological properties, a clay concentration of 39 kg/m^3 was used. Three samples, all soaked for 30 min before mixing in the mixer for 10 min using the high, medium, and low speed. The Fann V-G viscometer was then used to measure the viscosity and gel strength.

Mixing time. If high speed is the optimum mixing speed, then the question is how long should the slurry be mixed to obtain the best dispersed slurry system, which will give the desired viscosity and gel strength. An efficiently mixed slurry may require only minimal amount of clay.

Four mixing times, 2, 5, 10, and 20 min were selected for the test. The clay concentration used was 39 kg/m^3. As the mixing time increases, the temperature of the mixed slurry increases. The mixed slurry was then cooled down to room temperature by pouring back and forth to keep the slurry agitated as well as to get rid of the air bubbles resulting from mixing in the mixer at high speed. The maximum increase in temperature observed was about 12°C, caused by mixing for 20 min. Just before running the Fann V-G viscometer test, the sampled was agitated for 1 min to ensure all the samples had the same stress history before testing.

In addition to the above test, a test was performed to show the effect of stress history prior to testing using the Fann V-G viscometer. Five samples were prepared at a clay concentration of 39 kg/m^3, four of them were left standing for different periods before running the viscometer test, and the last one was agitated vigorously for 1 min just before running the test.

Results and Discussion

Figure 4-8 depicts the results of the soaking test. It shows that by soaking the Florigel H-Y clay would not help much in improving the rheological properties of the slurry. This information is important and practical in that soaking is not necessary and hence time may be saved in slurry preparation.

The results of the mixing speeds are shown in Figures 4-9 and 4-10. It shows that mixing at medium and high speed gives about the same effective viscosity. Similarly, Figure 4-10 shows that the plastic viscosity and the yield point do not increase beyond the medium speed. It seems that the viscosity and the yield point approach a plateau after reaching a certain speed. Or it may be said that beyond a certain mixing speed, the mixer is not efficient in breaking the particles down to a smaller size and the dispersion approaches the maximum. Figure 4-10 also shows that the gel strengths increase slightly with increasing mixing speed.

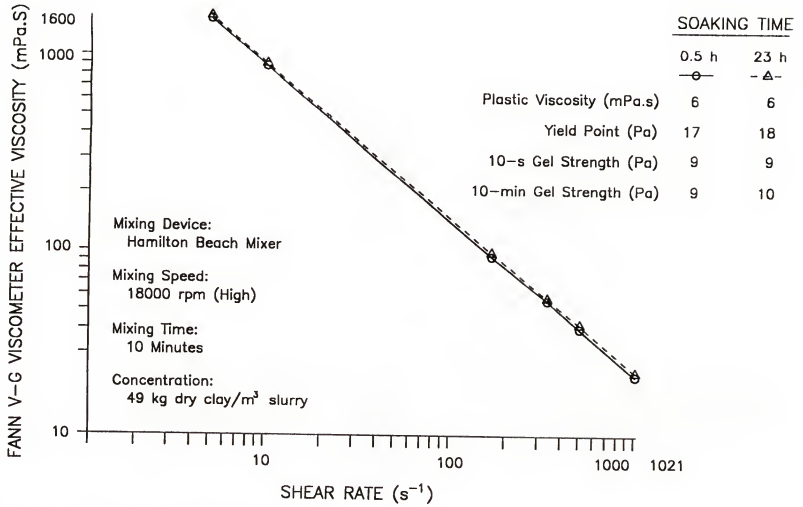

Figure 4-8. Effect of soaking time on effective viscosity at various shear rates, plastic viscosity, yield point, and gel strengths of Florigel H-Y clay slurry.

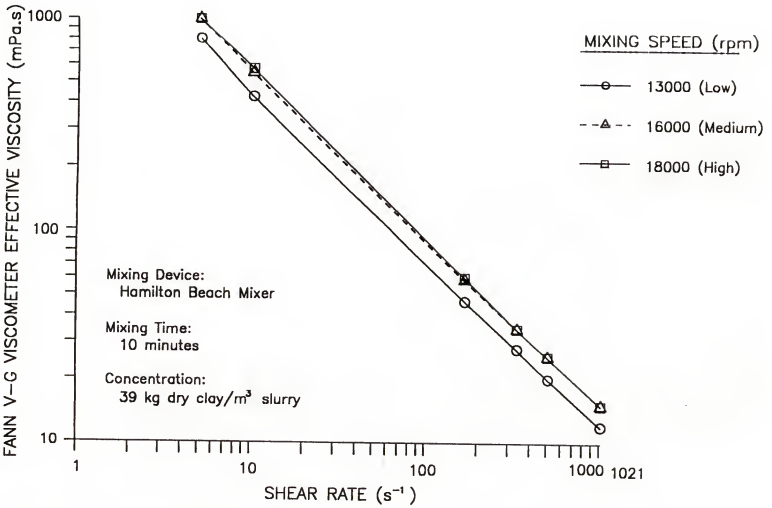

Figure 4-9. Effect of mixing speed on effective viscosity at various shear rate of Florigel H-Y clay slurry.

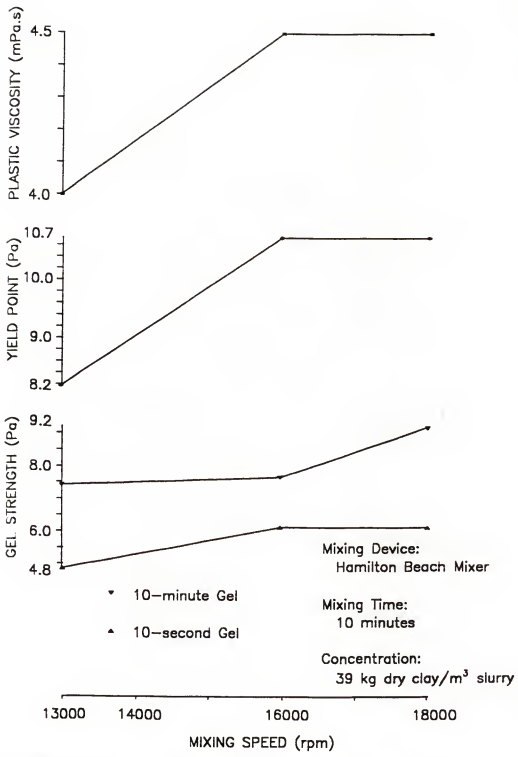

Figure 4-10. Effect of mixing speed on plastic viscosity, yield point, and gel strengths of Florigel H-Y clay slurry.

Figures 4-11 and 4-12 show the results of the mixing time tests. As the mixing time approaches 10 min, a further increase in mixing time to 20 min only increases the viscosity by an insignificant amount. The explanation may be similar to that of mixing speed where a certain amount of time is required to disperse the clay particles at a specific speed. When the dispersion has reached the maximum for a specific speed, a further increase in mixing time will not help much in increasing the viscosity. In Figure 4-12, the yield point increases slightly for mixing time longer than 5 min, whereas the gel strengths show no increase when mixing for longer than 5 min.

As mentioned before, the cooled down samples were agitated for 1 min before running the viscosity test. The effect of stress history prior to testing is shown in Figure 4-13. There is a difference in viscosity between agitated sample and non-agitated samples. Those samples that had been left standing, even for only 5 min, were affected by the gel forming property of the slurry. In other words, the thixotropic effect had occurred and influenced the viscosity measurement.

From the results of the above tests, a procedure was established for preparing slurry for the pH tests. The slurry concentration was based on the desired viscosity to be achieved. A high mixing speed was adopted for both the clay and polymer slurry. The mixing time used for the clay

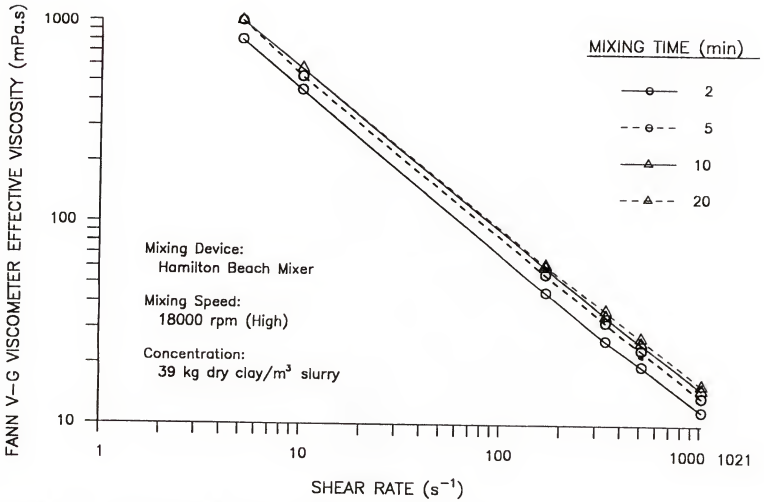

Figure 4-11. Effect of mixing time on effective viscosity at various shear rates of Florigel H-Y clay slurry.

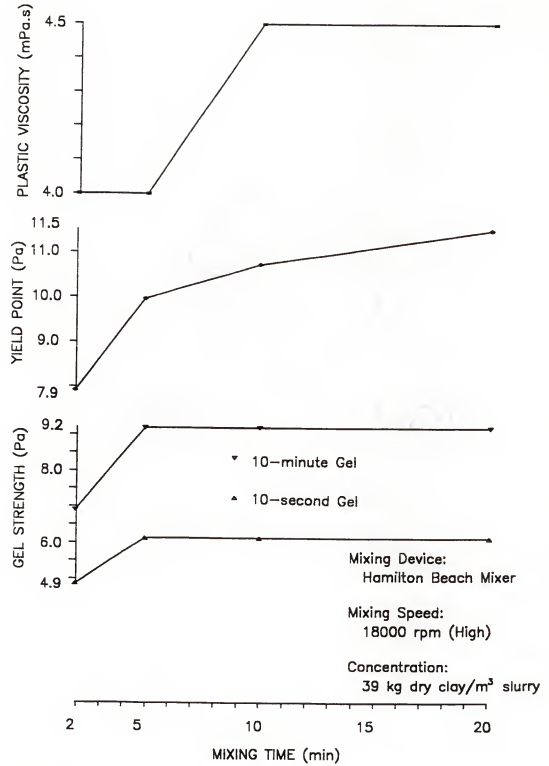

Figure 4-12. Effect of mixing time on plastic viscosity, yield point, and gel strengths of Florigel H-Y clay slurry.

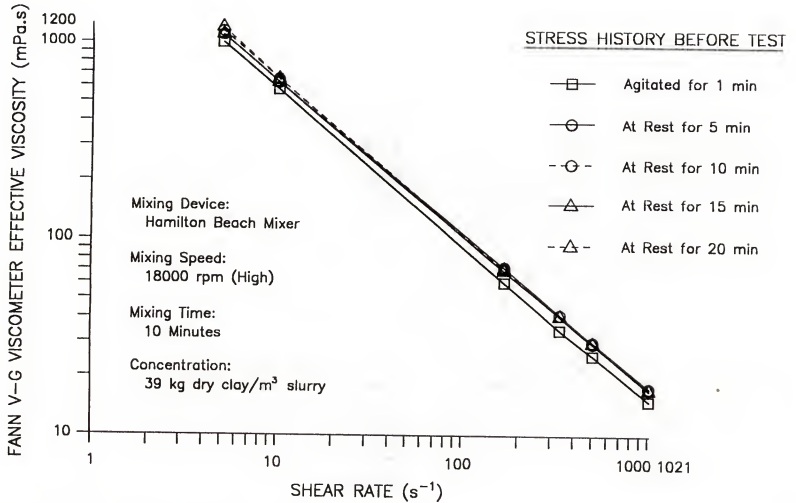

Figure 4-13. Effect of stress history on effective viscosity at various shear rates of Florigel H-Y clay slurry.

slurry was 10 min, but 1 min was adequate for the polymer slurry. For the clay slurry, the dry clay was soaked for 30 min before being transferred to the mixer cup for mixing. After mixing for 10 min, the clay slurry was cooled to near room temperature and agitated for about 1 min just before running the viscosity test.

Effect of pH

Methodology

Floricel H-Y clay slurry

Two types of acids and two types of bases were used to lower and raise the pH of the slurry. An inorganic acid, hydrochloric acid (HCl), and an organic acid, tannic acid ($C_{76}H_{52}O_{46}$), were used. The bases used were sodium hydroxide (NaOH) and calcium hydroxide ($Ca(OH)_2$). Hydrochloric acid and sodium hydroxide are common inorganic acid and base, respectively. Tannic acid is a natural organic acid commonly found in Florida waters and has been reported by drillers to have an effect of viscosity reduction on the drilling slurry. Calcium hydroxide, which is commonly referred by the drilling industry as builder's lime, is an inexpensive chemical additive used to raise the pH of the slurry when its pH is lowered by ground water during drilling operations.

Both distilled and tap water were used to prepare the slurry, although in a field environment, a fire hydrant is

most likely to be the source of water. The use of distilled water had no practical significance, its use was only to compare what impact distilled and tap water had on the slurry rheological properties. Six sets of tests were performed. The combinations of acids, bases and types of water were as follows:

1) Hydrochloric acid with distilled water,
2) Sodium hydroxide with distilled water,
3) Hydrochloric acid with tap water,
4) Sodium hydroxide with tap water,
5) Tannic acid with tap water, and
6) Calcium hydroxide (builder's lime) with tap water.

A clay concentration of 49 kg/m^3 was chosen for this study. The slurry makeup water was prepared by adding the acid or base to distilled or tap water. The pH of tap water varied between 8.4 and 8.6 and that of distilled water was from 5.5 to 5.8. A water test was conducted by the Extension Soil Testing Laboratory at the University of Florida for both the tap and distilled water. The results of the water test are given in Appendix D. The range of slurry pH examined was from 5.5 to about 12. Since the pH of the clay slurry prepared with tap water ranges from 9.0 to 9.3, and with distilled water alone ranges between 9.5 and 9.6, acids and bases were used to obtain slurry of pH below 9 and above 10, respectively. The Hamilton Beach mixer was used as a mixing device to prepare slurries.

Slurry preparation of combinations 1 to 4 above followed the same procedure. Five different amounts, 0.1, 0.2, 0.3, 0.4, and 0.5% (by volume) of the slurry makeup water, of 1 normal hydrochloric acid or sodium hydroxide solution were used to prepare five different slurry samples. Each of the five samples was prepared by slowly adding the clay powder to the makeup water (distilled or tap water added with a fixed amount of acid or base solution) while mixing at low speed. The sample was then mixed at high speed for 10 min. The pH of the slurry sample was measured and checked the next day to ensure a stabilized pH had been achieved.

For combination 4 (tannic acid with tap water), a tannic acid solution was prepared by dissolving 0.01 formula weight of the light yellow tannic acid powder in a liter of distilled water. Note that this concentration was obtained through trial and error because of the low solubility of the tannic acid powder in water. The tannic acid solution was then added with eight different quantities, 1.67, 3.33, 5.00, 6.67, 8.33, 13.33, 18.33, 25.00% (by volume) of the slurry makeup water, to tap water. Eight slurry samples were mixed and prepared the same as for combinations 1 to 4.

The preparation of slurry with various pH values using calcium hydroxide was different from the above where solutions of acid or base were prepared and used. In this

case, it was impossible to prepare calcium hydroxide solutions with different desired pH values under an open system due to the existence of carbon dioxide in the atmosphere. When carbon dioxide dissolved in the calcium hydroxide solution, carbonic acid formed and its carbonate ions formed complexes with calcium ions and precipitated as calcium carbonate. The pH of the solution kept decreasing until equilibrium was reached. Consequently, powder form calcium hydroxide was added to the powder clay before mixing.

The amount of calcium hydroxide added was 1, 2, 3, 4, and 5% of the weight of the clay powder. The powder mixtures were mixed well before pouring slowly into the mixer cup, which contained a fixed amount of tap water, and was mixed at a low speed. The slurry was then mixed at a high speed for 10 min.

Super Mud polymer slurry

According to the manufacturer of the Super Mud polymer, the pH of the makeup water of the Super Mud slurry should be above 8. The pH of the polymer itself was about 7. The range of slurry pH tested was from 3.0 to 9.2. The viscosity of the polymer slurry was measured using the Marsh funnel.

The first part was to observe the effect that pH had on the slurry viscosity at various concentrations. The range of concentration was chosen so that the Marsh funnel

viscosity ranged from 26 to 40 s. The slurry was prepared by using tap water alone, tap water with tannic acid, and tap water with soda ash. The range of pH of the makeup water ranged from 6 to 10 and the resulted slurry pH ranged from 6.4 to 9.2.

The second part was to investigate the viscosity of the slurry at very acidic conditions (pH of 3 to 6), as well as the effectiveness of soda ash (Na_2CO_3) to raise the pH of the acidic slurry. Hydrochloric acid and tannic acid were used in this investigation to lower the slurry pH to below 6. The soda ash was then added to raise the pH of the slurry to 9. The Marsh funnel viscosities of the slurry before and after added soda ash was compared.

Results and Discussion

Florigel H-Y slurry

Slurry with distilled water. Figure 4-14 shows the change of effective viscosity with pH at various shear rates for slurries with hydrochloric acid. The range of slurry pH obtained is from 8.5 to 5.7. In general, the effective viscosity decreases with decreasing pH. This may be caused by the dissolution of clay and carbonates, thus diluting the solid concentration. Between pH of 7.9 to 7.3, the slurry seems to have no change in viscosity. At the lowest shear rate (5.1 s^{-1}), the effective viscosity reduces from 1100 mPa.s to 650 mPa.s, which is reduced by

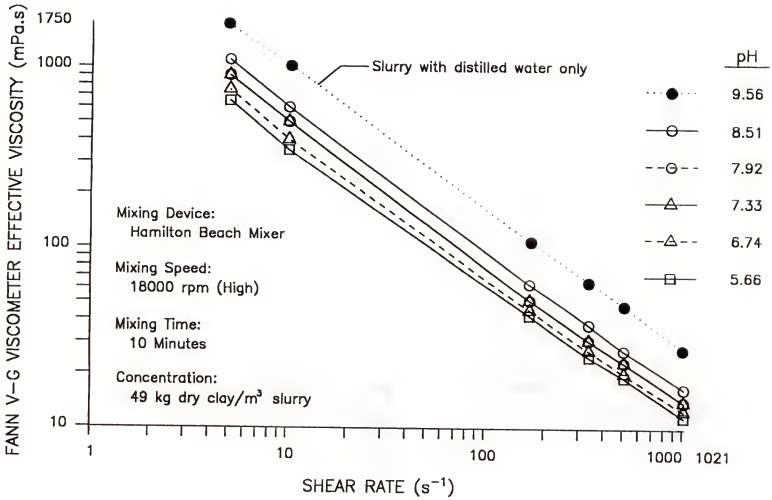

Figure 4-14. Variation of effective viscosity at various shear rates with pH of Florigel H-Y clay slurry made of hydrochloric acid and distilled water.

about one-half, over the pH range from 8.5 to 5.7, whereas at the highest shear rate (1021 s^{-1}), the reduction is only from 16.5 to 11.5 mPa.s.

Figure 4-15 shows the change of effective viscosity with pH at various shear rates for slurries with sodium hydroxide. As the pH increases from 10.6 to 11.2 the effective viscosity drops dramatically, from 1200 to 50 mPa.s at the lowest shear rate, and from 11.5 to 4.3 mPa.s at the highest shear rate. Above pH 11.2, the effective viscosity increases. Note that the curve indicated as "Slurry with distilled water only" is the same as the one shown in Figure 4-14, because it is the result of the same test.

The change of plastic viscosity with pH is shown in Figure 4-16. Figure 4-16 is a combination of the results of plastic viscosity obtained from slurries with hydrochloric acid and sodium hydroxide. The pH shown thus ranges from 5.7 to 11.9. Figures 4-14 through 4-16 all indicate that the highest viscosity occurs when the slurry was prepared with distilled water only. Also, the effective viscosity and the plastic viscosity show similar trend over the pH range.

Figure 4-17 shows the change of yield point with pH and Figure 4-18 shows the change of gel strengths with pH. Again, the results show that for slurry with distilled water only, a stronger gel was formed. The lowest yield

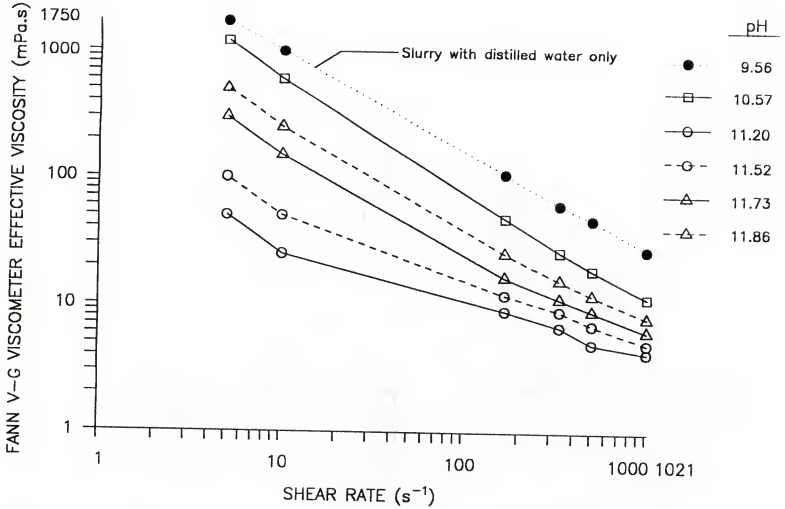

Figure 4-15. Variation of effective viscosity at various shear rates with pH of Florigel H-Y clay slurry made of sodium hydroxide and distilled water.

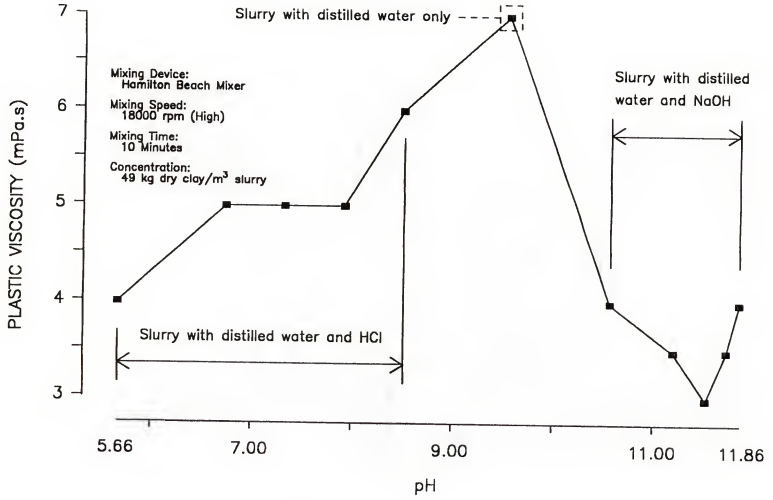

Figure 4-16. Variation of plastic viscosity with pH of Florigel H-Y clay slurry made of distilled water with hydrochloric acid and sodium hydroxide.

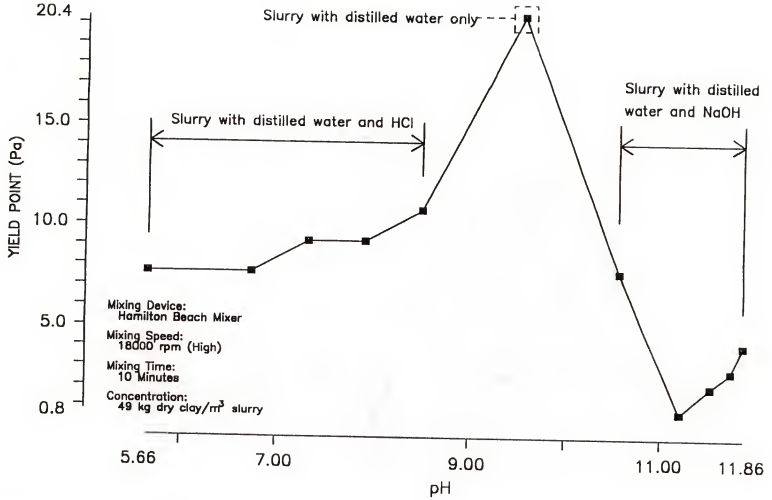

Figure 4-17. Variation of yield point with pH of Florigel H-Y clay slurry made of distilled water with hydrochloric acid and sodium hydroxide.

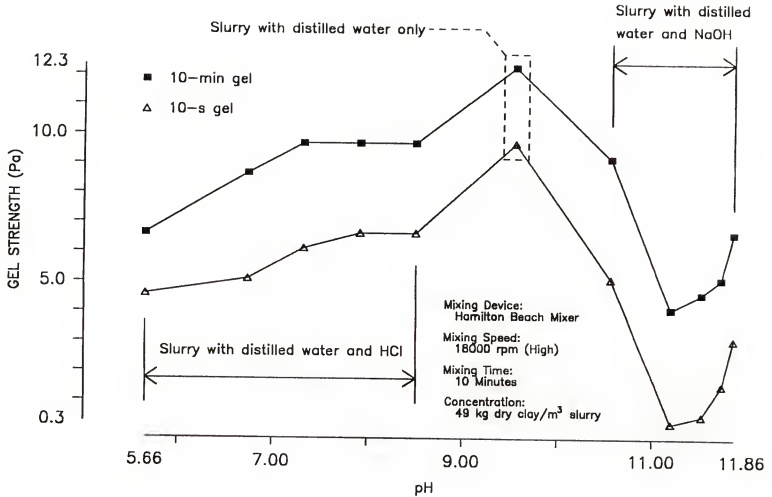

Figure 4-18. Variation of gel strengths with pH of Florigel H-Y clay slurry made of distilled water with hydrochloric acid and sodium hydroxide.

point and the lowest gel strengths occur at pH of 11.2, which is the same as that of the effective viscosity shown in Figure 4-16. On the average, the rate of gel strength increase is about 3.5 Pa, over the pH range of 5.7 to 11.9, from 10 s to 10 min.

Slurry with tap water. Figure 4-19 delineates the change of effective viscosity with pH at different shear rates for slurries with hydrochloric acid. The effective viscosity is about the same from pH 7.4 to 5.5. Although effective viscosity decreases with decreasing pH, the decrease is small over the tested pH range (from 8.2 to 5.5). At the highest shear rate, the reduction of effective viscosity is from 12.5 to 10.0 mPa.s, and at the lowest shear rate the reduction is from 750 to 500 mPa.s.

The change of effective viscosity with pH at different shear rates of slurries with sodium hydroxide is shown in Figure 4-20. Similar to slurry prepared with sodium hydroxide and distilled water (Figure 4-15), an enormous reduction of effective viscosity takes place when the pH is raised from 10.2 to 11.1 (from 2300 to 150 mPa.s for the lowest shear rate, and from 23.5 to 5 mPa.s for the highest shear rate). Above pH 11.6 viscosity increases gradually.

Figure 4-21 presents the results of change of effective viscosity with pH at different shear rates for slurries with tannic acid. The range of pH analyzed was

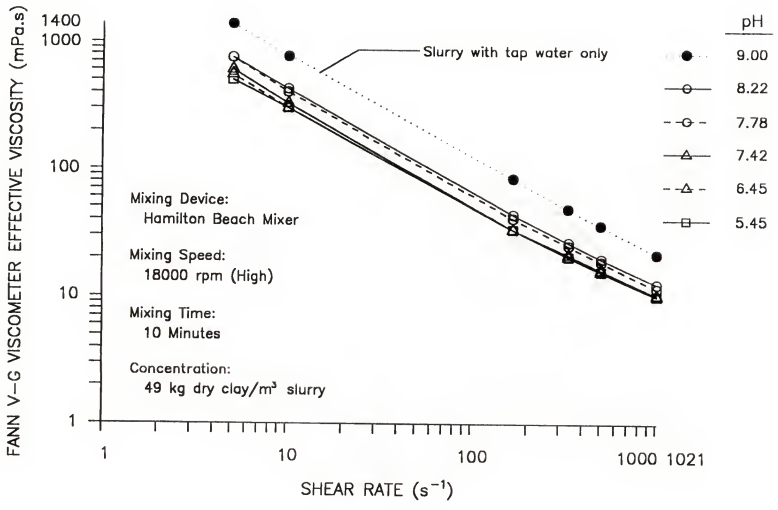

Figure 4-19. Variation of effective viscosity at various shear rates with pH of Florigel H-Y clay slurry made of hydrochloric acid and tap water.

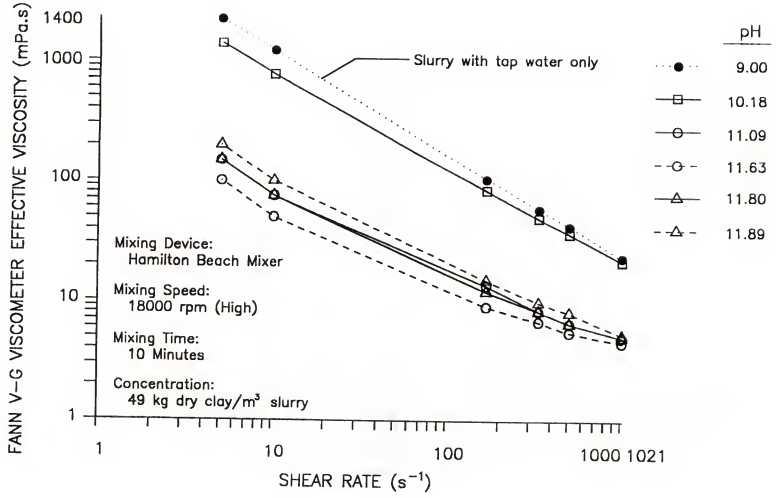

Figure 4-20. Variation of effective viscosity at various shear rates with pH of Florigel H-Y clay slurry made of sodium hydroxide and tap water.

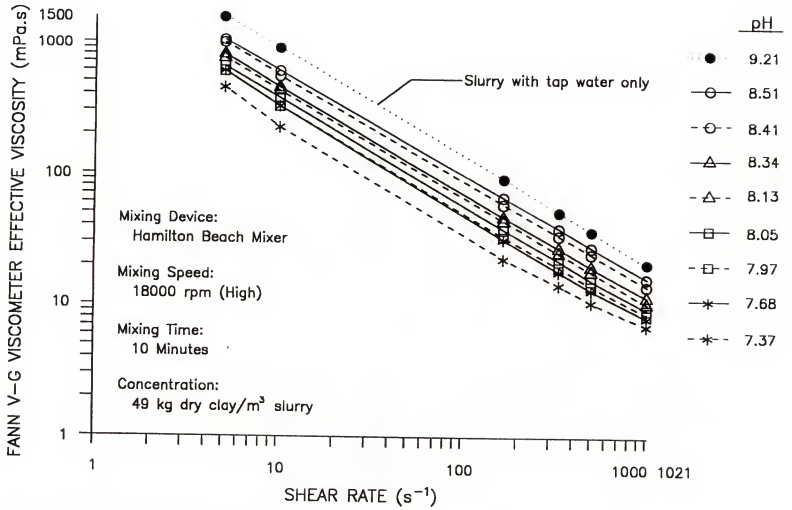

Figure 4-21. Variation of effective viscosity at various shear rates with pH of Florigel H-Y clay slurry made of tannic acid and tap water.

from 8.5 to 7.4. Within about a 1 unit change of pH (from 8.5 to 7.4), the effective viscosity decreases from 1050 to 450 mPa.s at the lowest shear rate, and from 16 to 7 mPa.s at the highest shear rate.

Figure 4-22 shows the change of effective viscosity with pH at different shear rates for slurries with calcium hydroxide. The range of pH achieved for this test is from 10.2 to 11.7. The slurry samples were observed to be different from the above samples as these samples show flocculation. Due to the flocculated structure it was not easy on occasions to obtain stable readings from the viscometer. The whole set of tests had to be repeated. The effective viscosity reduces from 1275 to 300 mPa.s at the lowest shear rate and from 22 to 13 mPa.s at the highest shear rate. The effective viscosity in general decreases with increasing pH, except at the higher shear rate, the slurry of pH 11.1 shows a higher viscosity than that of pH 10.2.

The change of plastic viscosity with pH for slurries with hydrochloric acid, sodium hydroxide, tannic acid, and calcium hydroxide is shown in Figure 4-23. Note that the overall change of plastic viscosity with pH is only 5 mPa.s, i.e., from 2.5 to 7.5 mPa.s, and 1 mPa.s is equivalent to 1 division of the viscometer dial reading. This magnitude is small as compare to the change of effective viscosity as mentioned above. Since the primary

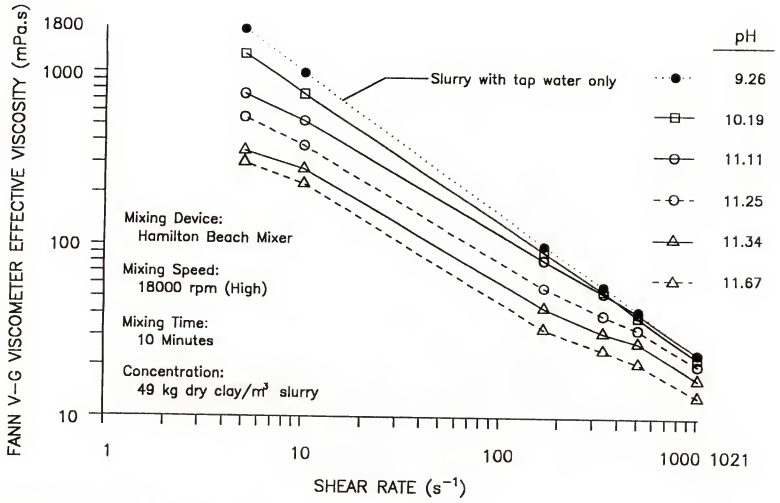

Figure 4-22. Variation of effective viscosity at various shear rates with pH of Florigel H-Y clay slurry made of calcium hydroxide and tap water.

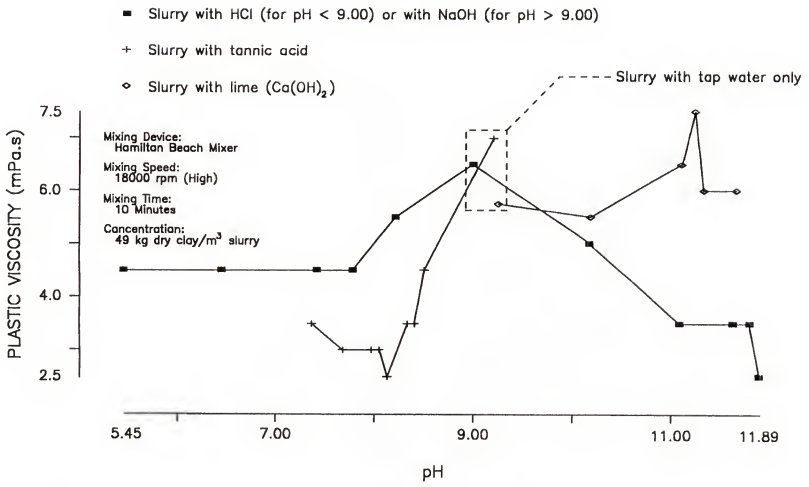

Figure 4-23. Variation of plastic viscosity with pH of Florigel H-Y clay slurry made of tap water with hydrochloric acid, tannic acid, sodium hydroxide, and calcium hydroxide.

cause of plastic viscosity is the mechanical friction between solid particles and between solid particles and the liquid surrounding them, chemical treatment which mainly affect the interparticle attractive and repulsive forces has little influence on the viscosity.

The change of yield point with pH for slurries with hydrochloric acid, sodium hydroxide, tannic acid, and calcium hydroxide is shown in Figure 4-24. In general, the variation of yield point shows similar trend as that of the effective viscosity. For slurry with sodium hydroxide, the yield point at pH 10.2 is greater than that of slurry with tap water only (pH 9.0). This does not agree with the trend of the effective viscosity and plastic viscosity shown in Figures 4-20 and 4-23, respectively. However, the result is not unreasonable since yield point is caused mainly by the interparticle forces. Although the effective viscosity is also influenced by the interparticle forces, the extend of influence is less than that of the yield point.

The change of gel strengths with pH for slurries with hydrochloric acid, sodium hydroxide, tannic acid, and calcium hydroxide is shown in Figure 4-25. Note that the trend of the variation of gel strengths of slurry with sodium hydroxide is the same as that of the yield point. Since gel strength is controlled by the interparticle forces, the similar trend in yield point and gel strength

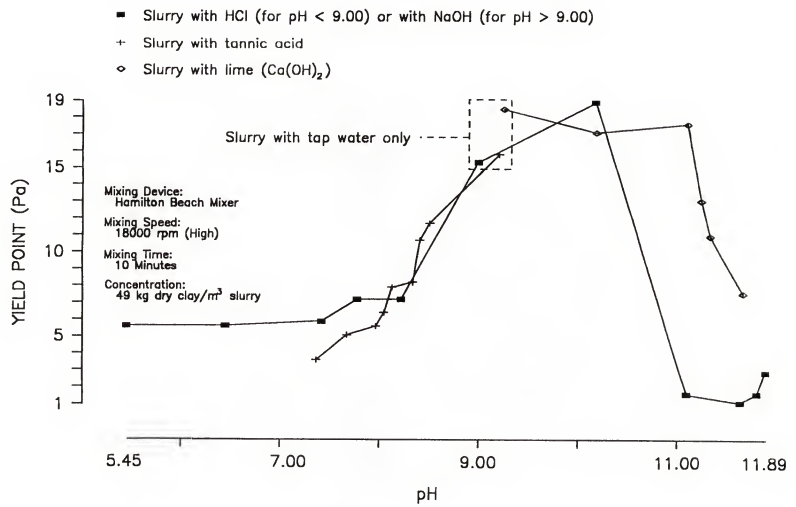

Figure 4-24. Variation of yield point with pH of Florigel H-Y clay slurry made of tap water with hydrochloric acid, tannic acid, sodium hydroxide, and calcium hydroxide.

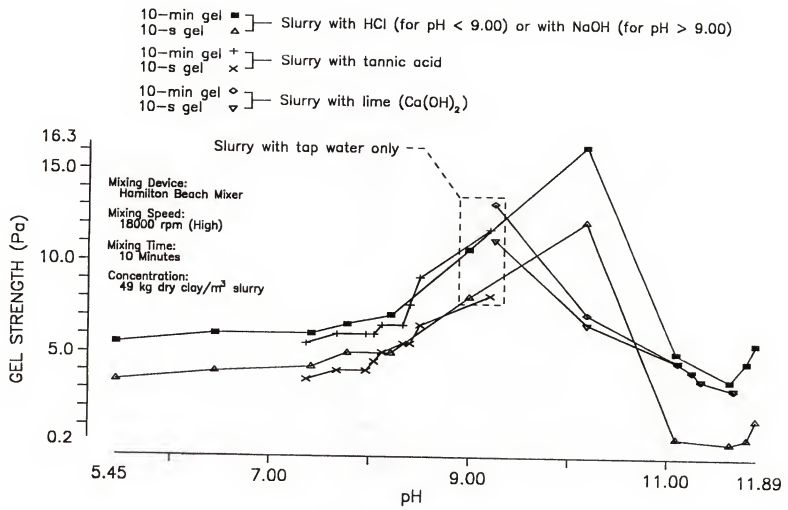

Figure 4-25. Variation of gel strengths with pH of Florigel H-Y clay slurry made of tap water with hydrochloric acid, tannic acid, sodium hydroxide, and calcium hydroxide.

substantiate the explanation that the high yield point at pH 10.2 is caused by interparticle forces. The rate of gel strength increase is about 2 Pa from 10-s to 10-min for slurries with hydrochloric acid and tannic. The rate of gel strength increase is 4 Pa from 10-s to 10-min for slurry with sodium hydroxide. However, for slurry with calcium hydroxide, the 10-min and 10-s gel strength are about the same. This suggests that the gel strength reaches its maximum as early as 10 s after it comes to rest.

Tap and distilled water slurries with HCl. In general, tap and distilled water both give decreasing viscosity, yield point and gel strengths as the pH of slurry decreases. The addition of hydrochloric acid created salt in the slurry system. This is because Florigel H-Y clay contains carbonates which when reacted with HCl, liberates CO_2 and forms chloride salts. Increase of salt concentration in the clay-water system suppresses the double layer. Counter-ions of both the edge and face surfaces shift toward the surfaces and decrease the effective attracting charges on these surfaces. Compression of the double layer may be in favor of the interparticle repulsive force. A slight unbalance of interparticle repulsive and attractive force would be significant enough that the card-house structure, i.e., edge to edge (EE) and edge to face (EF) particle

association, breaks down and results in lower viscosity, yield point, and gel strengths.

Tap and distilled water slurries with NaOH. Both tap and distilled water slurries show rapid reduction in viscosity, yield point and gel strengths. At higher pH, there is a greater tendency for H^+ from the clay particles to go into solution, and hence a greater effective negative charge of the particle. In addition to this, the alumina, which is amphoteric and ionizes negatively at high pH causes an edge charge reversal which then leads to the domination of interparticle repulsion, thus promotes dispersion and reduction of viscosity. Only a small amount of sodium hydroxide is needed for deflocculation because of the small edge surface. Beyond the minimum point (or point of reversal), further increase of sodium hydroxide only increases the viscosity slightly.

Slurries with HCl and tannic acid. Figures 4-19 and 4-21 show that at the same pH, the slurry prepared with tannic acid gives a viscosity lower than that of hydrochloric acid. For example, at pH of about 8, the effective viscosity of slurry with tannic acid ranges from 9 to 650 mPa.s, and with hydrochloric acid ranges from 12 to 750 mPa.s for shear rate between 5.1 and 1021 s^{-1}. Also, slurry of tannic acid at pH 7.4 shows about the same effective viscosity as slurry of hydrochloric acid at pH of 5.5. Also, as shown in Figure 4-23, the plastic viscosity

of slurry with tannic acid is lower than that of slurry with hydrochloric acid. The reduction of gel strengths (from 6.6 to 3.6 Pa for 10-s gel and from 9.2 to 5.6 Pa for 10-min gel) of slurry with tannic acid when the slurry pH drops from 8.5 to 7.4, is almost double that of slurry of hydrochloric acid (from 5.1 to 3.6 Pa for 10-s gel and from 7.2 to 5.6 Pa for 10-min gel) when the pH range drops from 8.2 to 5.5.

According to Van Olphen (1977), experiments have shown that organic anions of tannic acid adsorbed at the edge surfaces of the clay particles by complexing with the exposed octahedral aluminum ions. Consequently, the edge charge is reversed and a negative double layer is created by which EF and EE association is prevented. This may explain why tannic acid is more effective in reducing the slurry viscosity, yield point, and gel strength than HCl.

Slurries with NaOH and $Ca(OH)_2$. Figures 4-20, 4-22, 4-23, 4-24, and 4-25 indicate that Na^+ and Ca^{2+} render different rheological properties. Lime causes no sudden decrease in viscosity, yield point and gel strengths but forms flocs. Although high pH reverses the positive edge charge to negative, the divalent cation compresses the double layer. The double effects, high pH and Ca^{2+}, result in a structure that is flocculated but with flocs not extended throughout the available volume, i.e., not complete gelation. As pH increases, the gel becomes more

incomplete and hence gives lower viscosity, yield point and gel strengths. The gel strength in Figure 4-25 shows only prominent initial gel strength but no increase in gel strength after longer rest time; this may be attributed to the unique structure formed.

Super Mud polymer slurry

Figure 4-26 shows that by varying the pH between 6.4 and 9.2, there is an insignificant effect on the viscosity for the range of slurry concentration used. When only the tap water was used as the makeup water, the Marsh funnel viscosity was slightly lower than when the makeup water was either tap water with tannic acid or soda ash.

Figures 4-27 and 4-28 show the effect of Marsh funnel viscosity when the slurry pH had been lowered below 6. The results do show a significant drop in Marsh funnel viscosity. The triangular data points in the Figures depict the addition of soda ash to attempt to recover the viscosity. The slurry that was added with tannic acid did show slight recovery on the viscosity, but not that with hydrochloric acid. Thus it is important not to allow the pH of the polymer slurry in the drilled shaft to drop below 6 since this will "kill" the viscosity permanently.

Comments on Current Slurry Specifications

1. The test results indicate that a 40 - 50 s Marsh funnel viscosity Florigel H-Y clay slurry gives a 5 - 6.5 mPa.s Fann plastic viscosity and a 40 - 45 s Marsh

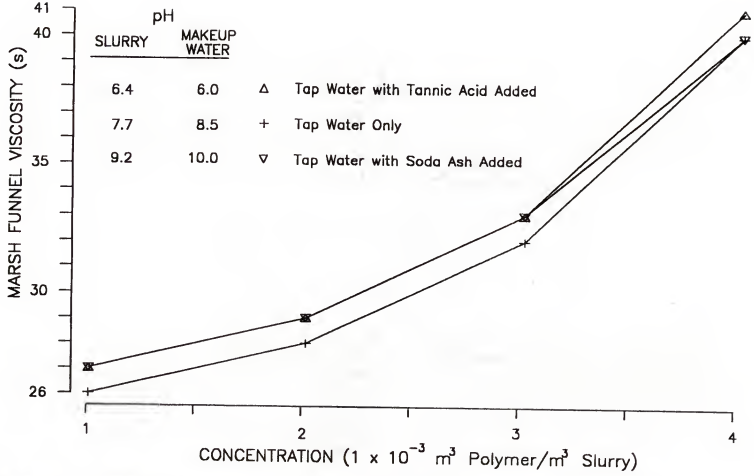

Figure 4-26. Effect of pH on Marsh funnel viscosity of Super Mud polymer slurry at various concentrations.

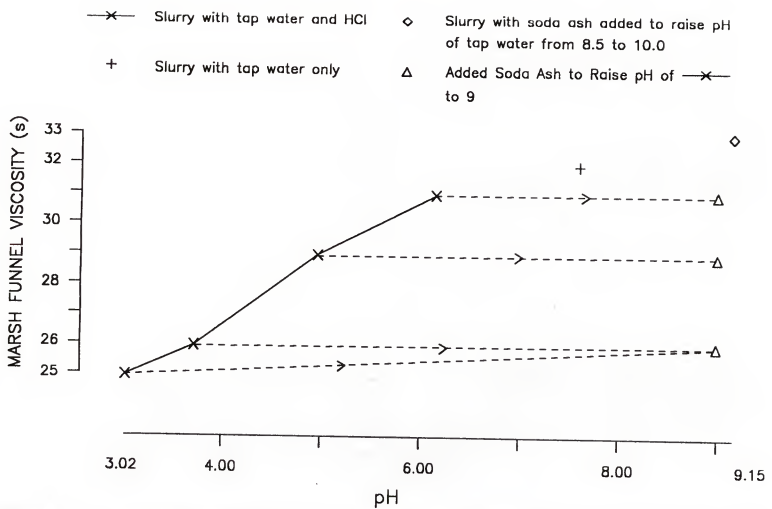

Figure 4-27. Effect of hydrochloric acid on Marsh funnel viscosity of Super Mud polymer slurry.

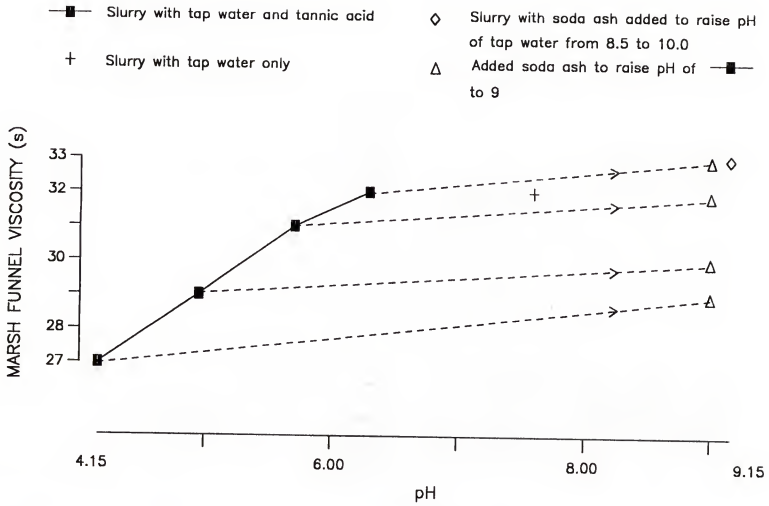

Figure 4-28. Effect of tannic acid on Marsh funnel viscosity of Super Mud polymer slurry.

funnel viscosity Super Mud polymer slurry gives a 5.5 to 7.5 mPa.s Fann plastic viscosity. Therefore, slurry specifications which require the viscosity of a fresh slurry to be either less than 40 s (or 50 s) Marsh funnel viscosity or less than 20 mPa.s (20 cP) Fann plastic viscosity is not appropriate for these two slurries. The 20 cP Fann viscosity limit is too high for the corresponding 40 s (or 50 s) Marsh viscosity.

2. In general, the results suggest that specifying a pH range of 8 to 11 may be more reasonable than the 8 to 12 range currently under consideration for the proposed slurry specifications of the Florida Department of Transportation. And when tannic acid is suspected at the drilling location, it may be preferable not to allow the pH to drop below 8.5.

CHAPTER 5
SETTLING CHARACTERISTICS OF SANDS IN SLURRIES

Introduction

The study of settling characteristics of sands in slurries is presented in this chapter. Both the Florigel H-Y clay slurry and the Super Mud polymer slurry were investigated. The sands used in the settling tests were both uniformly graded coarse and fine sands (see Figure 3-6), although it was known that in field conditions, slurries may also suspend silty and clayey soils besides clean sands. The purpose of using two distinct sand sizes was to determine whether particle size was a major factor in sand settlement.

The settling characteristics of sands in slurries were studied using 18 in. (457.2 mm) sedimentation cylinders (Figure 5-1) and a 20 ft (6.096 m) settling column (Figure 5-2). The sedimentation cylinder tests were small scale settling tests used to gain qualitative information about the settling characteristics of sands in slurries. The quantitative information was obtained from the full scale settling column tests. Comparisons were made between the qualitative settling information and the quantitative

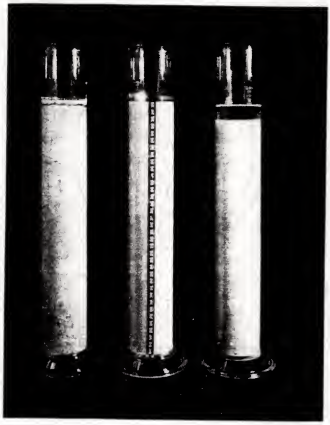

Figure 5-1. Settling of sands in Florigel H-Y clay slurry after 1 h standing time using sedimentation cylinders.

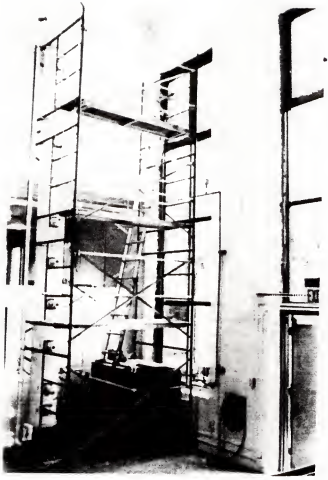

Figure 5-2. Set up of the settling column.

settling information to see if the former could be a predictor of the latter.

The settling column designed and constructed for the settling tests was described. Also the effect of sand content on Marsh funnel viscosity was investigated. Finally, comments on current slurry specifications were made based on the settling tests results.

Settling Tests with Sedimentation Cylinders

Prior to conducting the full scale settling column tests, small scale settling tests were performed using sedimentation cylinders. These are glass cylinders 2.5 in. (63.5 mm) in diameter, with a marked volume of 1000 mL.

Floriqel H-Y clay slurry. Two slurry viscosities, 27 and 38 s Marsh, two sand grain sizes, coarse and fine, and two sand contents, 4 and 14% (by volume), made up eight different slurry combinations, i.e., eight cylinders were set up for the tests. Each slurry was poured into the cylinder to about 400 mL, sand was then added, and the slurry was later filled to the 1000-mL mark. The open end of the cylinder was covered and the cylinder was turned upside down and back for a period of 3 min to ensure that the sand and slurry were well mixed. The settling test began right after the agitation. The settling characteristics of the sand were monitored for a day.

Figure 5-1 shows three of the cylinders that have the most prominent settling characteristics after 1 h of

standing time. The cylinder in the middle contained a 27 s Marsh slurry with a 4% fine sand. No sedimentation occurred. The cylinder on the right contained the same slurry viscosity (27 s Marsh) but with a 14% coarse sand. Sedimentation occurred and a layer of water appeared on the surface. The formation of the water layer is an indication of the settlement of clay particles. The third cylinder contained a 38 s Marsh slurry and a 14% coarse sand. No observable sedimentation occurred. The coarse sand particles were not suspended uniformly throughout the cylinder. Localized concentration of coarse particles were observed along the cylinders.

Another set of similar settling tests was also performed. Through monitoring the two sets of cylinders for a day, observations revealed several interesting phenomena. The high viscosity (38 s Marsh) slurry, was able to suspend the coarse and fine sands to as high as 14% by volume, with no observable sedimentation. However, the low viscosity (27 s Marsh) slurry failed to suspend coarse sand of 14% but was able to partially suspend the 4% coarse sand. The low viscosity slurry could suspend the 4% fine sand without any sedimentation but not the 14% fine sand, where sedimentation did occur.

Super Mud polymer slurry. The tests of the Super Mud polymer slurry were performed in a similar manner as that of the Florigel H-Y clay slurry. Eight cylinders were set

up with different combinations of the following: two slurry viscosities, 26 and 40 s Marsh, two sand grain sizes, coarse and fine, and two sand contents, 4 and 14% (by volume). It was observed that all sands settled to the bottom of the cylinders in less than 10 min. The polymer slurry was unable to hold even the 4% fine sand in suspension.

Effect of Sand Content on Marsh Funnel Viscosity

Since the clay slurry to be measured by the Marsh funnel in the settling column tests would contain sand particles, it was necessary to determine whether the existence of sand in the slurry sample would alter the Marsh funnel viscosity of the clean slurry. Figure 5-3 is a plot of Marsh funnel viscosity versus fine sand content in the clay slurry. Four different viscosities, ranging from 27 to 41 s Marsh were tested. The plot shows insignificant variation in viscosity as a function of sand content.

Similar tests for the coarse sand were performed. Only sand particles smaller than the screen opening, 1.6 mm, of the Marsh funnel (described in Chapter 3) could pass through the screen and be measured with the slurry. Consequently, based on the grain size distribution curve of the coarse sand as shown in Figure 3-6, about 30% of the coarse sand in the slurry was estimated to be retained by the screen. Similar results as that of the fine sand

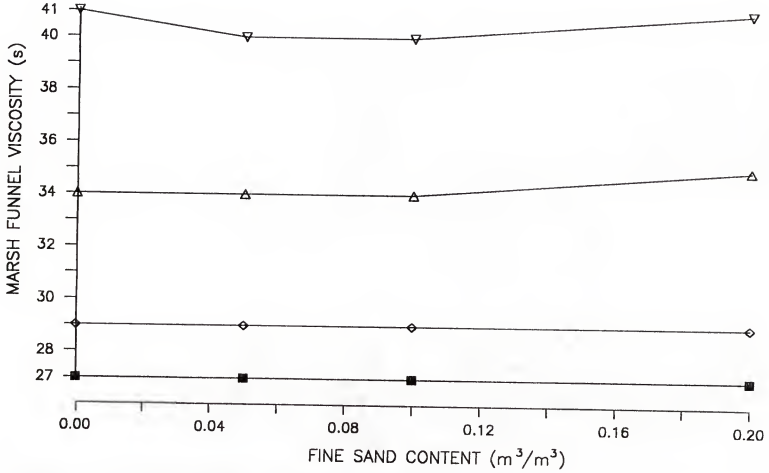

Figure 5-3. Marsh funnel viscosity versus fine sand content of the Florigel H-Y clay slurry.

(Figure 5-3) were obtained. Thus, it is unlikely that both the fine and coarse sands would affect the Marsh funnel viscosity for sand content less than 20% by volume.

Description of Settling Column

The 20 ft long column is made of a 16 in. (0.4064 m) diameter polyvinyl chloride (PVC) pipe. Ten sampling ports are mounted along the side of the column. The ports are spaced at 2 ft (0.6096 m) intervals, with the exception of the bottom two ports, which are 1 ft (0.3048 m) apart. Figure 5-4 is a schematic diagram of the column with a mixing tank, two centrifugal pumps, piping, and valves. The functions of valves 1 to 8 are indicated in Figure 5-4. Valve 9 is a discharge valve for discharging slurries with coarse sand. Valve 10 is used to facilitate priming of the pump located near the bottom of the column. A photograph of the entire setup of the settling column is shown in Figure 5-2. Scaffolding and a stairway are provided for access to slurry sampling.

The small 1 in. (25.4 mm) pump on top of the mixing tank is shown in Figure 5-5. The functions of the pump are, to premix the slurry through circulating in the tank, to pump the fresh slurry into the column, and to pump the used slurry out from the column. Also, shown in Figure 5-5, is a rectangular piping system with 4 spray heads. The piping system was designed so that the slurry could achieve a thorough mixing while circulating in the tank. Figure 5-

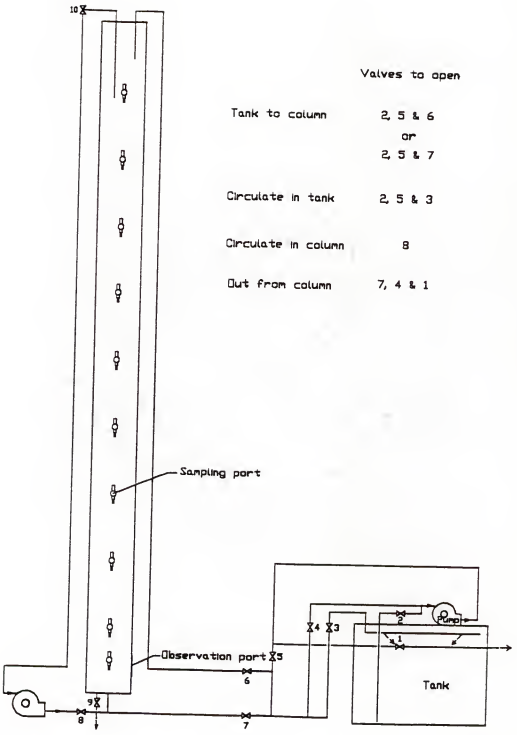

Figure 5-4. Schematic diagram of the settling column with a mixing tank, pumps, piping and valves.

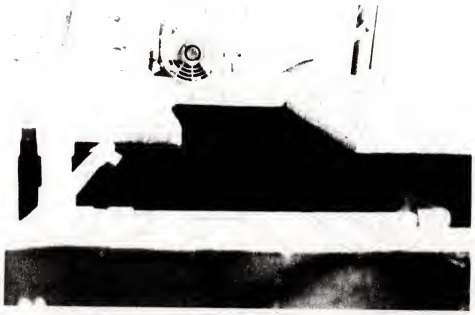

Figure 5-5. The rectangular piping system and the small pump.

6 shows a closer view of the bottom of the settling column with a slurry sampler. The 6.75 in. (171.45 mm) by 3.75 in. (95.25 mm) clear acrylic observation port is for observing any sedimentation of sand at the bottom of the column. The pump that is located beside the column, is a large 2 in. (50.8 mm) pump for circulating the slurry with and without sand in the column.

The slurry sampler is a simple yet novel device. Figure 5-7 shows an assembled sampler and the components of it. The components are easily obtained PVC pipes, a steel rod, spring, rubber stopper, rubber tube, and fittings. The rod is positioned inside and along the axis of the PVC pipe casing. A rubber stopper is connected at one end of the rod and a spring at the other end. The rubber stopper is screwed onto the rod and held in position by nuts and a washer. The spring is fitted at the other end with a locking rubber disc and nut. A short, about 1.5 in. (38 mm), PVC tube spacer is outside the spring. The rubber tube (shown in Figure 5-7) is to seal the part of the sampler that is inside the column. The sealing is achieved by using a hose clamp on one end and 'O' rings on the other end of the rubber tube. The sampler can be conveniently attached and detached from the column for maintenance and cleaning if necessary.

The sampling mechanism is illustrated in Figure 5-8. The sampler is fabricated to extend to the center of the

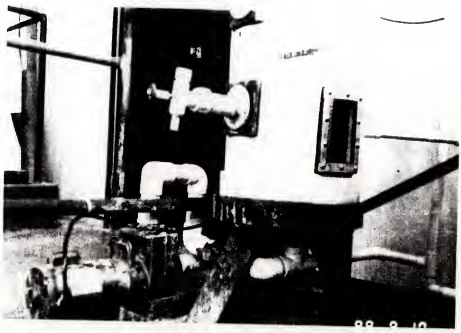

Figure 5-6. Bottom of settling column showing the observation port and the large pump.

Figure 5-7. Slurry sampler and its components.

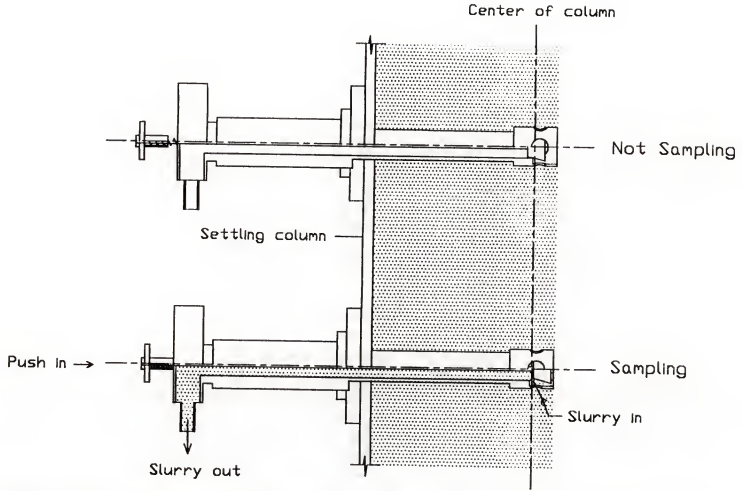

Figure 5-8. Schematic diagram showing the sampling mechanism of the slurry sampler.

column. By pushing in the rubber disc, thus compressing the spring, the rubber stopper at the other end of the sampler moves and creates an opening for the slurry to flow into the sampler, thus sampling is achieved. At the end of sampling, the rubber disc is released, and the recoil of the spring causes the rubber stopper to close the opening and to stop the slurry from flowing into the sampler, thus end sampling.

The ease of slurry outflow from the sampler depends upon the slurry viscosity. The length of the PVC tube spacer can be adjusted to control the opening (where the slurry flowed into the sampler), and the rate of slurry outflow.

Settling Column Tests

The sand content and density of the slurries at ten different depths along the column were determined at five different elapsed times, hence, variations of sand content and density with depth and elapsed time could be obtained. Each type of slurry, Florigel H-Y clay slurry and Super Mud polymer slurry, was prepared at three different viscosities. The three viscosities were designated as high viscosity, medium viscosity, and low viscosity, and ranged between 27 to 41 s Marsh. The Marsh funnel viscosities at the top, middle, and bottom of the column were also measured to see how the slurry viscosity varied during the settling period.

Testing Procedures

Florigel H-Y clay slurry

The clay slurries for the settling column tests were mixed in a special way. For each slurry, the clay powder was slowly added to the mixing tank while water was added. At the same time, the slurry was circulated in the tank through the rectangular piping system (see Figure 5-5) to ensure that a uniform mixture was obtained.

After the specific amount of clay was added to the tank to obtain the desired concentration, the slurry was pumped up to the settling column. Effective mixing was done by circulating the slurry in the column. Figure 5-9 shows the amount of time required to achieve a constant Marsh funnel viscosity. Each of the data point represents an average Marsh funnel viscosity of the three slurry samples, which were obtained, at the top, middle, and bottom of the column. Based on Figure 5-9, slurries of different viscosities attained the maximum viscosity in 2 h. Therefore, all the clay slurries were circulated in the column for 2 h. After circulated for 2 h the slurry was left in the column overnight.

On the next day, the slurry was again circulated for 30 min. The Marsh funnel viscosity of the slurry was checked before adding sand from the top of the column. The amount of sand added was 100±5 lb (≈ 43.2 to 47.7 kg), which corresponds to about 4 - 5% sand content. The

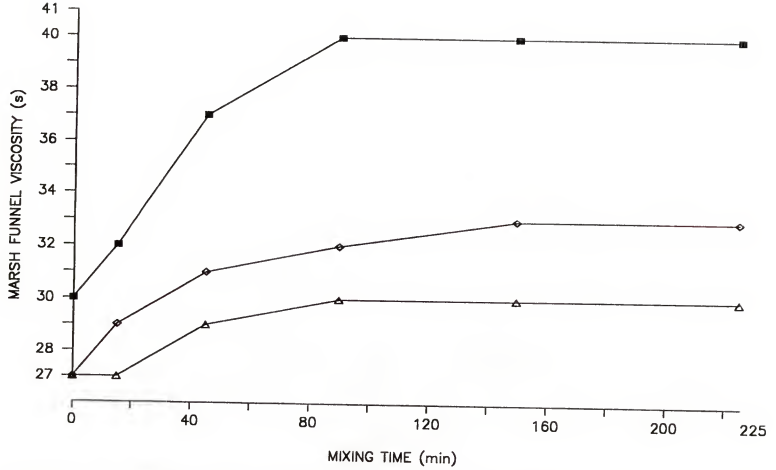

Figure 5-9. Marsh funnel viscosity versus mixing time of the Florigel H-Y clay slurry in the settling column.

mixture of slurry and sand was continuously circulated for another 20 min. The test was then started. Slurry samples, about 500 mL, from the ten sampling ports were sampled at five different elapsed times, 0, 1, 3, 7, and 24 h. The time taken to sample from top to bottom of the column was about 10 to 15 min. Sand content and density tests were then performed on all the 50 samples. Due to the large quantity of slurry required to perform the Marsh funnel viscosity test, the Marsh funnel test was only performed on the samples obtained from the top, middle, and bottom sampling ports, where a large volume, 2500 mL, of slurry samples were sampled.

At the end of each settling test, the column, the tank, and the piping were flushed clean with water, before another test was performed. Three different slurry viscosities, two sand sizes, and two replicates for each combination of slurry viscosity and sand size, made up a total of twelve settling column tests for the clay slurry.

Super Mud polymer slurry

The preparation of Super Mud polymer slurries was different from that of the clay slurries. For each polymer slurry, the polymer was added very slowly through a small funnel with the water jetting towards the polymer. In this way, the polymer could be mixed properly to form a uniform slurry. The slurry was left in the tank until the next day.

On the second day, the slurry was circulated in the tank for about 5 min, before being pumped up to the column. The slurry was then circulated in the column for 10 min before checking the Marsh funnel viscosity. The sand was poured from the top of the column while circulating the slurry. The sand slurry mixture was circulated for another 10 min before starting the test. The sampling time intervals were the same as that for the clay slurries. The total number of settling column tests for the polymer slurry was eight, four less than the clay slurry. Two of the four tests that were not performed were the replicates for the high and low viscosity slurries with the coarse sand. The other two tests were medium viscosity slurry with the coarse sand and its replicate. These four tests were intentionally omitted because they would not yield additional information.

Results and Discussion

Florigel H-Y clay slurry

Sand content. The results of the sand content distributions with depth of slurries in the column are shown in Figures 5-10 through 5-15. At each elapsed time, the figures show a pair of distribution curves, which represent the results of the two replicate tests of a certain slurry viscosity with a particular sand size. The legend of the graph symbols, the average Marsh viscosity, is the average of the Marsh viscosities measured at the

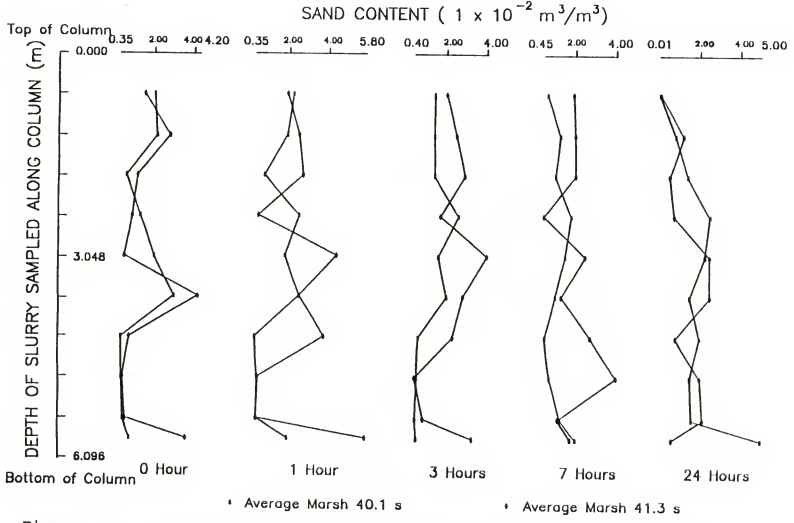

Figure 5-10. Distributions of sand content with depth of high viscosity Florigel H-Y clay slurry mixed with coarse sand at 5 different elapsed times after mixing.

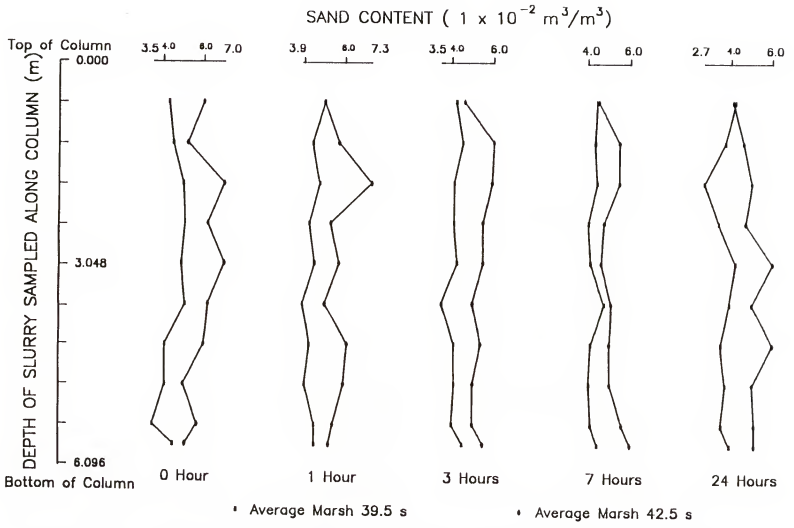

Figure 5-11. Distributions of sand content with depth of high viscosity Florigel H-Y clay slurry mixed with fine sand at 5 different elapsed times after mixing.

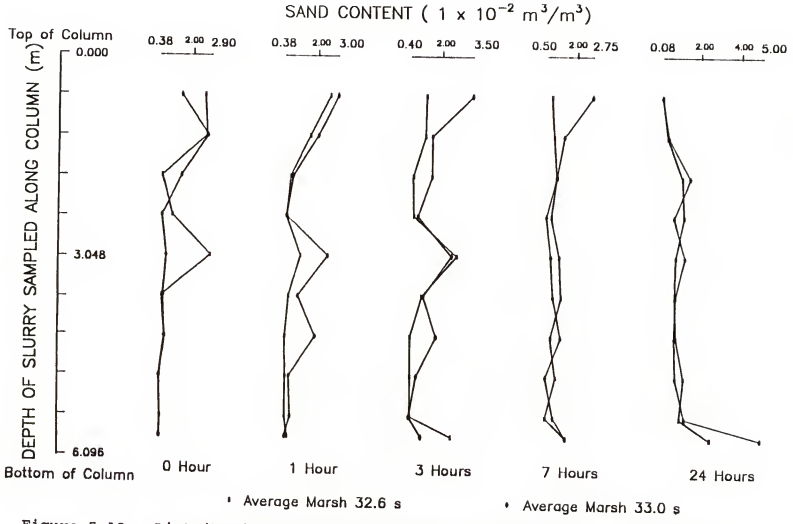

Figure 5-12. Distributions of sand content with depth of medium viscosity Florigel H-Y clay slurry mixed with coarse sand at 5 different elapsed times after mixing.

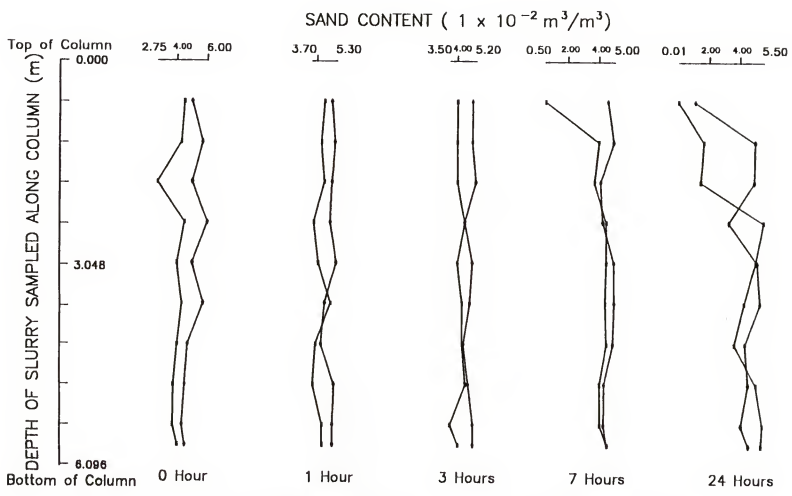

Figure 5-13. Distributions of sand content with depth of medium viscosity Florigel H-Y clay slurry mixed with fine sand at 5 different elapsed times after mixing.

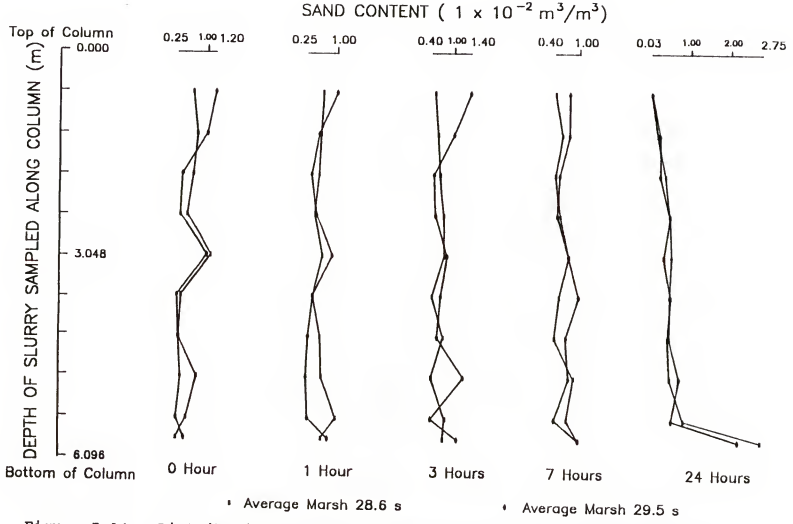

Figure 5-14. Distributions of sand content with depth of low viscosity Florigel H-Y clay slurry mixed with coarse sand at 5 different elapsed times after mixing.

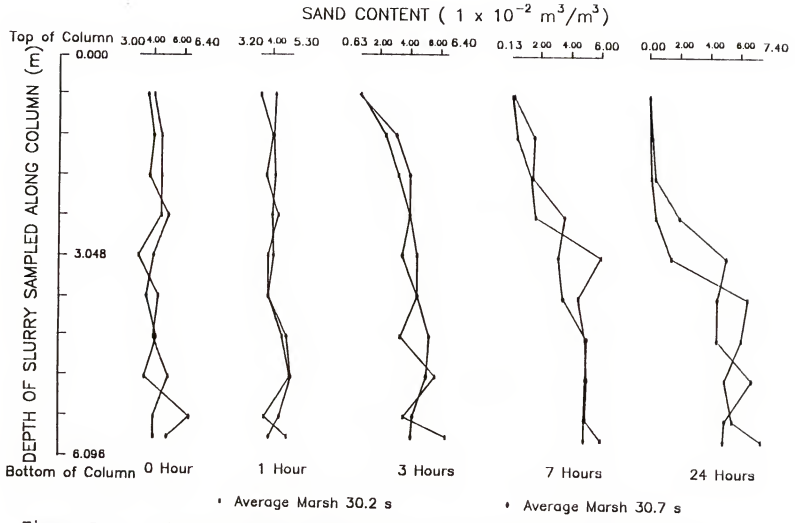

Figure 5-15. Distributions of sand content with depth of low viscosity Florigel H-Y clay slurry mixed with fine sand at 5 different elapsed times after mixing.

five elapsed times from slurries sampled along the top, middle and bottom of the column. The sand content was measured as volume of sand in a fixed volume of slurry.

Figures 5-10 and 5-11 show the sand content distribution curves of the high viscosity (39 to 42 s Marsh) slurries. The high viscosity slurries hold about 3.5 to 5.5% fine sand for 24 h and about 0.5 to 2.5% coarse sand for 7 h. The distributions of the coarse sand are more erratic than the fine sand. This phenomenon was observed during the sedimentation cylinder tests, where localized concentration of coarse particles was noticed. Through observations during the sand content tests on the slurries with the coarse sand, the low sand contents in Figure 5-10, less than 0.5%, are attributed to the finer particles of the coarse sand. The higher sand contents in Figure 5-10 result from measuring either the mixture of the coarser and finer particles of the coarse sand or the coarser particles of the coarse sand alone. Some of the coarse sand settle to the bottom of the column as shown in Figure 5-10, where there is an increase in sand content at the bottom of the column.

Figures 5-12 and 5-13 show the sand content distribution curves of the medium viscosity (about 33 s Marsh) slurries. The medium viscosity slurries hold approximately 3 to 5.5% fine sand for 24 h and 0.5 to 2% coarse sand for only 3 h.

The sand content distribution curves of the low viscosity (29 to 30 s Marsh) slurries are shown in Figures 5-14 and 5-15. The low viscosity slurries are unable to suspend the coarse sand as depicted in Figure 5-14, where the sand contents are low, less than 1%. Since the bottom sampling port is 1 ft above the bottom of the column, and the thickness of the coarse sand sediment is less than 1 ft, the sedimentation of the coarse sand does not clearly reflect in Figure 5-14. In Figure 5-15, it shows that the low viscosity slurries suspend about 3.5 to 5% fine sand for about an hour, thereafter, settling of sand occurs. At the end of 24 h, fine sand in the upper half of the column settles to the bottom half of the column.

Density. In general, the trend of the density distribution curves is similar to that of the sand content distribution curves.

Figure 5-16 shows the density distribution curves of the high viscosity (40 to 41 s Marsh) slurries with the coarse sand. The density distributions range from 1035 to 1060 kg/m^3 at the end of 7 h. The density of the high viscosity slurries with no sand was measured to be between 1030 and 1035 kg/m^3. During the two settling tests of the high viscosity slurry with the coarse sand, it was observed that at the end of 3 h, a layer of water, 50 mm (≈ 2 in.), appeared on top of the clay slurry. The thickness of the water layer increased to 380 mm (≈ 15 in.) at the end of 24

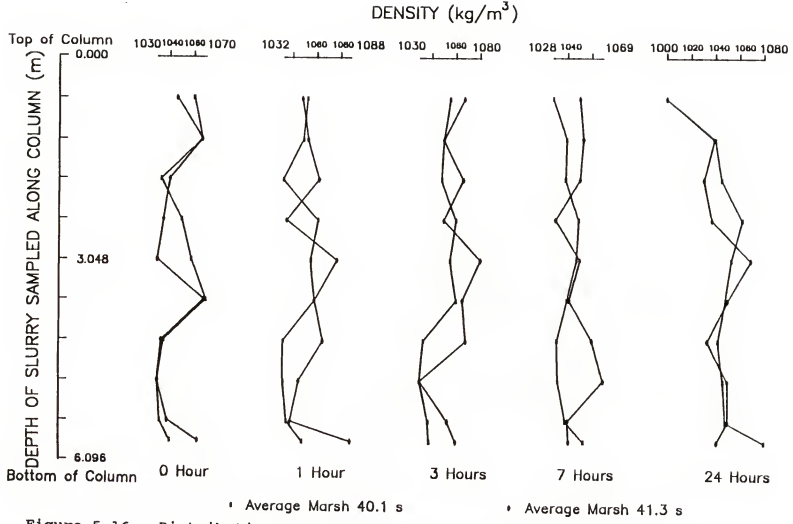

Figure 5-16. Distributions of density with depth of high viscosity Florigel H-Y clay slurry mixed with coarse sand at 5 different elapsed times after mixing.

h. Due to the lowering of slurry level caused by sampling, about 90 mm (≈ 3.5 in.) for each sampling, and the formation of water layer, the sample obtained from the top of the column was a very dilute clay suspension. Hence, Figure 5-16 shows a density of 1000 kg/m^3 for the sample obtained from the top of the column, at the end of 24 h.

Figure 5-17 shows that the density distributions of the high viscosity (40 to 42 s Marsh) slurries with fine sand are fairly constant along the column for about a day of standing. The densities vary in a narrow range of approximately 1055 to 1070 kg/m^3 at the end of 24 h. Slurries of high viscosity with fine sand showed only a 100 mm (≈ 4 in.) thick layer of water on top of the slurry after standing for 24 h.

The density distribution curves of the medium viscosity (about 33 s Marsh) slurries are shown in Figures 5-18 and 5-19. The densities of the medium viscosity slurries with no sand were determined to be between 1020 and 1025 kg/m^3. Figure 5-18 shows a density range of 1025 to 1040 kg/m^3 at the end of 3 h, and Figure 5-19 shows a density range of 1055 to 1070 kg/m^3 at the end of 24 h. The higher densities (Figure 5-19) were obtained by suspending the fine sand. The lower densities (Figure 5-18) resulted from most of the coarser particles in the coarse sand settled to the bottom, with mainly the finer particles being suspended and thus measured. The increase

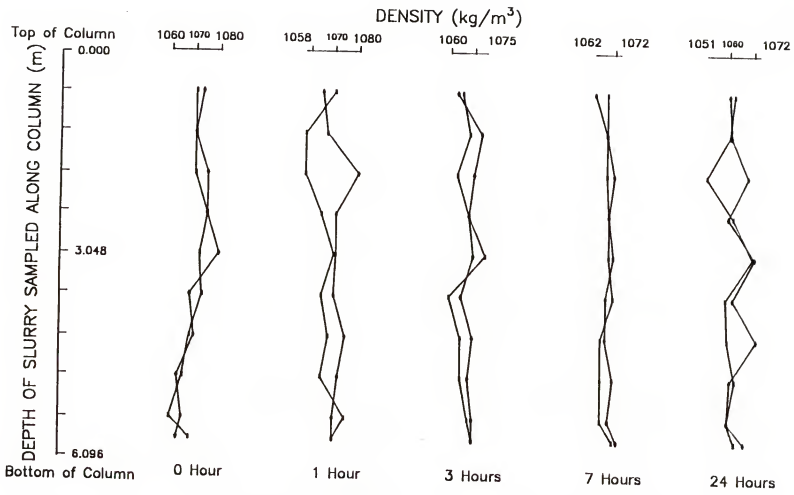

Figure 5-17. Distributions of density with depth of high viscosity Florigel H-Y clay slurry mixed with fine sand at 5 different elapsed times after mixing.

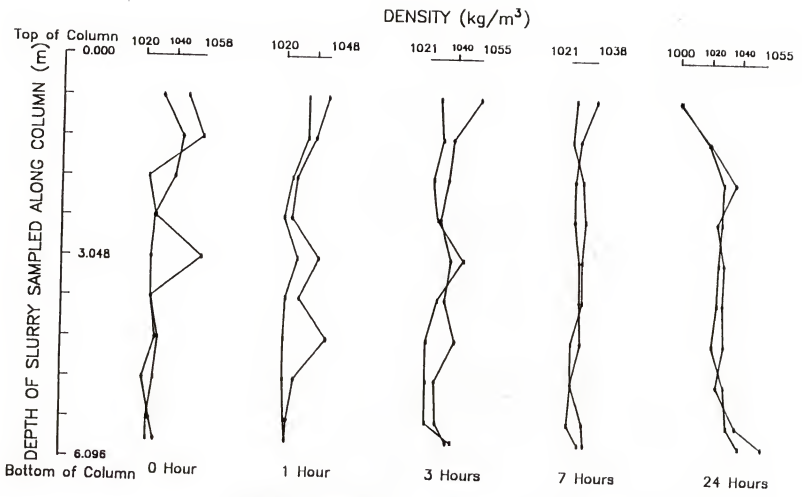

Figure 5-18. Distributions of density with depth of medium viscosity Florigel H-Y clay slurry mixed with coarse sand at 5 different elapsed times after mixing.

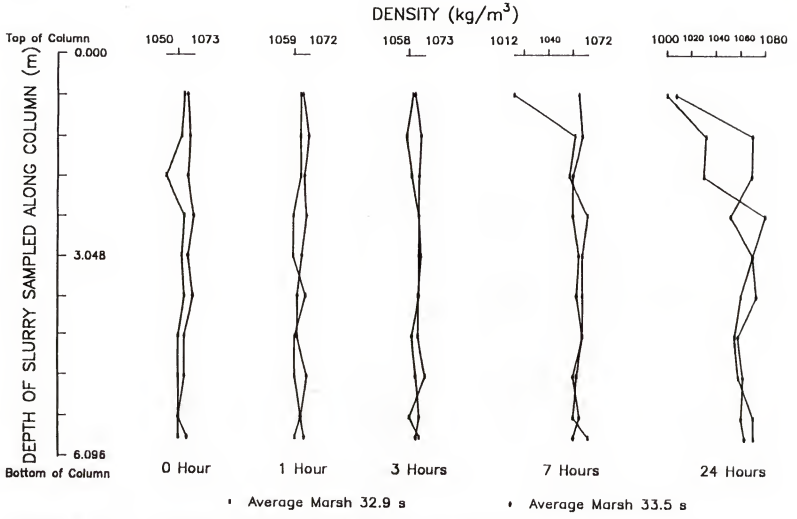

Figure 5-19. Distributions of density with depth of medium viscosity Florigel H-Y clay slurry mixed with fine sand at 5 different elapsed times after mixing.

in density with depth was also partly caused by the settling of clay. The 1000 kg/m^3 density at the topmost sampling port at the end of 24 h, as shown in Figures 5-18 and 5-19, is attributed to the layer of water formed on top of the clay slurry. When comparing Figures 5-18 and 5-19, the density distributions, with Figures 5-12 and 5-13, the sand content distributions, they are very similar.

Figures 5-20 and 5-21 present the density distribution curves of the low viscosity (29 to 30 s Marsh) slurries. With no sand, the densities of the slurries are between 1015 to 1020 kg/m^3. Because the low viscosity slurries are unable to suspend coarse sand, the densities obtained are low, about 1020 kg/m^3, as shown in Figure 5-20. Similar to the settling tests of low viscosity slurry with coarse sand conducted using the sedimentation cylinders (see Figure 5-1), the settling of clay particles in the settling column created a surface water layer of 50 mm (≈ 2 in.) only after standing for 1 h.

Figure 5-21 shows that the low viscosity slurries cannot suspend fully the fine sand after 1 h of elapsed time. The densities after 1 h range between 1055 to 1070 kg/m^3. It can be seen that slurries in the lower half of the column have densities as high as 1060 to 1090 kg/m^3 at the end of 24 h, which indicate that the fine sand settles with the slurries to the lower half of the column.

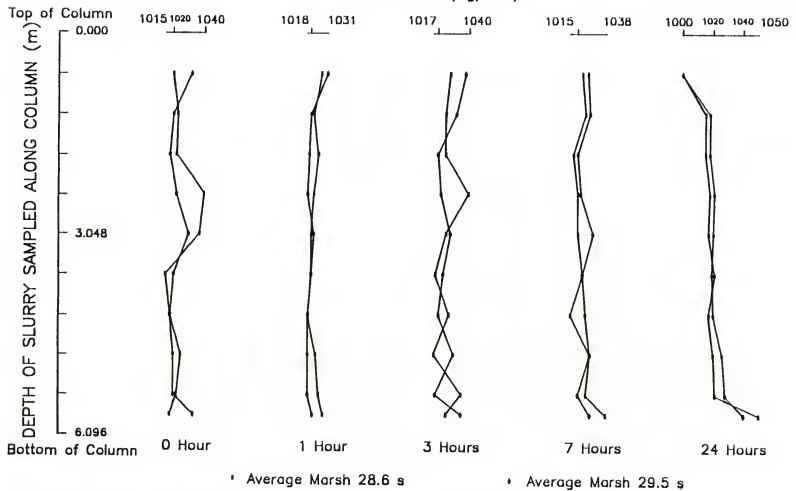

Figure 5-20. Distributions of density with depth of low viscosity Florigel H-Y clay slurry mixed with coarse sand at 5 different elapsed times after mixing.

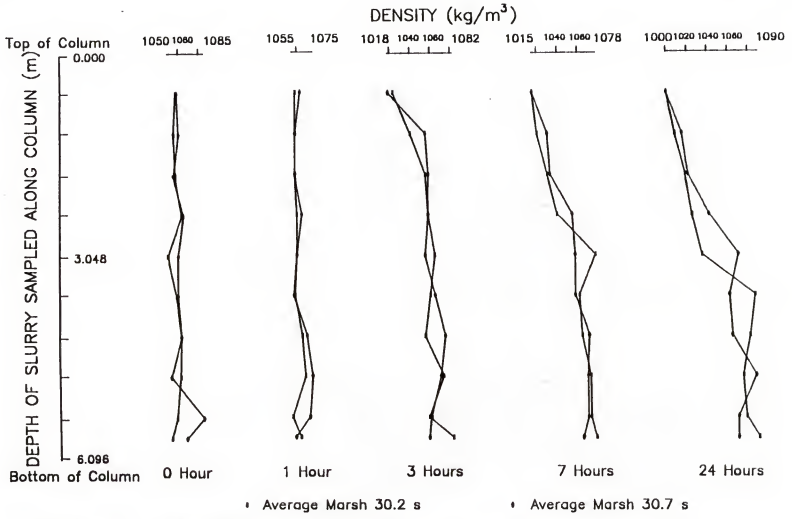

Figure 5-21. Distributions of density with depth of low viscosity Florigel H-Y clay slurry mixed with fine sand at 5 different elapsed times after mixing.

Marsh funnel viscosity. The Marsh funnel viscosity distributions for high viscosity slurries with coarse sand are shown in Figure 5-22. The viscosities are uniform throughout the whole column until the 7th h. At the 7th h, a decrease in viscosities of slurries sampled at the topmost sampling port indicates the settlement of clay particles. At the end of 24 h, the 25 s Marsh viscosity signifies viscosity of water. Figure 5-22 suggests that the slurries settle and concentrate in the lower half of the column. In the case of the high viscosity slurries with fine sand, Figure 5-23 shows little variation in the viscosity. At the end of 24 h, Figure 5-22 and 5-23 both show a trend of slight decrease in viscosity in the lower half of the slurry column. The decreasing trend of the viscosities may be explained by the settling of clay particles from the middle of the column to the bottom (below the bottommost sampling port) of the column.

In the medium viscosity slurries, the distribution curves of the Marsh funnel viscosity of the slurries with the coarse sand are uniform for the first 7 h, as shown in Figure 5-24. The low viscosities, 25 to 26 s, of the topmost samples at 24 h are due to the settling of clay particles and thus the layer of water on the surface. Figure 5-25, which shows the distributions of the Marsh viscosity of medium viscosity slurries with the fine sand,

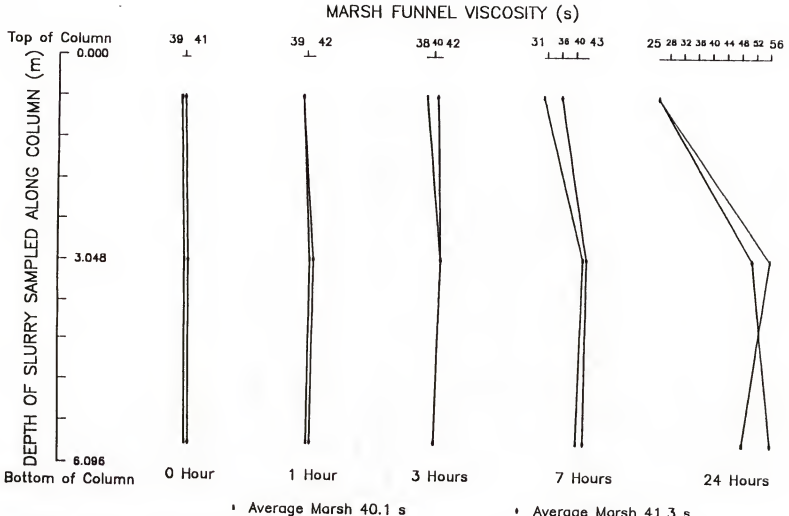

Figure 5-22. Distributions of Marsh funnel viscosity with depth of high viscosity Florigel H-Y clay slurry mixed with coarse sand at 5 different elapsed times after mixing.

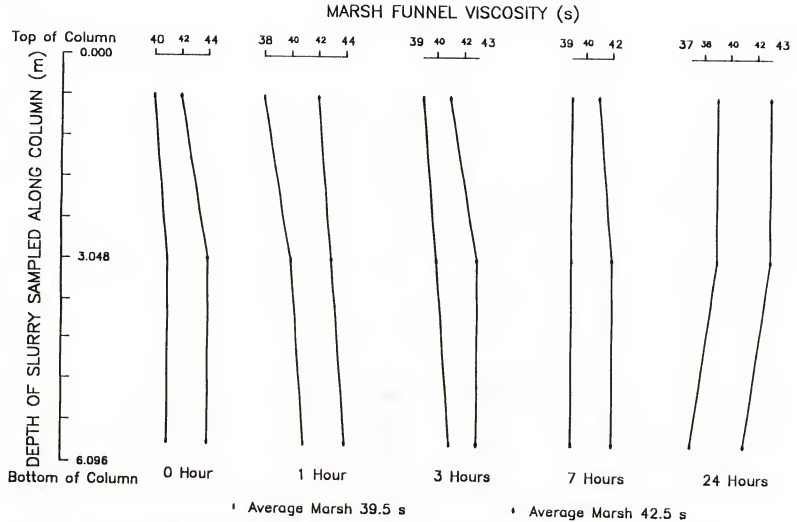

Figure 5-23. Distributions of Marsh funnel viscosity with depth of high viscosity Florigel H-Y clay slurry mixed with fine sand at 5 different elapsed times after mixing.

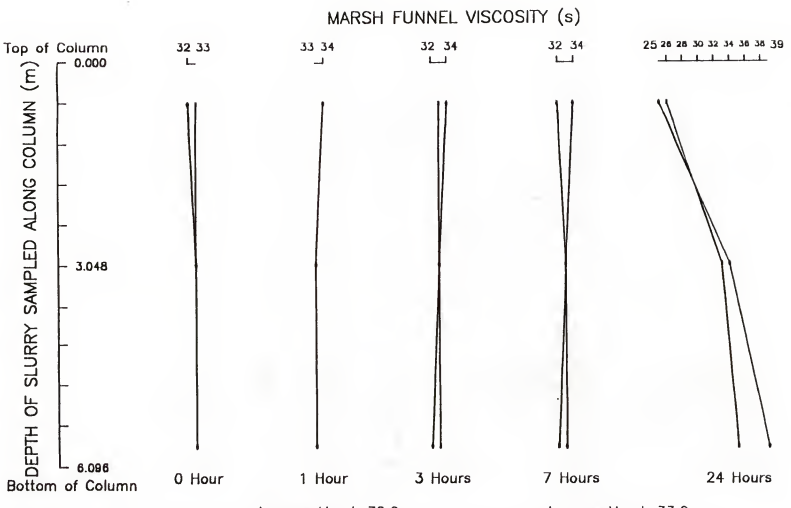

Figure 5-24. Distributions of Marsh funnel viscosity with depth of medium viscosity Florigel H-Y clay slurry mixed with coarse sand at 5 different elapsed times after mixing.

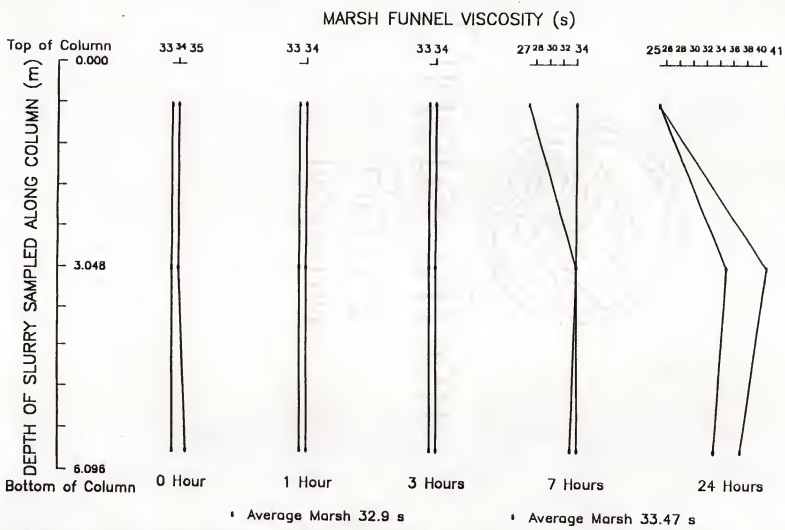

Figure 5-25. Distributions of Marsh funnel viscosity with depth of medium viscosity Florigel H-Y clay slurry mixed with fine sand at 5 different elapsed times after mixing.

indicates an early settling of clay particles at the 7th h of one of the tests.

The distributions of the Marsh funnel viscosity of the low viscosity slurries are shown in Figures 5-26 and 5-27. Similar trend as that shown in Figures 5-24 and 5-25 for the medium viscosity slurries. The viscosity distribution curves at 24 h as shown in Figure 5-27 show two different trends. One increases with depth and the other increases to the mid-depth and then decreases slightly. The explanation for this discrepancy is the different rates of settling of the clay particles.

Summary of sand content and density. Table 5-1 shows the sand content and density of slurry with different viscosities suspending the coarse and fine sands. The elapsed time in parenthesis indicates the duration the sand stays in suspension.

To relate the particle size of the suspending sand with the slurry gel strength, the relationships of both Weiss and Cardwell (given in Chapter 2) were used. Since the gel strengths of the actual slurries tested were not measured, Figures 4-3 and 4-4 together with the actual slurry Marsh viscosities were used to estimate the gel strengths. Note that both the 10-s and 10-min gel strengths were used. Table 5-2 shows the calculated particle sizes.

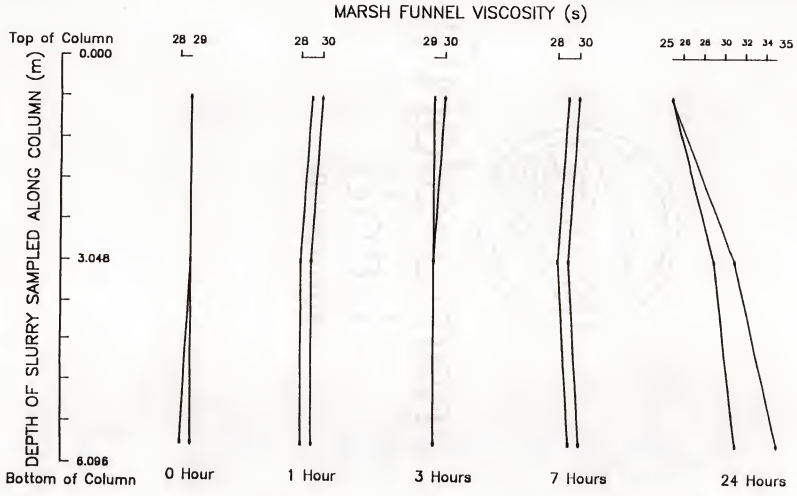

Figure 5-26. Distributions of Marsh funnel viscosity with depth of low viscosity Florigel H-Y clay slurry mixed with coarse sand at 5 different elapsed times after mixing.

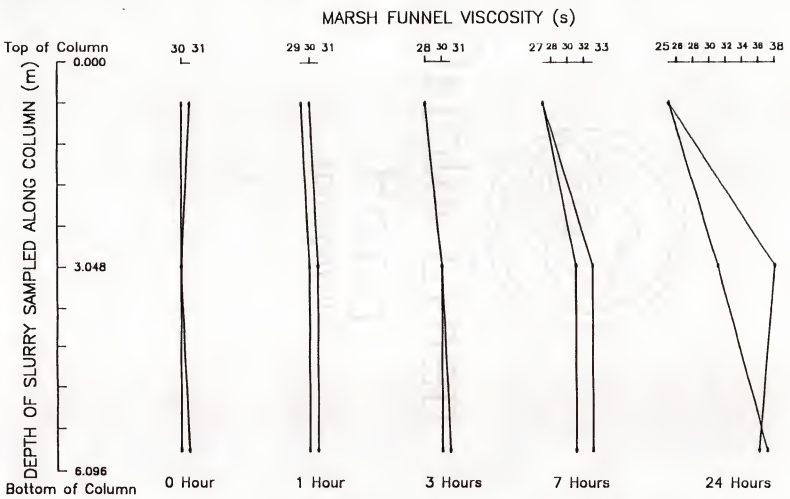

Figure 5-27. Distributions of Marsh funnel viscosity with depth of low viscosity Florigel H-Y clay slurry mixed with fine sand at 5 different elapsed times after mixing.

Table 5-1. Summary of the sand content and density results of the Florigel H-Y clay slurry from the settling column tests.

Slurry	Sand content (%)	Density kg/m^3
High viscosity (39 - 40 s Marsh) no sand		1030 - 1035
Medium viscosity (33 s Marsh) no sand		1020 - 1025
Low viscosity (29 - 30 s Marsh) no sand		1015 - 1020
High viscosity coarse sand (7 h)	0.5 - 2.5	1035 - 1060
High viscosity fine sand (24 h)	3.5 - 5.5	1055 - 1070
Medium viscosity coarse sand (3 h)	0.5 - 2.0	1025 - 1040
Medium viscosity fine sand (24 h)	3.0 - 5.5	1055 - 1070
Low viscosity coarse sand (0 h*)	0.5 - 1.0	1020 - 1025
Low viscosity fine sand (1 h)	3.5 - 5.0	1055 - 1070

* Note that sampling time from the top sampling port to the bottom sampling port is about 10 to 15 min.

Table 5-2. Diameter of suspending particle calculated using equations of Weiss and Cardwell

Viscosity (Marsh s)	Density (kg/m^3)	Gel Strength 10-s	Gel Strength 10-min (Pa)	Diameter Weiss	Diameter Cardwell (mm)
39 - 40	1.033	7.8		0.72	2.89
39 - 40	1.03		9.2	0.85	3.41
33	1.023	6.3		0.58	2.32
33	1.023		7.7	0.71	2.84
29 - 30	1.018	2.3		0.21	0.85
29 - 30	1.018		3.3	0.30	1.21

From Figure 3-6 the grain size of coarse sand ranges from 0.5 to 3 mm and fine sand ranges from 0.1 to 0.5. The sand content in Table 5-1 and the grain size of the fine and coarse sands suggest that the particle size calculated by the Weiss's equation agrees quite well with the tests results. Cardwell's equation seems to overestimate the particle size.

Super Mud polymer slurry

Sand content. The small scale settling tests from the sedimentation cylinders have demonstrated that the polymer slurry is not capable of suspending sand particles. The results of the full scale settling column tests, shown in Figures 5-28 through 5-32, substantiate the previous observations. Even at a Marsh funnel viscosity of about 38 s, the polymer slurry can only suspend small amount of fine sand for 1 h (Figure 5-29). In Figure 5-32, the increase

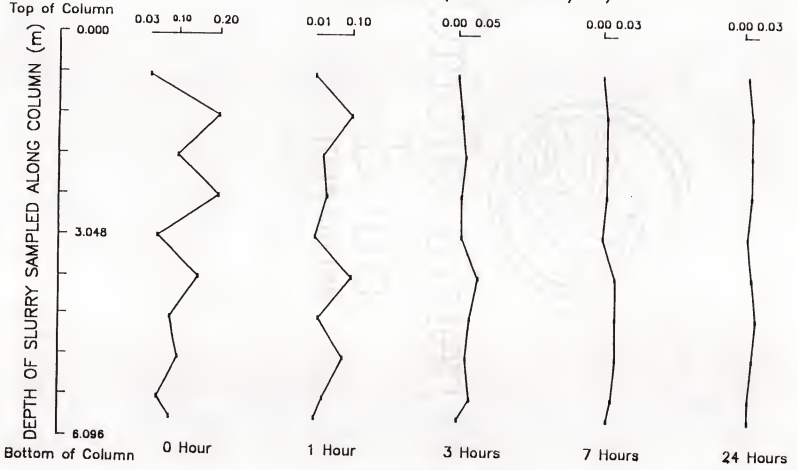

Figure 5-28. Distributions of sand content with depth of high viscosity Super Mud polymer slurry mixed with coarse sand at 5 different elapsed times after mixing.

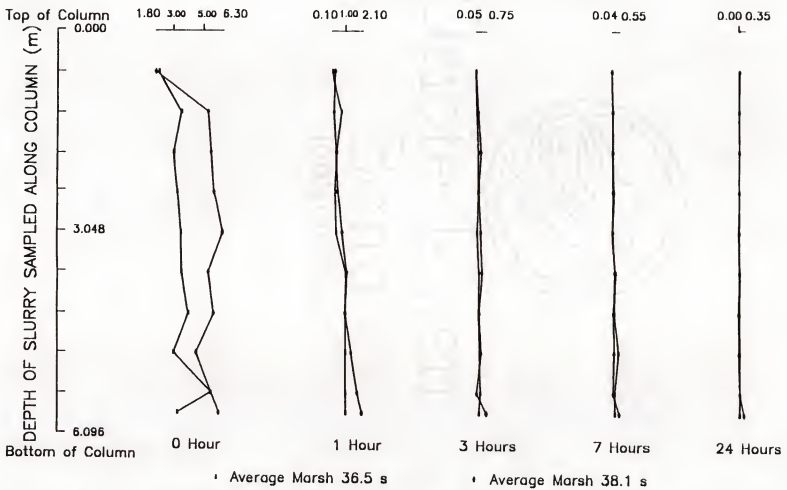

Figure 5-29. Distributions of sand content with depth of high viscosity Super Mud polymer slurry mixed with fine sand at 5 different elapsed times after mixing.

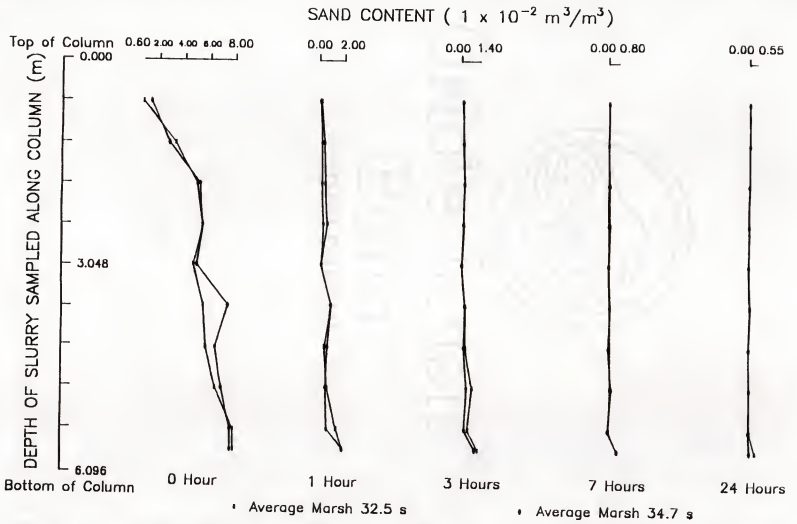

Figure 5-30. Distributions of sand content with depth of medium viscosity Super Mud polymer slurry mixed with fine sand at 5 different elapsed times after mixing.

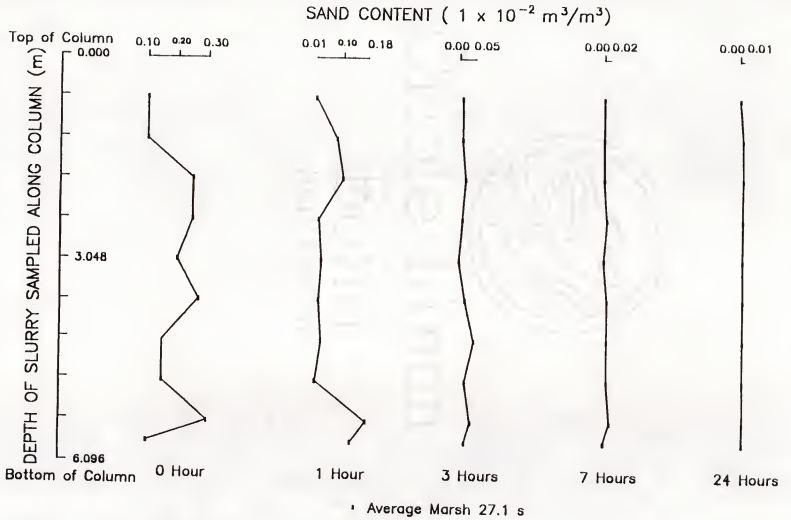

Figure 5-31. Distributions of sand content with depth of low viscosity Super Mud polymer slurry mixed with coarse sand at 5 different elapsed times after mixing.

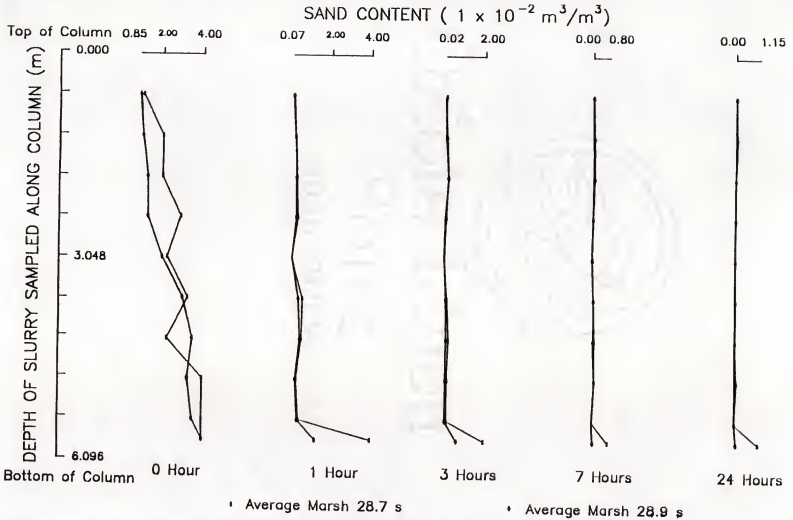

Figure 5-32. Distributions of sand content with depth of low viscosity Super Mud polymer slurry mixed with fine sand at 5 different elapsed times after mixing.

in sand content from the bottom sampling port is caused by the sediment which has a thickness of about 0.3 m (≈ 1 ft). During the settling tests of the polymer slurries, unlike the clay slurries, sand build-up was clearly visible from the observation port located near the bottom of the column. It was observed that 90% of the sand sediment formed within 30 min.

Density. Since the polymer slurry is unable to suspend sand particles, results of the slurry densities shown in Figures 5-33 through 5-37 are obvious. The density of the clean polymer slurry was measured to be 1000 kg/m^3. The densities shown in Figures 5-33 through 5-37 indicate that the majority of the slurry samples are almost clean slurry.

Marsh funnel viscosity. The distributions of Marsh viscosity along the column are presented in Figures 5-38 through 5-42. In general, the variations of the viscosities of the polymer slurry are smaller than that of the clay slurry, and are insignificant. This may be due to the lack of solid particles in the polymer slurries.

Comparison of Settling Test Results from Settling Column and Sedimentation Cylinder Tests

The sedimentation cylinder test can be used to predict whether the particles will suspend or settle in the slurry; for example, the sedimentation cylinder tests predict correctly that Super Mud polymer slurry has no suspending

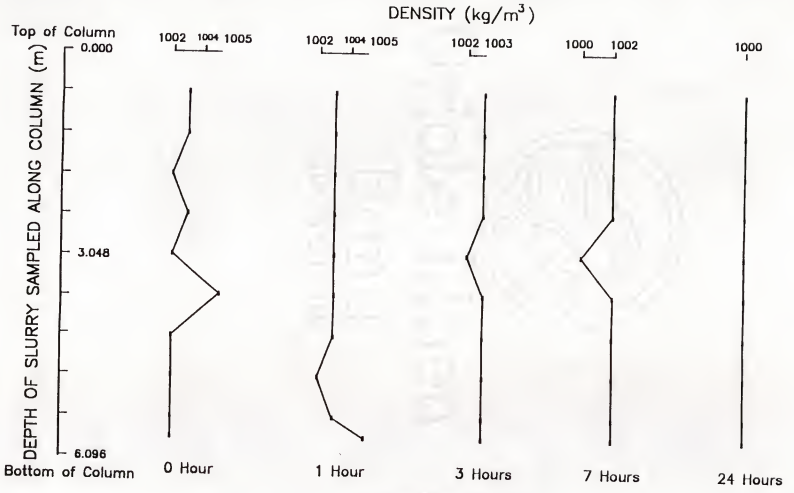

Figure 5-33. Distributions of density with depth of high viscosity Super Mud polymer slurry mixed with coarse sand at 5 different elapsed times after mixing.

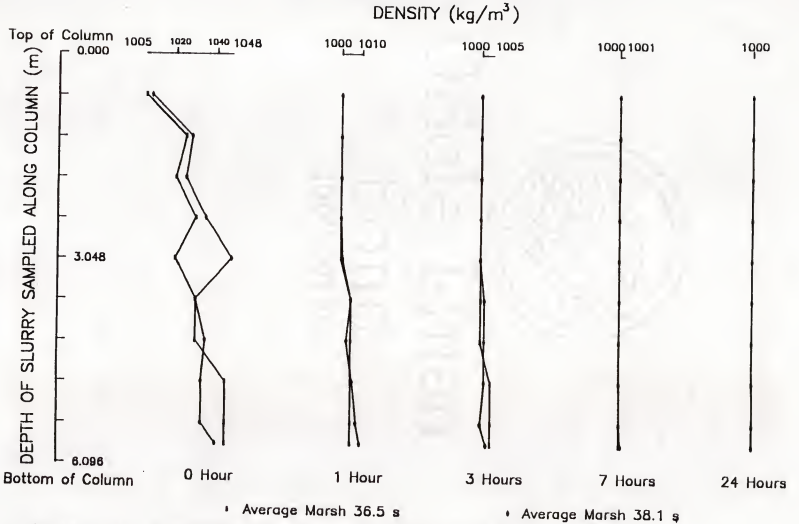

Figure 5-34. Distributions of density with depth of high viscosity Super Mud polymer slurry mixed with fine sand at 5 different elapsed times after mixing.

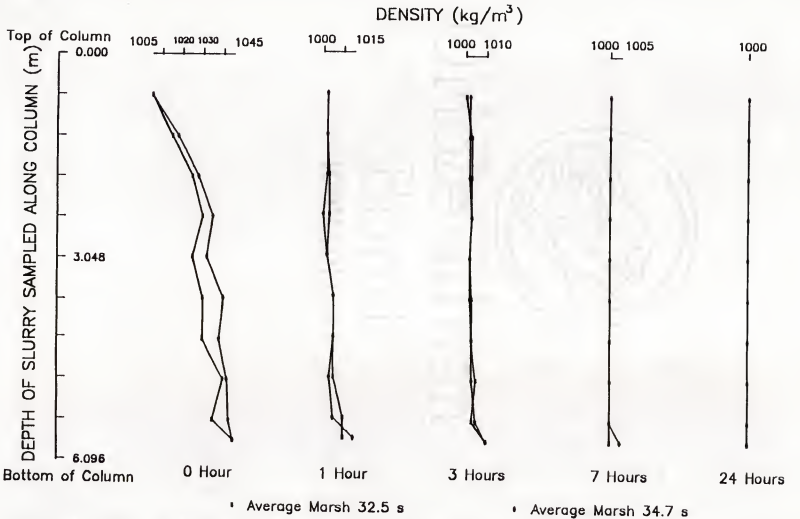

Figure 5-35. Distributions of density with depth of medium viscosity Super Mud polymer slurry mixed with fine sand at 5 different elapsed times after mixing.

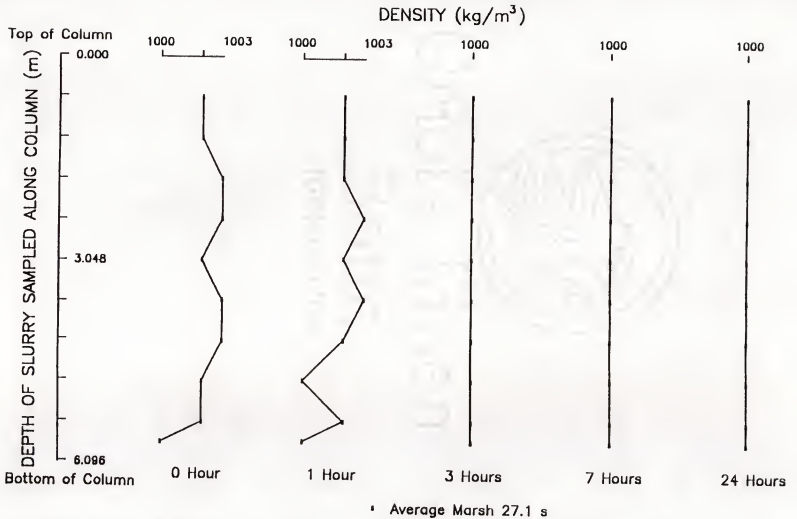

Figure 5-36. Distributions of density with depth of low viscosity Super Mud polymer slurry mixed with coarse sand at 5 different elapsed times after mixing.

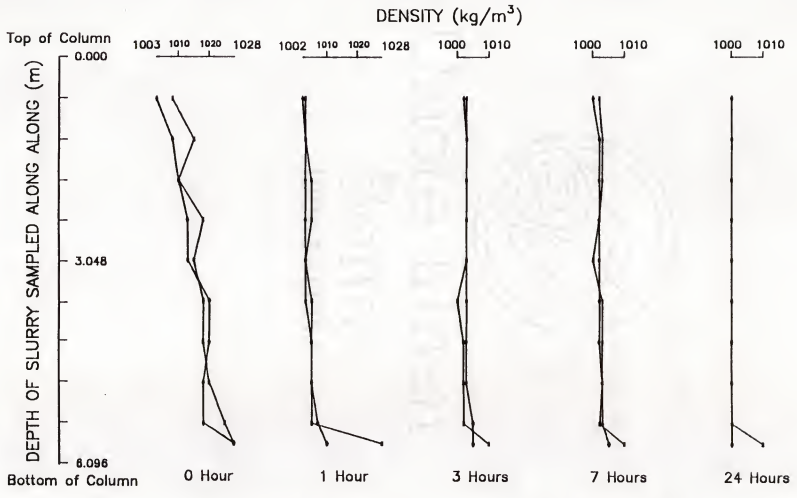

Figure 5-37. Distributions of density with depth of low viscosity Super Mud polymer slurry mixed with fine sand at 5 different elapsed times after mixing.

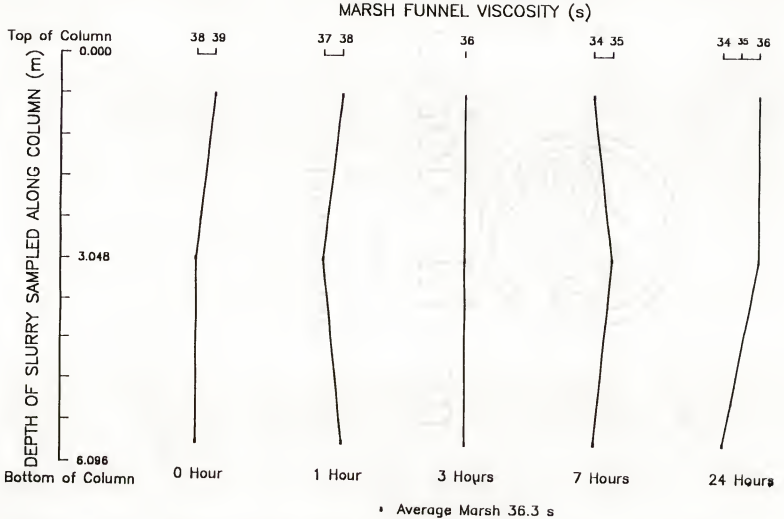

Figure 5-38. Distributions of Marsh funnel viscosity with depth of high viscosity Super Mud polymer slurry mixed with coarse sand at 5 different elapsed times after mixing.

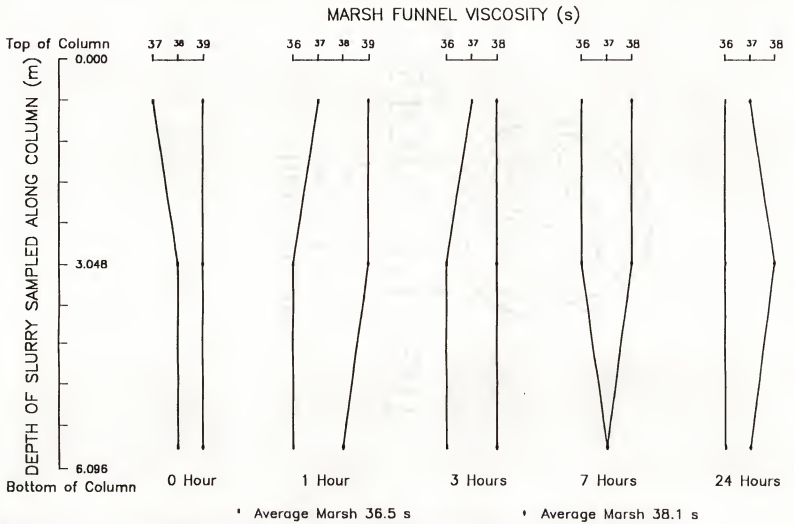

Figure 5-39. Distributions of Marsh funnel viscosity with depth of high viscosity Super Mud polymer slurry mixed with fine sand at 5 different elapsed times after mixing.

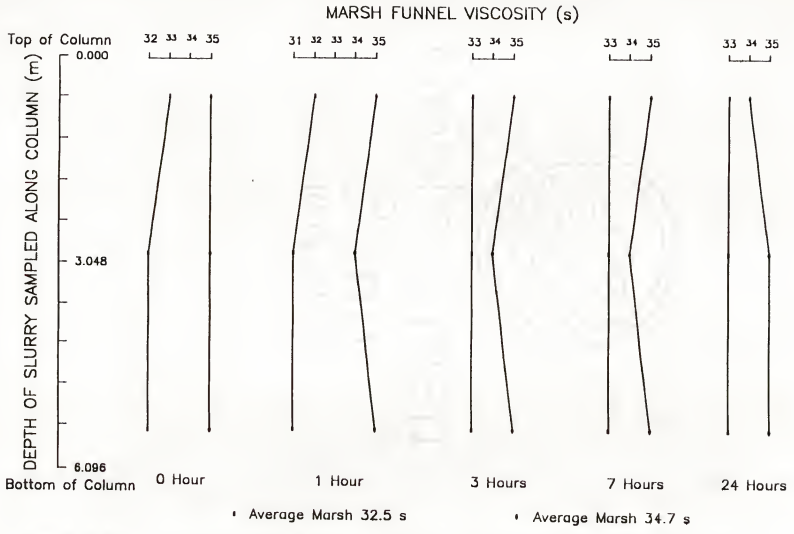

Figure 5-40. Distributions of Marsh funnel viscosity with depth of medium viscosity Super Mud polymer slurry mixed with fine sand at 5 different elapsed times after mixing.

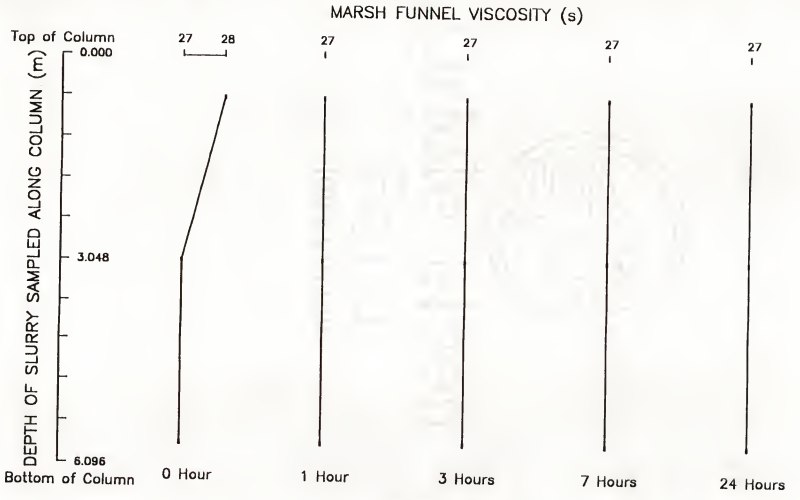

Figure 5-41. Distributions of Marsh funnel viscosity with depth of low viscosity Super Mud polymer slurry mixed with coarse sand at 5 different elapsed times after mixing.

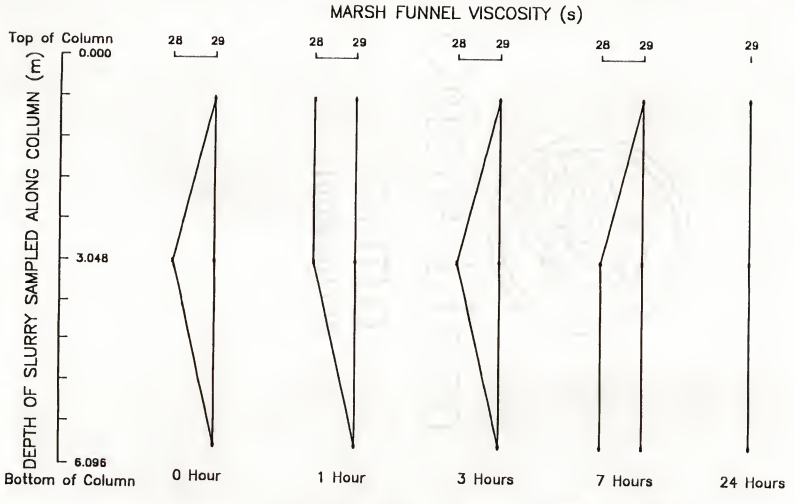

Figure 5-42. Distributions of Marsh funnel viscosity with depth of low viscosity Super Mud polymer slurry mixed with fine sand at 5 different elapsed times after mixing.

ability. However, the color of the slurry and sand may make it difficult to judge, especially for fine sand in clay slurry. Although the variation of sand content with depth cannot be predicted, visual observation can give useful information. For example, it was observed during the sedimentation tests of high viscosity Florigel H-Y clay slurry with coarse sand that particles were locally concentrated along the cylinder and this agrees with the erratic sand content values obtained from the settling column tests. In general, distinct phenomena such as water interface, sedimentation, can be easily predicted.

Comments on Current Slurry Specifications

1. The results in Table 5-1 show that a 5% sand content corresponds to a density of 1070 kg/m^3 (≈ 66.8 lb/ft^3). The maximum density (70 to 75 lb/ft^3) before concreting in the current slurry specifications corresponds to a sand content that is much higher than 5% or even 10%.
2. The gel strength of 2 - 10 Pa for fresh slurry is a reasonable limit for the Florigel H-Y clay slurry. Slurry specifications that allow the gel strength of fresh slurry to have an upper limit of 40 Pa is not suitable for the Florigel H-Y clay slurry.

CHAPTER 6
CENTRIFUGE MODELING OF SLURRY IN DRILLED SHAFT

Introduction

The objective of the centrifugal modeling test program was twofold; one, to determine whether or not the centrifuge was a viable tool to study slurry performance in drilled shaft construction, and two if so, can the hole integrity and filter cake thickness be studied. A perusal of available literature found no information on the modeling of drilled shaft construction, thus this series of experiments hopefully would lay the ground work for further study.

The Principle of Centrifugal Model Testing

The idea of centrifugal model testing is to construct a scaled-down model similar in geometry, material properties, and boundary conditions to the full-scale prototype, and to subject the model to a rotational action such that the radial acceleration induces an increase in self-weight stresses that match those at corresponding points in the prototype.

The following example illustrates the uniqueness of the centrifuge modeling technique. If the prototype is a column of 6 m deep slurry (density of 1030 kg/m^3) in a

drilled hole, the hydrostatic pressure at the bottom of the hole is

$$1030\ kg/m^3 \times 9.807\ m/s^2 \times 6\ m = 60607.26\ N/m^2$$

where the acceleration of gravity, $g = 9.807\ m/s^2$

If a model were constructed using the same slurry but reduced linear dimensions by a factor of 40, the height of the model would be

$$6\ m / 40 = 0.15\ m$$

By increasing the acceleration of gravity 40 times through centripetal acceleration, the hydrostatic pressure at the bottom of the model will be the same as that of the prototype as shown below:

$$1030\ kg/m^3 \times 40 \times 9.807\ m/s^2 \times 0.15\ m = 60607.26\ N/m^2$$

It shows that, in centrifugal model testing, by accelerating a 1/N scaled model so that its self weight increases by N times, same stresses can be achieved in the model and in the full scale prototype at corresponding points if they have the same material and same boundary conditions.

University of Florida Centrifuge

The University of Florida Geotechnical Centrifuge was originally designed and built in 1957 for the Sperry Rand Corporation by the Rucker Company (Davidson and Bloomquist 1980). It was donated to the University of Florida's Department of Mechanical Engineering, and later acquired by the Department of Civil Engineering in 1972. Since then,

modifications on the operating voltage, sample capacity, and slip rings of the centrifuge had been performed to suit various geotechnical centrifuge modeling research (Millan 1985, Ryan 1983, and Davidson and Bloomquist 1980).

The centrifuge is a Rucker Model 57-2380 (Figure 6-1). A protective metal housing encloses the entire assembly. The overall dimensions of the centrifuge are 2.5 m (≈ 98 in.) in diameter, and 1.17 m (≈ 46 in.) in height. Access to the platform is possible through a swinging side door (Figure 6-2) and hinged top panels. Figure 6-3 shows the cross section of the centrifuge. Two rotating arms, 180° apart, each support a platform on which a sample or a counterweight is mounted. The distance from the axis of rotation to the centroid of the platform is 87 cm. (≈ 34 in.). The centrifuge can accelerate 25 kg to 85 g (2125 g-kg capacity).

The original 2.75 hp (2051.5 W) electric motor and varidrive unit were replaced in 1989 by a Parajust electronic direct-current (DC) motor controller as well as a larger 5 hp (3730 W) electric motor. This enhancement allows for longer flights at elevated g levels in addition to providing more accurate speed control.

A slip ring assembly, consisting of 32 leads, is located along the central rotating spindle. It provides electrical power and/or data acquisition to the model platform. A schematic diagram of the slip ring assembly is

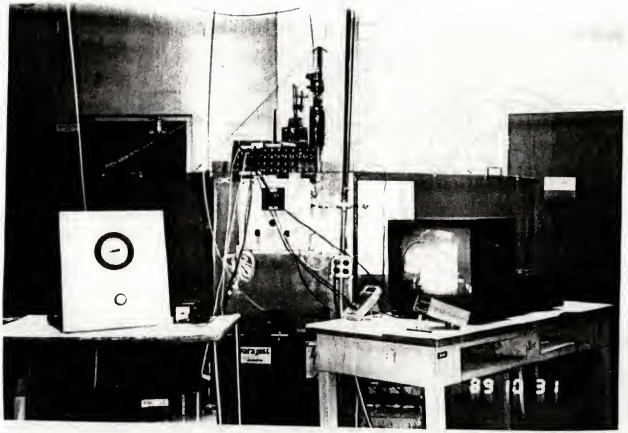

Figure 6-1. University of Florida Centrifuge (Rucker Model 57-2380).

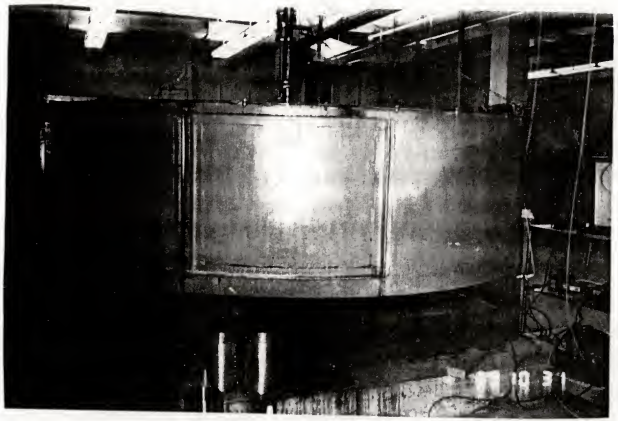

Figure 6-2. Swinging side door of the centrifuge.

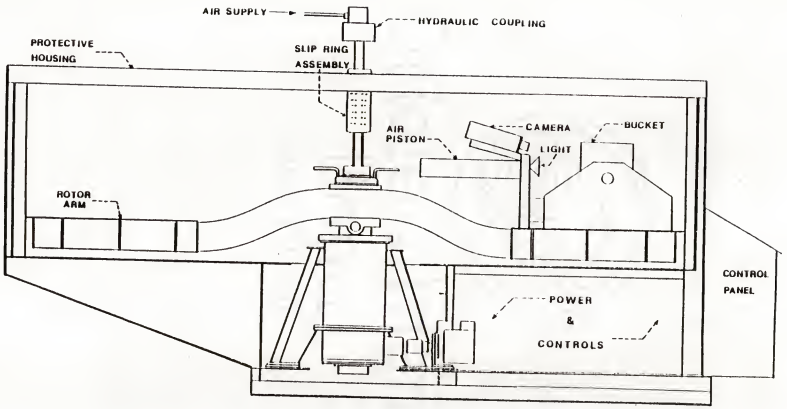

Figure 6-3. Cross-section view of the centrifuge. [Adapted from Davidson and Bloomquist 1980]

shown in Figure 6-4. External power is supplied to the slip ring terminals and brought out through the rotor arm terminals to the model sample.

Air pressure can be supplied by a hydraulic coupling which is located at the top of the rotating spindle. An air line is placed down through the slip ring and out to the model platform.

Model Bucket Assembly

In order to simulate a drilled shaft construction process in the centrifuge, a plexiglass model container was designed and constructed.

The model bucket assembly is shown in Figure 6-5. The bucket assembly consists of an aluminum bucket, an aluminum bucket housing, and a plexiglass container.

The bucket is constructed of 6061-TA aluminum (Millan 1985). It is 9.5 in. (≈ 241 mm) in diameter and 13.625 in. (≈ 346 mm) in height. The thickness of the bucket is 0.3125 in. (≈ 8 mm). The bucket pivots on two 1 in. (25.4 mm) diameter threaded rods which are supported by the 0.25 in. (≈ 6 mm) thick aluminum housing.

The bucket is designed to support a load of 36 kg at 80 g's in the base with a factor of safety of 5.5. The factor of safety against shear along the pivoting holes and against failure of the pivots has been calculated to be 14 and 6.3, respectively. The housing has a factor of safety of 4 against shear failure in the pivoting holes.

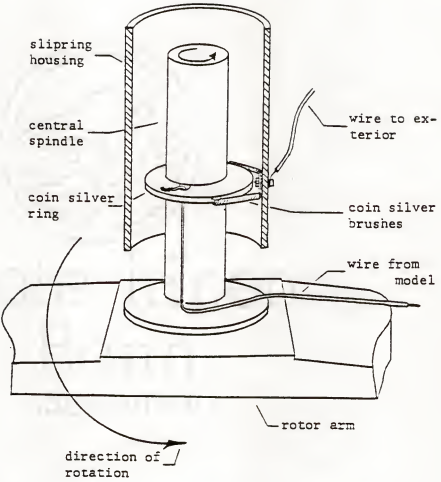

Figure 6-4. Schematic diagram of the slip ring assemble. [From Ryan 1983]

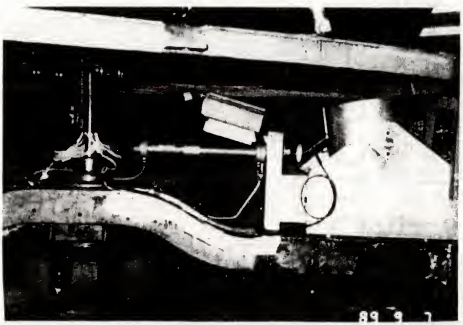

a)

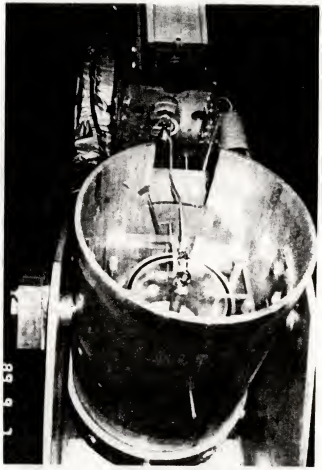

b)

Figure 6-5. The model bucket assembly. a) Side view; b) Top view.

An air piston (Bimba Model 318-DXP), a video camera (Panasonic WV-1414), and a light source are attached to the bucket housing. The total weight of all components and accessories is 36 kg.

Figure 6-6 shows a schematic diagram of the plexiglass container. The container consists of a cylinder, a top plate, and a bottom plate. The cylinder has a 140 mm diameter and is 180 mm in height. The plates are both 25 mm thick. The ends of the cylinder are grooved, and an 'O' ring is placed between the cylinder and the plate. At the center of the base plate is a 8 mm deep circular depression which is connected to a pressure transducer through a channel in the base plate and tubing. A narrow groove is cut along the circumference of the depression to fit a small 'O' ring. An acrylic tube of 13 mm internal diameter, 1.5 mm thick, and 230 mm long, is inserted into the circular depression. The 'O' ring is used to prevent leakage of the slurry which is placed in the tube. The cylinder and plates are assembled using threaded rods, washers, and nuts.

Centrifuge Test Program

Sample Preparation

Based on the results of slurry preparation in Chapter 4, a Florigel H-Y clay slurry of 34 s Marsh viscosity was prepared by using a concentration of 49 kg/m^3 and by mixing

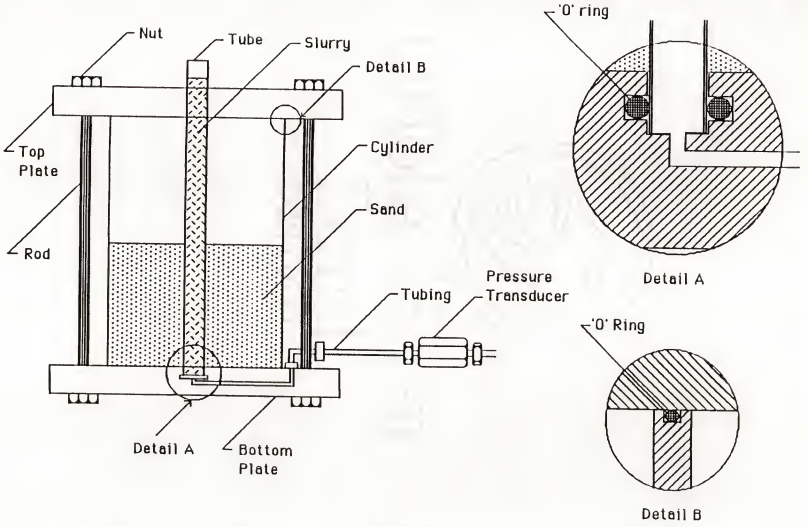

Figure 6-6. Schematic diagram of the plexiglass model container.

with the Hamilton Beach mixer at high speed for 2 min. The density of the clay slurry was determined to be 1025 kg/m^3. A Super Mud polymer concentration of 3 x 10^{-3} m^3/m^3 was used to obtain a 33 s Marsh viscosity polymer slurry by mixing at high speed for 1 min. The density of the polymer slurry was determined to be 1000 kg/m^3.

The procedure of preparing a model sample is illustrated in Figure 6-7. The connection to the pressure transducer from the bottom plate was through a flexible tubing (Figure 6-7 a). The space from the channel in the bottom plate, through an elbow fitting and tubing, to the pressure transducer, was saturated with water. The tube was inserted in the center depression and filled with slurry as shown in Figure 6-7 b. The cylinder was placed, with the tube in the center, on the bottom plate. Sand was slowly poured in the container to a height of 2.5 in. (63.5 mm) (Figure 6-7 c). The top plate was then placed on top of the cylinder and secured by washers and nuts on the rods. The assembled sample container is shown in Figure 6-7 d.

Note that the thickness of the sand layer was controlled by the amount of slurry in the tube. The slurry not only needed to fill the volume of the hole, it was also needed to form a filter cake. For a full tube of slurry, the maximum thickness of the sand layer was 2.5 in.

a)

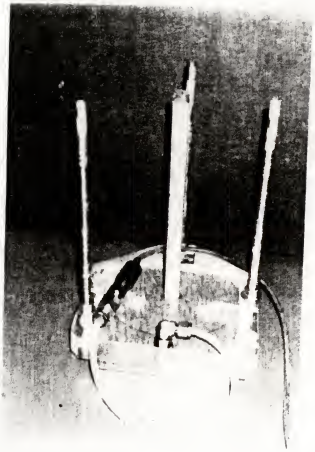

b)

Figure 6-7. Model preparation procedure. a) Connect pressure transducer to bottom plate; b) Insert tube and fill slurry; c) Place cylinder and pour sand; d) Secure top plate.

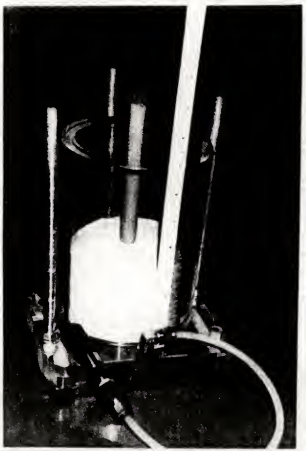

c)

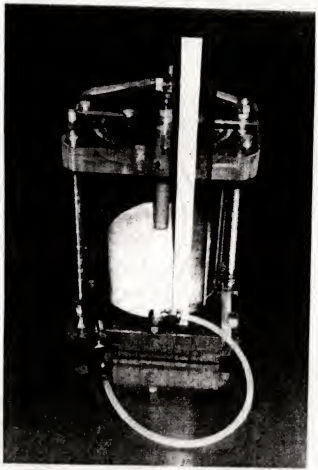

d)

Figure 6-7--continued

Centrifuge Experiments

Four series of experiments were performed to validate the centrifuge modeling concept. The experiments conducted involved the study of the stress levels (at 10 g, 20 g, 30 g, and 40 g), the sedimentation of slurry (at 30 g), the hole integrity (at 40 g), and the cake thickness (at 40 g).

Stress levels. This experiment was to investigate how accurate the pressure transducer could measure the corresponding stresses, at the bottom of a column of slurry, at various g levels. Water, the Florigel H-Y clay slurry, and the Super Mud polymer slurry were tested. Each of the tested materials was filled to a height of 7 in. (177.8 mm) in the 230 mm (≈ 9 in.) long acrylic tube. The setup of the sample was similar to that described in the above "Sample Preparation" section, except that no sand was placed in the container. The sample was then accelerated in the centrifuge to 40 g. Readings from the pressure transducer were recorded at various g levels. A total of three tests were performed.

Slurry sedimentation. Since the clay slurry was observed to settle about 1 in. (25.4 mm) in the 20-ft settling column (described in Chapter 5) in 13 h (780 min), it would be interesting to investigate whether a scaled-model clay slurry would settle the same amount in a scaled time frame. Based on the height of the settling column, 20 ft, and the desired head (8 in.) of slurry in the tube, a

scaling factor of 30 was adopted. The diameter of the slurry tube was also scaled down 30 times.

Only one test was performed for this experiment. The setup of the sample was as described in the "Sample Preparation" section with the exception that no sand was placed in the container. The tube of slurry was run at 30 g for 780/30 min = 26 min. At the end of the test, the depth of the water/slurry interface was measured.

Hole integrity. The study of the integrity of a slurry-filled hole using centrifuge modeling consisted of two parts. The first part was forming a slurry-filled hole under 1 g condition and then subjected the sample to an acceleration of 40 g and see if the hole collapsed. The second part was forming a slurry-filled hole at a desired g level (40 g) to test the stability of the hole.

The sample preparation procedure was illustrated in Figure 6-7 and was described in the "Sample Preparation" section. Three sand (where the slurry-filled hole was formed) conditions were tested: dry fine sand, wet fine sand, and wet coarse sand. The sand grain sizes are described in Chapter 3. For wet sands, the level of water was the same as the sand, i.e., 2.5 in. high. Note that the water was introduced into the container through two holes in the top plates.

To form a slurry-filled hole at 1 g, the tube was slowly pulled by hand. As the tube was raised, the slurry

seeped into the sand and the slurry level in the tube dropped. The tube was pulled again after the lowering of slurry level became unobservable. The length of time required for the tube to be completely withdrawn from the sand ranged from 20 to 30 min.

To form a slurry-filled hole when in flight, a special slurry tube pull-out mechanism was designed and constructed. Figure 6-8 is a schematic diagram showing how the mechanism works. When a certain g level was achieved, an air regulator was slowly opened which supplied air to the piston on board. By extending the piston, it pulled the tube out of the bottom plate of the sample container, via a pulley. When the tube was completely pulled out, a vacuum was applied to retract the piston back to its original position. Note that an elastic stretch cord was used to hold back the piston, preventing it from extending out at high g level.

Only the Florigel H-Y clay slurry was tested for hole integrity, because the Super Mud polymer slurry did not appear to form a filter cake during the preliminary 1 g pull-out tests. For dry sand, the polymer slurry kept seeping into the sand and dry sand turned into moist sand. For wet sand, the polymer slurry seeped into the sand and forced the surrounding water level to rise. Therefore a total number of six clay slurry tests were performed for

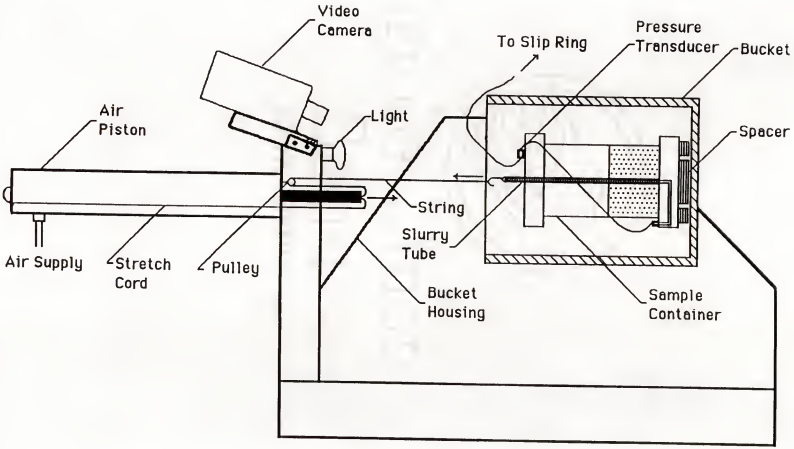

Figure 6-8. Schematic diagram of the slurry tube pull-out mechanism.

this experiment; three for the first part and three for the second part.

Filter cake thickness. This experiment was to observe the thickness of the filter cake formed at 1 g and 40 g levels. The sand conditions were the same as above; i.e., dry fine, wet fine, and wet coarse.

For the 1 g tests, the slurry-filled hole was formed as described above, i.e., by pulling the slurry tube gradually out from the sand. The sample container was then carefully dismantled and the filter cake thickness was measured. A total of three 1 g tests were performed.

For filter cake thickness formed at 40 g, the samples from the first part of the "Hole integrity" tests were used, i.e., the slurry-filled hole was formed at 1 g and then subject to an acceleration of 40 g. At the end of the hole-integrity test, the sample container was carefully dismantled and the filter cake thickness was measured. Strictly speaking, the samples from the second part of the "Hole integrity" tests should be used. However, as shown in the following section, all the slurry-filled holes formed at 40 g collapsed and measurement of filter cake thickness was impossible.

Results and Discussion

Stress Levels

The results of the stress level tests are presented in Figures 6-9 through 6-11. The pressure transducer recorded higher stresses than the corresponding theoretical stresses at high g levels. This error may be explained by the different levels of acceleration and thus different magnitude of stresses throughout the sample length. Since the centripetal acceleration is proportional to the radial arm, at a certain g level, the acceleration at the bottom of the sample is higher than that at the top of the sample.

The length of the sample, l, (7 in.) is about 18% the distance from the axis of rotation to the sample surface, R, (38.5 in.), i.e., $l/R \approx 0.18$. The error of height (or stress) from Figures 6-9 through 6-11 is about 10%. Davidson and Bloomquist (1980) show that the stress error is half the centripetal acceleration error, and the centripetal acceleration error is equals to l/R. Although the stress error determined (10%) is slightly higher than half l/R (18%), the results are reasonable.

Slurry Sedimentation

A 2 in. depth water/slurry interface was obtained at the end of the test. If this interface depth were scaled up to the prototype dimensions, it would be a 5 ft deep water/slurry interface appeared at the end of a 13 h

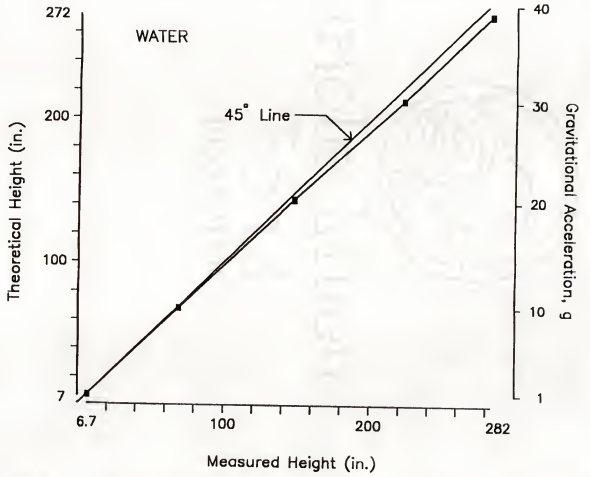

Figure 6-9. Theoretical height versus measured height of column of water in the centrifuge.

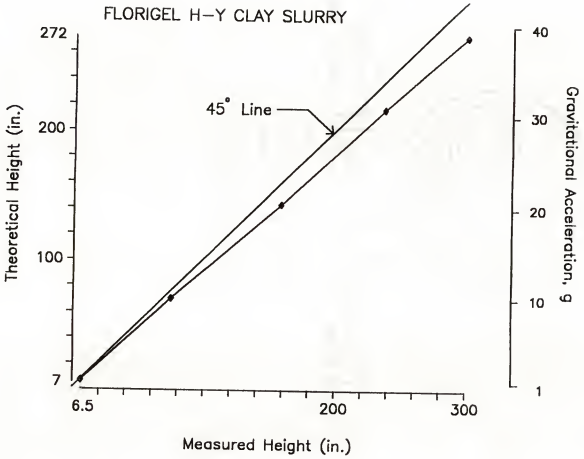

Figure 6-10. Theoretical height versus measured height of column of Florigel H-Y clay slurry in the centrifuge.

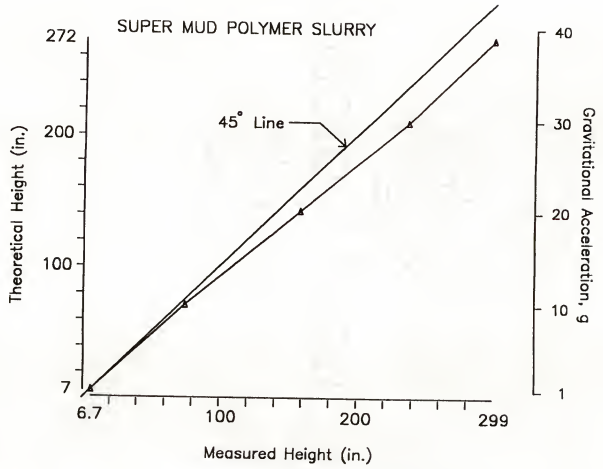

Figure 6-11. Theoretical height versus measured height of column of Super Mud polymer slurry.

sedimentation time. However, there was only about 1 in. deep interface observed during the settling column tests (Chapter 5). Since only one centrifuge test was performed for this sedimentation experiment, no concluding remark could be drawn from the result. However, this test can be served as a reference for future research having similar experimental conditions.

Hole Integrity

Of all the six tests performed, only one test showed an almost intact hole. It was the condition with dry fine sand and the slurry-filled hole was formed at 1 g and later accelerated to 40 g to test the hole integrity. Figure 6-12 shows photographs of the sample taken immediately after the test. The slurry appeared to concentrate at the bottom of the hole.

Another two tests where the slurry-filled hole was formed at 1 g were sands (fine and coarse) in wet condition. Two factors may attribute to the collapse of hole. First, the hydrostatic stress induced by the slurry may not be adequate to support the hole at high stresses because of denser sand at high g levels. Second, weaker filter cake formed at the sand and slurry interface in the wet conditions as compare to the dry conditions. The slurry penetrated shorter distance than that under the dry sand conditions because of the resisting hydrostatic pressure of water. Because of the smaller plastering

Figure 6-12. Sample of dry fine sand with slurry-filled hole formed at 1 g and later accelerated to 40 g.
a) Sample in the cylinder;
b) Sample with cylinder removed;
c) Cross-section view of the sample.

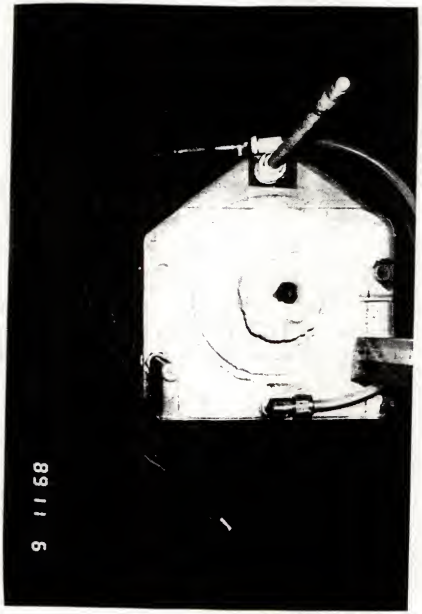

b)

Figure 6-12--continued

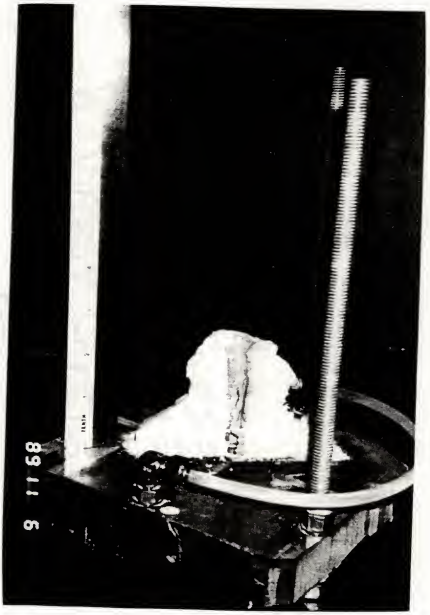

c)

Figure 6-12--continued

effect of the filter cake on the interface, any vibration caused by the centripetal acceleration may cause the collapse of the hole.

For the tests of slurry-filled hole formed at 40 g, all the holes collapsed. Figures 6-13 through 6-15 show the conditions of dry fine sand, wet fine sand, and wet coarse sand immediately after the tests. The major cause of the collapse of hole was due to the difficult control of the pulling rate of the slurry tube. Because of the compressibility of air, instant control of the piston was not achieved. The formation of filter cake, which is one of the controlling factors of hole stability, was thus affected.

Filter Cake Thickness

The filter cake thickness of the almost intact hole from a 40 g test shown in Figure 6-12 was measured. The thickness of the cake was 0.5 mm at the top and 2.5 mm at the bottom of the hole. The filter cake thickness of the same sand conditions formed at 1 g was measured to be the same as that tested at 40 g. Holden (1983) recommends a maximum filter cake thickness of 1 mm. The cake thickness measured has a mean thickness of 1.5 mm which is close to the recommended thickness. The thicker filter cake at the bottom was due to the longer contact time between the slurry and the interface.

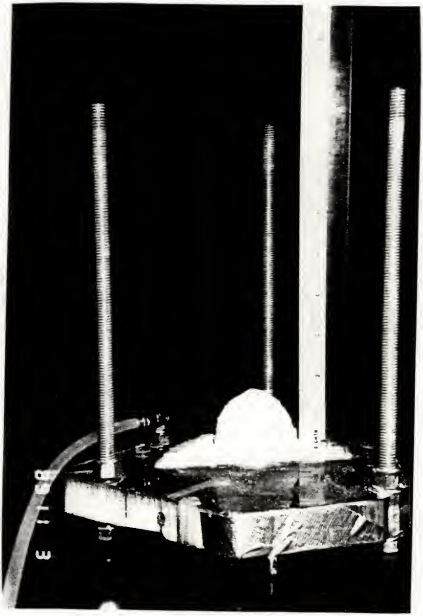

Figure 6-13. Cross-section view of the sample of dry fine sand with slurry-filled hole formed at 40 g.

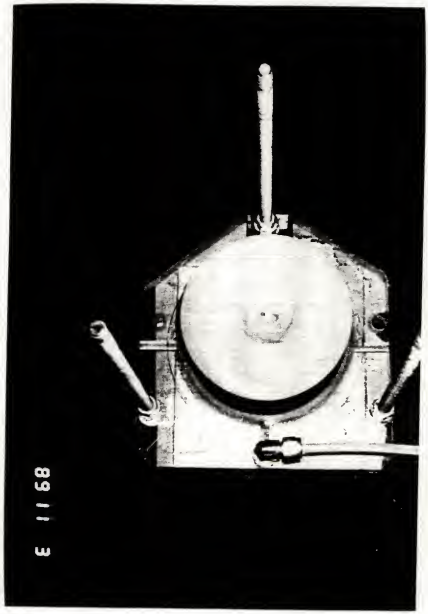

Figure 6-14. Sample of wet fine sand with slurry-filled hole formed at 40 g.

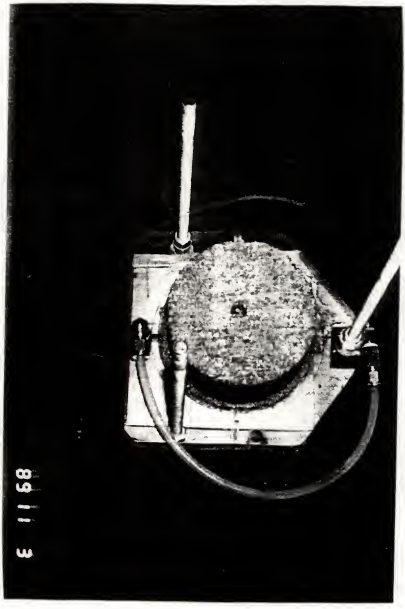

Figure 6-15. Sample of wet coarse sand with slurry-filled hole formed at 40 g.

Summary

The results of the stress-levels experiment indicate that the pressure transducer can measure a fairly accurate stress during centripetal acceleration. The clay slurry sedimentation in the centrifuge model was different from that in the prototype. Further tests are required to verify this finding. The hole-integrity tests show that under a dry fine sand condition, a clay slurry-filled hole is likely to stay open. The polymer slurry did not appear to form a filter cake at the interface. The thickness of the filter cake formed by the clay slurry is close to that recommended by Holden (1983). The tube pulling mechanism during flight condition need to be improved to control the pulling rate.

CHAPTER 7
CONCLUSIONS AND RECOMMENDATIONS

Conclusions

Conclusions are drawn based on the laboratory studies described in the previous chapters on the Florigel H-Y clay slurry and the Super Mud polymer slurry and are enumerated as follows:

1. The preparation of Florigel H-Y clay slurry required either powerful mixing with a short mixing time or less powerful mixing with a long mixing time. Pregel (pre-soak) of the clay showed no advantage on the rheological properties.
2. The preparation of Super Mud polymer slurry did not require powerful mixing. A uniform slurry was obtained as long as the polymer dissolved completely in the makeup water.
3. The density of the Florigel H-Y clay slurry increased linearly with its concentration. But the Super Mud polymer slurry gave a density of 1000 kg/m^3 for viscosity as high as 50 s Marsh.
4. Both the Florigel H-Y clay and Super Mud polymer slurries behaved in a non Newtonian manner. The slurry viscosity decreased with increasing shear rate.

5. At low shear rate (5.11 s^{-1}), the Florigel H-Y clay slurry was much more viscous than the Super Mud polymer slurry. But, the viscosities of the two types of slurry at high shear rate (1021 s^{-1}) were about the same.

6. The Florigel H-Y clay slurry is thixotropic. Its viscosity proved to be a function of the stress history. Therefore it is important to determine the slurry viscosity immediately after sampling.

7. The Super Mud polymer slurry showed no thixotropy. Insignificant gel strength was measured: for a 40 s Marsh polymer slurry, the gel strength is less than 1 Pa.

8. The slurry specifications on viscosity, which require the fresh slurry to be either less than 40 s Marsh (or 50 s Marsh) or less than 20 cP Fann plastic viscosity are not appropriate for both the Florigel H-Y clay and Super Mud polymer slurries. Because, a 40 to 50 s Marsh slurry viscosity was found to correspond to only 5 to 8 cP Fann plastic viscosity.

9. The pH value is merely a measure of acidity and acidity is not the only chemical variable that chemically control the slurry rheological properties. Slurries with the same pH but with different types of electrolytes and electrolyte concentrations showed different rheological properties.

10. Both the Tannic acid and hydrochloric acid lowered the viscosity, yield point, and gel strength of the Florigel H-Y clay slurry. Also, organic tannic acid was more effective than the inorganic hydrochloric acid in lowering these parameters.
11. Sodium hydroxide caused a sudden drop in viscosity, yield point, and gel strength of the clay slurry, and the slurry turned fluid when the pH was raised to above 11.
12. Calcium hydroxide (lime) did not have such a drastic effect as sodium hydroxide had on the Florigel H-Y clay slurry, but it also lowered the viscosity and caused the slurry to flocculate.
13. Super Mud slurry maintained a constant viscosity for slurry pH above 6. But, the slurry viscosity decreased when the slurry pH dropped below 6. Rejuvenating the viscosity by adding soda ash was almost futile.
14. The Marsh funnel viscosity of the Florigel H-Y clay slurry was found to be almost the same for clean slurry (no sand) and for slurry with less than 20% sand content by volume.
15. Although the slurry gel strength, yield point, and viscosity were known to control the sand (cuttings) suspending ability of the slurry, the results of the settling tests showed that the gel strength was the key controlling property. The super Mud polymer

slurry, with almost no gel strength, could not keep the sand particles in suspension, whereas the Florigel H-Y clay slurry, which was able to develop gel strength, was capable of suspending the sand particles.

16. For Florigel H-Y clay slurry, the size of the sand particles that could be suspended and the length of time the particles stayed in suspension, were found to depend on the slurry viscosity. Higher viscosity could suspend larger particles and reduce the settling rate.

17. Stress levels could be measured fairly accurately under centripetal acceleration. The sedimentation of Florigel H-Y clay slurry in the centrifuge requires further research.

18. The study of hole integrity using centrifuge modeling is a delicate task. The results of the centrifuge tests show promise in using centrifuge modeling in examining hole integrity and filter cake thickness. However, a more sophisticated mechanism is required to control the forming of slurry-filled hole in flight.

Recommendations for Future Research

The following are recommendations for future research related to this work:

1. Filter cake is an important part in stabilizing the drilled hole. The current API filter cake test uses a

filter press with a 100 psi applied pressure. The 100 psi may be too high for drilled shaft construction. An investigation on the effect of different applied pressures on the filter cake properties will be useful.

2. Whether the filter cake reduces the skin friction of the drilled shaft is still debatable. At present, there is no way to determine the shear strength of a filter cake in the laboratory. A device that can simulate the shearing action of the displacement of slurry by concrete, and measure the strength of the filter cake, will enable the studying of the effect the filter cake has on the skin friction.
3. For the study of hole integrity using centrifuge modeling, it is recommended that hydraulic pressure, instead of air pressure to be used to pull the slurry tube. Also, a design to have a continuous supply of slurry in flight will enable modeling of a deeper slurry hole.

APPENDIX A
PROCEDURES FOR MINERALOGICAL, PHYSICAL, AND CHEMICAL ANALYSES

The procedures described below are for the mineralogical, physical, and chemical analyses of the Florigel H-Y clay. The results of these analyses are presented in Chapter 3.

X-ray Diffraction Analysis (XRD)

Two samples were prepared for the XRD. The first was a random powder mount of the whole sample. The second was a clay fraction glass slide oriented mount. The clay fraction was obtained by dispersing the sample with sodium hexametaphosphate solution (4 g/L). The suspension at the end of 8 h and at the depth of 10 cm was pipetted onto the glass slide. The clay fraction in the suspension had a equivalent particle diameter of about 2 microns. The time and depth of sampling for the 2 microns clay fraction were based on Stokes' law and a nomograph developed by Tanner and Jackson (1947).

The powder mount sample was packed into an aluminum holder with as less pressing as possible to produce a random sample. Only one X-ray scan was run on this sample. For the glass slide oriented sample, three scans were run. The first was the untreated slide, the second was after

glycolated for 3 days, and the last was after heated at 550°C for 2 h.

A GE 11GN1 X-ray diffractometer was used for the XRD work. The operation conditions, except the range, for all the scans are as follows:

Radiation: Cu	Filter: 0.007 in. Ni
KV: 35 mA: 15	Take off angle: 4°
Counter: Proportional	Counter voltage: 1650 V
Time constant: 1.0	
Amplification gain: coarse 12, fine maximum; Linear	
Pulse height selector EL 60 V	
Chart speed: C	Scanning speed: 2°/min
Beam slit: 1°	Dectector slit: 0.1°
Soller slit: Medium reslolution	

Differential Thermal Analysis (DTA)

No grinding has been done on the powdered Florigel H-Y sample due to the interest in obtaining the thermal property of the whole sample. A calcined aluminum oxide was used as a reference material and the air dry clay sample was the reacting material. The DTA instrument used was the D6000 Deltatherm III. The operation procedure in the instruction manual was followed. The DTA was run up to 700°C, with a heating rate of 10°/min, chart speed of 2 in./100°C and delta sensitivity of 0.5°/in.

Grain Size Distribution Analysis

The test was performed according to the ASTM D422-63 (American Society for Testing and Materials 1989) with slight modification on the sample size. A 20 g air-dry sample was dispersed in a 125 mL sodium hexametaphosphate solution (40 g/L). The smaller amount of sample, 20 g instead of the normal 50-60 g, was chosen to reduce the gelation of the suspension. Note that the specific gravity of the Florigel H-Y clay was determined by the ASTM D854-83 and a value of 2.45 was obtained and was used in the hydrometer analysis calculation.

Atterberg Limits Test

The ASTM D4318-84 (American Society for testing and Materials 1989) standard test procedure was adopted for the test. Note that, after water was added to the sample, curing time of 1-2 h was allowed for clay particles to absorb water.

Total Surface Area Determination

The procedure of Carter, Mortland, and Kemper (1986) have been simplified and adopted. No pretreatment was done on the sample. Three replicates of the air dry sample, each weighed 2.00 g were placed in a desiccator chamber which had a bowl of liquid ethylene glycol monoethyl ether (EGME). The desiccator was then evacuated for 45 min and allowed to stand at room temperature for 4 to 6 h. The

weights of the sample replicates were taken after releasing the vacuum. They were then returned to the desiccator chamber and the chamber was evacuated for 45 min. The sample replicates were weighed at convenient time interval, evacuated between weighing, until a constant weight was achieved.

Cation Exchange Capacity (CEC) Determination

The CEC at pH 7 determination was performed on three replicate samples. The procedures were as follows:

1. The clay was sieved through a #200 sieve. Exactly 2.00 g minus #200 sample was then weighed.
2. The sample was placed in a Erlenmeyer flask and added 100 mL 2 normal (N) ammonium acetate (≈ pH 7). The flask was shaken briskly and allowed to soaked overnight.
3. On the next day, the sample was poured on a filter paper in a Büchner funnel, which was attached to a vacuum line.
4. The sampled was slowly washed with additional 2 N ammonium acetate while applying the vacuum. After all of the sample was removed from the flask, it was then washed thoroughly 3 to 4 times with neutralized methyl alcohol (pH 7).
5. The filter paper and clay sample were transferred to an ammonia distilling apparatus.

6. The end of the condenser was placed in a beaker containing exactly 20 mL of standard sulfuric acid and 4 drops of Brom Thymol Blue indicator.
7. Approximately 25 mL of concentrated (6 N) sodium hydroxide was run onto the clay sample. The sample was then distilled for 5 min.
8. The excess sulfuric acid in the beaker was back titrated with standard 0.1 N sodium hydroxide.
9. The total CEC was calculated as follows:

$$\text{Total CEC (me/100 g)} = \frac{(20 \text{ mL } H_2SO_4 - \text{mL NaOH})}{\text{g sample}} \times \text{N NaOH} \times 100$$

Note: 1 me/100 g = 1 cmol(+)/kg

APPENDIX B
DATA OF ATOMIC ABSORPTION SPECTROPHOTOMETRY

The readings obtained from the AAS for the four supernatants of Florigel H-Y clay suspension are as follow:

	AAS Readings	
Sample	Calcium	Magnesium
1M NaOAc (Blank)	0.019	0.014
A	0.021	0.681
B	0.018	0.634
C	0.018	0.760
D	0.019	0.547

APPENDIX C
VISCOSITY COMPUTATION OF THE FANN VISCOMETER

The following computations were used for the data reduction on slurry samples ran on the Fann V-G viscometer.

$$\text{Viscosity, } \mu = \frac{\text{Shear stress, } \tau \text{ (dynes/cm}^2\text{)}}{\text{Shear rate, s } (s^{-1})}$$

$$\tau = k_1 k_2 \theta$$

$$s = k_3 N$$

where k_1 is the torsion constant in dyne-cm/degree deflection

k_2 is the shear stress constant for the effective bob surface, cm^{-3}

k_3 is the shear rate constant, s^{-1} per rpm

θ is the Fann Viscometer reading

N is the rate of revolution of the rotor sleeve

By expressing viscosity using the three instrument constants,

$$\mu \text{ (poise)} = \frac{k_1 k_2 \theta}{k_3 N}$$

Since $(k_1)(k_2) = 5.11$ dyne/cm^2/degree deflection

and $k_3 = 1.7023\ s^{-1}$

$$\mu \text{ (poise, P)} = 3.00\frac{\theta}{N}$$

$$\mu \text{ (centipoise, cP)} = 300\frac{\theta}{N}$$

Since,

1 cP = 1 mPa.s

Therefore, with reference to Figure 3-11,

$$\text{Effective viscosity, } \mu_e \text{ (mPa.s)} = 300\frac{\theta}{N}$$

$$\text{Plastic viscosity, PV (mPa.s)} = 300\frac{(\theta_{600} - \theta_{300})}{(600 - 300)}$$

$$= \theta_{600} - \theta_{300}$$

$$\text{Yield Point, YP (Pa)} = 1.065\ (\theta_{300} - \text{PV})$$

(1° Fann = 0.511 Pa)

The corresponding shear rates for the rates of revolution of the rotor sleeve are given below:

N (rpm)	s (s^{-1})
3	5.1
6	10.2
100	170.0
200	340.0
300	511.0
600	1021.0

APPENDIX D
RESULTS OF WATER TEST

	Tap water	Distilled water
Calcium (Ca), ppm	26	1
Magnesium (Mg), ppm	15	0
Iron (Fe), ppm	0.1	0.1
Sodium (Na), ppm	9	0
Chlorine (Cl), ppm	26	2
pH	8.6	5.8
Soluble salts, dS/m	0.33	0.00
Soluble salts, ppm	231	0
Hardness, ppm	126 (hard)	2.5 (relatively soft)
Total Carbonates, meq/liter	1.3	--

REFERENCES

Ambrose, H. A., and Loomis, A. G. 1931. Some colloidal properties of bentonite suspensions. Physics 1: 129-36.

Ambrose, H. A., and Loomis, A. G. 1933. Fluidities of thixotropic gels: Bentonite suspensions. Physics 4, no. 8: 265-73.

American Concrete Institute. 1989. Proposed revisions to: Standard specification for the construction of drilled piers (ACI 336.1-79)(revised 1985). ACI Structural Journal 86, no. 1: 94-103.

American Petroleum Institute. 1985. Standard procedure for field testing drilling fluids, API RP 13B. Dallas: American Petroleum Institute.

American Society for Testing and Materials. 1989. 1989 Annual Book of ASTM Standards, Section 4 Construction, Volume 04.08: Soil and Rock, Building Stones; Geotextiles. Philadelphia: American Society for Testing and Materials.

Bailey, S. W., G. W. Brindley, W. D. Johns, R. T. Martin, and M. Ross. 1971. Clay minerals society report of nomenclature committee 1969-1970. Clays and Clay Minerals 19: 132-33.

Bingham, E. C. 1916. An investigation of the laws of plastic flow. Bulletin of the Bureau of Standards 13: 309-53.

Bouse, E. E. 1987. Better mud viscosity data necessary, possible. Oil and Gas Journal 85 (June), no. 26: 60, 63-64.

Bouyoucos, G. J. 1936. Directions for making mechanical analyses of soils by the hydrometer method. Soil Science 42, no. 3: 225-29.

Boyes, R. G. H. 1975. Structural and Cut-off Diaphragm Walls. New York: Halsted Press.

Bradley, W. F. 1940. The structural scheme of attapulgite. American Mineralogist 25: 405-10.

Burke, W. H. 1935. Some factors affecting the viscosity of rotary muds. Transactions of the American Institute of Mining and Metallurgical Engineers 114: 53-61.

Carico, R. D. 1976. New field test improves fluid-suspension measurements. The Oil and Gas Journal 74, no. 27:81-8.

Carter, D. L., M. M. Mortland, and W. D. Kemper. 1986. Specific surface. In Methods of Soil Analysis, Part 1-Physical and Mineralogical Methods, 2d ed. by A. Klute, 413-23. Madison: American Society of Agronomy, Inc. and Soil Science Society of America, Inc.

Chilingarian, G. V., and P. Vorabutr. 1981. Drilling and Drilling Fluids. Amsterdam: Elsevier Scientific Publishing Co.

Chisholm, F., and S. Kohen. 1954. Measurement of plastic flow properties. The Petroleum Engineer 26: 87-90.

Davidson, J. L., and D. Bloomquist. 1980. Centrifuge Modeling of the Consolidation/Sedimentation Process in Phosphatic Clays. Engineering and Industrial Experiment Station, Research Report 245 W65. Gainesville: University of Florida.

Federation of Piling Specialists. 1985. Specification for cast in place piles formed under bentonite suspension. Ground Engineering 18: no. 4: 11-15.

Florida Department of Transportation. 1987. FDOT Standard Specifications for Roads and Bridges Construction, Section 455: Foundations of Structures (Draft). Tallahassee: Florida Department of Transportation.

Florida Department of Transportation. 1988. FDOT Standard Specifications for Roads and Bridges Construction, Section 455: Foundations of Structures (Draft). Tallahassee: Florida Department of Transportation.

Gray, G. R., and H. C. H. Darley. 1980. Composition and Properties of Oil Well Drilling Fluids. Houston: Gulf Publishing Co.

Green, H. 1949. Industrial Rheology and Rheological Structures. New York: John Wiley & Sons.

Greer, D. M., and W. S. Gardner. 1986. Construction of Drilled Pier Foundations. New York: John Wiley & Sons.

Grim, R. E. 1962. Applied Clay Mineralogy. New York: McGraw-Hill Book Co.

Grim, R. E. 1968. Clay Mineralogy. New York: McGraw-Hill Book Co.

Haden, W. L., and I. A. Schwint. 1967. Attapulgite, its properties and applications. Industrial and Engineering Chemistry 59 (September), no. 9: 59-69.

Halbouty, M. T. 1937. Use of the viscosimeter in determining drilling mud viscosity and gel strength. The Oil Weekly 84, no. 10: 32-4.

Heggem, A. G., and J. A. Pollard. 1914. Mud-ladden fluid applied to well drilling. United States Bureau of Mines, Technical Paper 66, 5-20.

Herrick, H. N. 1932. Flow of drilling mud. Transactions of the American Institute of Mining and Metallurgical Engineers 98: 476-86.

Holden, J. C. 1983. Construction of Bored Piles in Weathered Rock, Part 4: Bentonite Construction Procedures, Technical Report No. 6. Australia: Road Construction Authority of Victoria.

Hostermann, J. W. 1985. Bentonite and fuller's earth resources of the United States. United States Geological Survey, Map MR-92.

Hutchinson, M. T., G. P. Daw, P. G. Shotton, A. N. James. 1975. The properties of bentonite slurries used in diaphragm walling and their control. In Diaphragm Walls and Anchorage, 33-39. London: Institute of Civil Engineers.

Ikuta, Y. 1974. Diaphragm walling in Japan. Ground Engineering 7, no. 5: 39-44.

Institution of Civil Engineers. 1977. A Review of Diaphragm Walls, A Discussion of 'Diaphragm Walls and Anchorages'. London: Institution of Civil Engineers.

Jessen, F. W., and C. N. Toktar. 1960. Gel development in drilling fluids. The Petroleum Engineer 32: 48-60.

Johnston, I., J. J. Pettit, A. Weltman, and D. Fairweather. 1977. Piling. Contract Journal 279, no. 5115: 49-67.

Kelly, J. 1983. Drilling fluids selection, performance, and quality control. Transaction of the Society of Petroleum Engineer 275: 889-98.

Lilienthal, W. B. 1952. Viscometry and mud control. The Oil and Gas Journal 51, no. 25: 124.

Loomis, A. G., H. A. Ambrose, and H. T. Kennedy. 1934. Some Rheologic Aspects of Petroleum Production. Physics 5: 207-16.

Lorenz, H. 1963. Utilization of thixotropic fluid. In Grouts and Drilling Muds in Engineering Practice. London: Butterworths.

Marsh, H. N. 1931. Properties and treatment of rotary mud. Transaction of American Institute of Mining and Metallurgical Engineers 92: 234-51.

Mayo, D. F. 1973. Development of nonpneumatic caisson engineering. Journal of Construction Engineering Division, American Society of Civil Engineering 99 (July), no. CO1: 155-73.

McKinney, J. R., and G. R. Gray. 1963. The use of drilling mud in large diameter construction borings. In Grouts and Drilling Muds in Engineering Practice, 218-221. London: Butterworths.

Melrose, J. C., and Lilienthal, W. B. 1951. Plastic flow properties of drilling fluids, measurement and application. Transactions of American Institute of Mining and Metallurgical Engineers 192: 159-64.

Millan, A. A. 1985. Centrifuge Modeling of Pile Groups in Sand. Ph.D. Dissertation. University of Florida.

Mitchell, J. K. 1960. Fundamental aspects of thixotropy in soils. Proceedings of the American Society of Civil Engineers 86 (June), no. SM3: 19-52.

Mitchell, J. K. 1976. Fundamentals of soil behavior. New York: McGraw-Hill Book Co.

Morgenstern, N., and I. Amir-Tahmasseb. 1965. The stability of a slurry trench in cohesionless soils. Geotechnique 15, no. 4: 387-95.

Nesbitt, L. E., and J. A. Sanders. 1981. Drilling fluid disposal. Transactions of the Society of Petroleum Engineers 271: 2377-81.

Polymer Drilling Systems Co. 1989. Construction of slurry displaced drilled shafts using Super Mud. Foundation Drilling 28 (Dec/Jan), no. 1: 36.

Reese, L. C. 1978. Design and construction of drilled shaft. Journal of the Geotechnical Engineering Division, American Society of Civil Engineering 104 (January), no. GT1: 95-116.

Reese, L. C., and O'Neill, M. W. 1987. Draft of Drilled Shafts: Construction Procedures and Design Methods. McLean, Virginia: U.S. Department of Transportation.

Rogers, W. F. 1953. Composition and Properties of Oil Well Drilling Fluids. Houston: Gulf Publishing Co.

Ryan, W. F. 1983. Centrifuge Testing of Model Piles in Sand. M.E. Report. University of Florida.

Skempton, A. W. 1953. The colloidal "activity" of clays. In Proceedings of the 3rd International Conference on Soil Mechanics and Foundation Engineering 1: 57-61.

Stebbins, E. E., and R. C. Williams. 1986. Slurry method of drilled shaft construction. A paper presented at Drilled Foundation Seminar held in Atlanta, Georgia 19-20 February 1986.

Tanner, C. B., and M. L. Jackson. 1947. Nomographs of sedimentation times for soil particles under gravity or centrifugal acceleration. Soil Science Society Proceedings 12: 60-65.

Terzaghi, K., and R. B. Peck. 1967. Soil Mechanics in Engineering Practice. New York: John Wiley and Sons.

Van Olphen, H. 1956. Forces between suspended bentonite particles. Clays Clay Minerals 4: 204-24.

Van Olphen, H. 1959. Forces between suspended bentonite particles, part II-Calcium bentonite. Clays Clay Minerals 6: 196-206.

Van Olphen, H. 1977. An Introduction to Clay Colloid Chemistry: For Clay Technologists, Geologists, and Soil Scientists. New York: John Wiley & Sons.

Van Olphen, H., and J. J. Fripiat, ed. 1979. Data Handbook for Clay Materials and Other Non-Metallic Minerals. New York: Pergamon Press.

Veder, C. 1953. Method for the construction of impermeable diaphragms at great depth by means of thixotropic muds. In Proceedings of 3rd International Conference of Soil Mechanics and Foundation Engineering 2: 91-94.

Xanthakos, P. P. 1979. Slurry Walls. New York: McGraw-Hill Book Co.

Zamora, M. and R. Bleier. 1977. Prediction of drilling mud rheology using a simplified Herschel-Bulkley model. Journal of Pressure Vessel Technology 99: 485-90.

BIOGRAPHICAL SKETCH

Hwee Yan Kheng was born on May 20, 1958. She was born and raised in the Republic of Singapore. She completed her primary school education from St. Nicholas Girls' School. She continued her secondary education with the same school and later transferred to Tanglin Technical School for her technical education. She graduated from Hwa Chong Junior College in 1976. In 1977, she entered the National University of Singapore for her engineering training. She received her Bachelor of Engineering (Civil) degree in 1981. After graduation, she worked for the Building Control Division, Ministry of National Development, Singapore.

In the fall of 1983, she came to the United States, and entered the West Virginia University for her graduate studies, specialized in geotechnical engineering. She received her Master of Science in Civil Engineering degree in December, 1984. She transferred to the University of Florida to continue her Doctor of Philosophy degree in the fall of 1985. She is currently working towards the degree in the field of geotechnical engineering.

I certify that I have read this study and that in my opinion it conforms to acceptable standards of scholarly presentation and is fully adequate, in scope and quality, as a dissertation for the degree of Doctor of Philosophy.

Paul Y. Thompson, Chair
Professor of Civil
Engineering

I certify that I have read this study and that in my opinion it conforms to acceptable standards of scholarly presentation and is fully adequate, in scope and quality, as a dissertation for the degree of Doctor of Philosophy.

David Bloomquist, Cochair
Assistant Professor of Civil
Engineering

I certify that I have read this study and that in my opinion it conforms to acceptable standards of scholarly presentation and is fully adequate, in scope and quality, as a dissertation for the degree of Doctor of Philosophy.

Frank C. Townsend
Professor of Civil
Engineering

I certify that I have read this study and that in my opinion it conforms to acceptable standards of scholarly presentation and is fully adequate, in scope and quality, as a dissertation for the degree of Doctor of Philosophy.

Douglas L. Smith
Professor of Geology

I certify that I have read this study and that in my opinion it conforms to acceptable standards of scholarly presentation and is fully adequate, in scope and quality, as a dissertation for the degree of Doctor of Philosophy.

James L. Eades
Associate Professor of Geology

I certify that I have read this study and that in my opinion it conforms to acceptable standards of scholarly presentation and is fully adequate, in scope and quality, as a dissertation for the degree of Doctor of Philosophy.

Roy D. Rhue
Associate Professor of Soil Science

This dissertation was submitted to the Graduate Faculty of the College of Engineering and to the Graduate School and was accepted as partial fulfillment of the requirements for the degree of Doctor of Philosophy.

December 1989

for Winfred M. Phillips
Dean, College of Engineering

Madelyn M. Lockhart
Dean, Graduate School